# Dilatancy of Silty Sand at Varied Densities

Major Project - II

Submitted in fulfilment of the requirement
For the award of the degree of

Master of Technology
(Geotechnical Engineering)

Submitted By:

***Paritosh Goyal***

(University Roll No: 04/GTE/2010)

Under the Guidance of
***Prof. A.Trivedi***
(Professor)
**&**
***Mr. Naresh Kumar***
(Assistant Professor)


DEPARTMENT OF CIVIL ENGINEERING
DELHI TECHNOLOGICAL UNIVERSITY
(Formerly Delhi College of Engineering)
2012

# Certificate

This is declare that the major project - II entitled **"Dilatancy of Silty Sand at Varied Densities "** is a bonafide record of work done by me for partial fulfilment of award of degree in M.Tech Civil Engineering (Geotechnical Engineering) at Delhi Technological University (Formerly Delhi college of Engineering), Delhi.

This project has been carried out under the supervision of **Prof. A.Trivedi**, **& Mr. Naresh Kumar**, Department of Civil Engineering, Delhi Technological University (Formerly Delhi College of Engineering), Delhi.

The work embodied in this major project has not been submitted to any other Institute/University for the award of any other Degree or Diploma.

(PARITOSH GOYAL)
University Roll No: 04/GTE/2010

---

**(Mr. Naresh Kumar)**
Department of Civil Engineering
Delhi Technological University,
(Formerly Delhi College of Engineering),
Delhi.

**(Prof. A.Trivedi)**
Department of Civil Engineering
Delhi Technological University,
(Formerly Delhi College of Engineering),
Delhi.

# Acknowledgement

It is distinct pleasure to express my deep sense of gratitude and indebtedness to my supervisor **Prof. A. Trivedi & Mr. Naresh Kumar**, Department of Civil Engineering**,** Delhi Technological University (Formerly Delhi College of Engineering), for his invaluable guidance, encouragement and patient reviews. His continuous inspiration only has made me complete this major project. Without his help and guidance, this major project would have been impossible. He remained a pillar of help throughout the project.

I am also grateful to Prof. **A.K. Gupta** Head Department of Civil Engineering, for providing the experimental facilities in various labs of the Department.

I express my sincere gratitude to the faculty and non teaching staff of Civil and Environmental engineering department and the library of Delhi Technological University, (Formerly Delhi College of Engineering) for providing the relevant information and help when needed during the course of my project work.

I am also thankful to Mr. Sadanand Ojha for sharing selected data from his PhD work entitled "Nonlinear Behaviour of Silty Sand and its Engineering Implication" for the purpose of comparison and his colleague particularly Sikandar and Mandeep Singh for their unconditional support during this project work.

I am also thankful to my friend Vijay Kumar Sukeriya for his unconditional support and motivation during this project work.

(PARITOSH GOYAL)

# Abstract

This work considers results of 180 drained tri-axial compression tests out of which 90 were successfully completed sharing up to large strain (20-25%). The results are analyzed with the aim to capture deviator stress v/s volumetric strain under different test conditions of relative densities and mean confining pressure. The sample was prepared in laboratory at varied relative densities. It is considers the effect of plastics fines on shear strength of sands. The properties of clean sands pertaining to shear strength have been studied extensively. The behavior of natural sands is normally influenced by the amounts of silt and / or clay. The critical state has been selected from tri-axial test data and care has been taken to ensure that true steady states arrived. Test procedures and the intrinsic properties of the material being tested are well controlled. The empirical shear strength fitting parameters (Q & R) for silty sands was compared with the existing literature for non-plastic silty sands. The values of shear strength fitting parameters (Q & R) found out for a selected sample was found to be slightly less than the conventional values. The main aim of this work is to identify the behavior of silty sand of different fineness at varied relative densities.

# Contents

# List of Tables & Figures

# List of Symbols

$C_u$ = coefficient of uniformity

s = shear strength

б = normal stress on the plane of shearing

$б_1$ = principal stress,

$б_3$ = confining stress

Φ = friction angle,

$Φ_c$ = critical friction angle

ψ = dilatancy angle

G = specific gravity

$γ_w$ = unit weight of water

$γ_{min}$ = minimum dry density

$γ_{max}$ = maximum dry density

$γ_d$ = dry density

$б_d$ = deviator stress

$ϵ_{axial}$ = axial strain

$ϵ_v$ = volumetric strain

$e_{max}$ and $e_{min}$ = minimum and maximum void ratio

$(б_1 / б_3)_c$ = effective principal stress ratio at critical state

$(б_1 / б_3)_p$ = effective principal stress ratio at peak state

$(б`_1 / б`_3)$ = effective principal stress ratio or stress obliquity

$dϵ_v$ = volumetric strain increment,

$dϵ_1$ = major principal strain increment

$D_r$ = relative density

$P`_p$ = mean effective stress at peak strength

$P_A$ = reference stress

Q & R = fitting parameters

# List of Symbols

Y.S. = Yamuna sand

$R_c$ = Degree of compaction

$I_N = I_R + \{D_r(\ln 100(P`_p / P_A)\}$

$D_mD_{r39.3}$ = Mean particle size & relative density at 39.3%

$D_mD_{r60.7}$ = Mean particle size & relative density at 60.7%

$D_mD_{r75}$ = Mean particle size & relative density at 75%

$D_mD_{r85.7}$ = Mean particle size & relative density at 85.7%

$D_mD_{r89.3}$ = Mean particle size & relative density at 89.3%

$D_mD_{r46.67}$ = Mean particle size & relative density at 46.67%

$D_mD_{r63.33}$ = Mean particle size & relative density at 63.33%

$D_mD_{r70.02}$ = Mean particle size & relative density at 70.02%

$D_mD_{r76.54}$ = Mean particle size & relative density at 76.54%

$D_mD_{r82.32}$ = Mean particle size & relative density at 82.32%

$D_mD_{r23.33}$ = Mean particle size & relative density at 23.33%

$D_mD_{r40}$ = Mean particle size & relative density at 40%

$D_mD_{r66.67}$ = Mean particle size & relative density at 66.67%

$D_mD_{r75.23}$ = Mean particle size & relative density at 75.23%

$D_mD_{r82.67}$ = Mean particle size & relative density at 82.67%

$D_mD_{r20}$ = Mean particle size & relative density at 20%

$D_mD_{r43.33}$ = Mean particle size & relative density at 43.33%

$D_mD_{r66.67}$ = Mean particle size & relative density at 66.67%

$D_mD_{r75.23}$ = Mean particle size & relative density at 75.23%

$D_mD_{r83.45}$ = Mean particle size & relative density at 83.45%

$D_mD_{r16.67}$ = Mean particle size & relative density at 16.67%

$D_mD_{r36.67}$ = Mean particle size & relative density at 36.67%

$D_mD_{r56.67}$ = Mean particle size & relative density at 56.67%

# List of Symbols

$D_mD_{r88.9}$ = Mean particle size & relative density at 88.9%

$D_mD_{r91.13}$ = Mean particle size & relative density at 91.13%

$D_mD_{r71.43}$ = Mean particle size & relative density at 71.43%

$D_mD_{r83.33}$ = Mean particle size & relative density at 83.33%

$D_mD_{r87.88}$ = Mean particle size & relative density at 87.88%

$D_mD_{r92.03}$ = Mean particle size & relative density at 92.03%

$D_mD_{r93.15}$ = Mean particle size & relative density at 93.15%

# Chapter 1

# Introduction

## 1.1 Introduction:-

Most sandy soils have mechanical and hydraulic properties that rapidly deteriorate when exposed to high moisture contents. In some cases, they turn into mud, almost losing completely shear strength; in other cases, they become impervious and prevent water from draining. These synthetic soils have hydraulic and shear strength properties different from those of natural soils. It is well established that soils behave as linear elastic materials at shear strains smaller than about $10^{-4}$–$10^{-3}$% (*Salgado et al. 2000*). For larger shear strains, the stress-strain relationship is nonlinear. Peak shear strength develops at relatively large strains (corresponding typically to axial strains in the range of 1–4%), and critical-state shear strength (corresponding to no volume change during shearing) develops for axial strains (*Schofield & Wroth 1968*). After the Mohr-Coulomb failure criterion is commonly used to describe shear failure in soils, friction angles determined at the peak and critical states can be defined.

The properties of clean sands have been extensively studied under laboratory and field conditions. These include Ottawa, Ticino, and Monterey sands [*Hardin and Richart (1963), Chung et al. (1984), Bolton (1986), Lo Presti (1987), Lo Presti et al. (1992)*]. However, in situ soils often contain significant amounts of plastic & non plastic fines.

The stress-strain response of silty sand at small-, intermediate, and large-strain levels depends upon soil state variables (the relative density $D_r$ of the sand, the effective stress state, and fabric) and other factors related to the nature of the sand (particle shape, particle size distribution, particle surface characteristics, and mineralogy). The factors related to the constitution and general nature of the sand particles are referred to as intrinsic variables [*Been et al. (1991), Salgado et al. (1997a,b)*].

Examples of intrinsic variables are the critical state friction angle $\Phi_c$ , the maximum and minimum void ratio's $e_{max}$ and $e_{min}$, and the dilatancy parameters Q and R of the peak friction angle correlation of *Bolton (1986*).

Past research has debated the effect of non-plastic silt content on the liquefaction behavior of sand. Many studies suggest that liquefaction resistance increases with increasing silt content [*Seed et al. 1983; Tokimatsu and Yoshimi 1983; Robertson and ,Campanella (1985), Seed et al. (1985), Kuerbis et al. (1988), Kuerbis (1989); Pitman et al. (19940, Salgado et al. (2000), Amini and Qi (2000), Polito and Martin (2001)*]. However, other studies conclude that loose silty sands are more prone to liquefaction [*Sladen and Hewitt (1989), Verdugo and Ishihara (1996), Lade and Yamamuro (1997), Yamamuro and Lade (1997), Zlatovic and Ishihara (1997)*]. Silty sand can be deposited into dense configurations that result in more dilatant behavior than clean sand *(Kuerbis 1989*). However, silty sand also has been show to have a greater potential for exhibiting much more volumetrically contractive behavior when deposited in very loose states (*Lade and Yamamuro 1997*).

Knowledge of the values of small-strain stiffness and critical-state and peak friction angles is very useful for applications based on constitutive models or analyses that attempt to capture material response from the initial stages of loading up to shear failure. More immediate application of such knowledge can be made in analyses that rely predominantly on small strain stiffness (such as the design of machine foundations), or on friction angles only (such as stability analyses of various forms, where deformations prior to collapse are not considered) (*Salgado et al. 2000*).

*Yamamuro and Lade (1997, 1998) and Yamamuro and Covert (2001)* concluded that complete static liquefaction (zero effective confining pressure and zero effective stress difference) in laboratory testing is most easily achieved in silty sands at very low pressures. *Kramer and Seed (1988)* also observed that liquefaction resistance increased with increasing confining pressure. Numerous studies [*Oda (1972a), (1972b), Ladd (1974), Mulilis et al. (1977), Tatsuoka et al. (1979), Miura and Toki (1982), Tatsuoka et al. (1986), Zlatovic and Ishihara (1997), Jang and Frost (1998), Vaid et al. (1999), Wood and Yamamuro (1999), Høeg et al. (2000)*] have reported that the behavior of sands can be greatly influenced by specimen reconstitution method. However, experimental data related to the effect of depositional method on the behavior of sand with non-plastic silt content is very limited because most prior studies have focused their efforts on clean sands.

Intrinsic variables are the critical state friction angle, peak state friction angle and the maximum and minimum void ratios $e_{max}$ and $e_{min}$. If the realistic analysis are to be done of soils mechanics problems involving these materials information is needed on their mechanical properties. It is work used to describe the small strains stiffness and the shear strength of clean sands may be used for silty sands, provided that the fines contents remain below some limit.

In this project, we evaluate how the intrinsic variables that appear in co- relation for the small strain stiffness and the shear strength of sands vary with the content of fines.

The critical state model (CSM) we studies a simplification and an idealization of soil behavior [*Schofield, A.N. and Wroth, C.P. (1968)*].CSM captures the behavior of soils that are of greatest importance to geotechnical engineers. CSM is that all soils will fail on a unique failure surface in a space.

CSM is a tool to make estimate of soil responses when you cannot conduct sufficient soils tests to completely characterize a soil at a site or when you have to predict the soil's response from changes in loading during and after construction. Although there is a debate on the application of the CSM to real soils, the ideas behind the CSM are simple.

## 1.2 Objective of the Present Work:-

- To estimate stress strain relations for silty sand
- To estimate volume change behavior of silty sand
- To stimate shear strength parameters (Q & R).

Soils in situ usually possess natural structure, which enables them to behave differently from the same material in a reconstituted state [e.g., *Burland, (1990), Leroueil and Vaughan, (1990), Cuccovillo and Coop, (1999)*]. Recently, there have been important developments in formulating constitutive models incorporating the influence of soil structure, such as those proposed by [*Gens and Nova (1993), Whittle (1993), Wheeler (1997), Rouainia and Wood (2000), and Kavvadas and Amorosi (2000*)]. In this work the constitutive model for silty sand is verified. Since this model is relatively simple and should have few parameters, each of which has a clear physical meaning and can be conveniently implemented. The model is also relatively easy to understand and apply.

# Chapter 2

# Literature Review

Ever since the development in the area of strength of materials, there had been numerous attempts to find out the strength properties of various materials. Prominent among them was that of Mohr (1900) who proposed to evaluate the stresses at a point amid a loaded element. A combination of normal and shear stresses once exceeded a critical value, the material fails. Some of the salient features of the strength theories which were found relevant to the present study are described below:-

## 2.1 Shear Strength:-

The shear strength of a cohesion less soil can be defined by the Mohr-Coulomb failure criterion with zero cohesive intercept,

$$s = б \tan\Phi_c \qquad (1)$$

where,

s = shear strength;

б = normal stress on the plane of shearing; and

$\Phi_c$ = friction angle.

For a tri-axial test, it is practical to write Φ in terms of the principal effective stresses,

$$\sin\Phi = (б`_1 - б`_3) / (б`_1 + б`_3) \qquad (2)$$

where,

$(б`_1 / б`_3)$ = effective principal stress ratio or stress obliquity

Coulomb in the eighteenth century understood that the strength of freshly remolded soils is of frictional nature, hence, stress dependent [*Heyman (1997); Schofield (1998)*]. *Reynolds (1885)* highlighted the tendency of granular materials to change volume when sheared, a fact that was well known by grain dealers at the time. Casagrande (1936) recognized that a critical density divides the tendency to volume change into contractive and dilative behaviors. Later, *Taylor (1948)* showed experimentally that dilatancy is stress dependent, and *Bishop (1950)* expressed the shear strength in terms of friction and dilatancy components. Finally *Schofield and Wroth (1958*) and *Schofield and Wroth (1968)* brought together stress-dependent strength and dilatancy in the unifying structure of critical state soil mechanics within the framework of plasticity theory. Researchers in critical state (CS) soil behavior have generally relied on drained, strain-rate-controlled tests on dilatants specimens to determine the critical state because the critical state strength can be achieved at a relatively low global strain level [*Been et al. (1991*), *Lee(1995*)]. According to the critical-state model, when a loose sample is sheared under high effective confining stress, the shear stress increases monotonically until it reaches a plateau, after which the sample continues to undergo shear straining without any change in shear stress or sample volume. The sample is then said to have reached the critical state, and the corresponding friction angle is known as the critical-state friction angle $\Phi_c$. This material supports structural rafts and deep foundations for multistoried buildings, underground excavations, tunnels and pipelines. There is a need to characterize this granular media as an engineering material. The role of non-plastic silt & plastic silt on the behavior of loose sand is a matter of interest for the engineers. Natural sands contain a significant and varying amount of fines, whereas the current knowledge is primarily based on clean sands [*Attkinson (2007*)]. Silty sands are one of the most common soils which are encountered during construction of footings.

A systematic experimental study is performed of the variation of minimum and maximum void ratios, angle of internal friction with contents of plastic fines for sands. It is shown that the fines content plays an important role in determining the minimum and maximum void ratios, angle of internal friction. Results of the laboratory tests shows that maximum and minimum void ratios of clean sand decreases as fine content increases from 2.9 to 4.3%. Results also indicate that angle of internal friction and bearing capacity decreases on the addition of fines due to compressibility of fines (*Gupta & Trivedi 2009*).

During the shearing of dense sandy soil, the sample contracts initially and then dilates. The effective principal stress ratio reaches a peak, associated with a peak friction angle, at which the dilation rate is maximum. Further incremental loading causes the shear stress to drop until it reaches the critical state. For practical purposes, the critical-state friction angle obtained from tri-axial tests is commonly taken as a unique value for a given granular soil, regardless of the initial relative density and initial confining stress.

The engineering behavior of low-plasticity silts is more difficult to characterize than is the behavior of sand. Due to their tendency to dilate during shear, establishing a consistent and practically useful failure criterion for low-plasticity silts can be very difficult. Consideration of how the un-drained shear strength of silt is related to changes in pore pressure provides a more useful and practical framework for understanding the un-drained strengths of these materials and for characterizing un-drained strengths for practical purposes. Most geotechnical engineers consider the behavior of plastic silts as being somewhere between the behavior of clays at one extreme, and the behavior of sands at the other. If the behavior of sands fell on some continuous spectrum of

gradational change this concept would be useful. This is not the case, always the sands have modes of behavior that are distinctly different in a number of respects, and the concept of somehow interpolating between them does not provide a realistic approach to dealing with the behavior of plastic silts. Non-plastic silts & plastic silts have characteristics in common with both sands and clays. They are more subject to compression by static pressures than sands. In general, a loose silty sand contracts and a dense silty sand expands as it approaches the critical state, usually defined as the state at which the sand is sheared without changes in either shear strength or volume. However, whether a sample of silty sand is contractive or dilatants depend not only on density but also on effective confining stress.

**2.2 Stress – Dilatancy Relations:-**

The data of a typical drained compression test on a dense, cylinderical sample with frictionless ends is required to interpret stress - dilatancy relations. Strains were inferred from boundary displacements and volume changes, and they therefore underestimate the strains in the rupture zone which developed between points (*Salgado et al.2000*). The achievement and accurate determination of the ultimate conditions are considerably hampered by the non-uniformity of the sample and the uncertainty regarding membrane correction following the formation of a rupture plane. Nevertheless such evidence as exists suggests that soil in rupture zones will dilate fully to achieve a critical state, at which shear deformation can continue in the absence of a volume change. The point of peak strength is usually associated with the maximum rate of dilation defined as $(d\varepsilon_1 / d\varepsilon_3)_{max}$ (*Salgado et al.2000, Trivedi 2010*).

It developed his stress-dilatancy theory based on the analogy between irregular packings of soil particles and regular assemblies of spheres or cylinders and on the hypothesis that.

a minimum energy ratio at failure is achieved. It questioned the energy minimization hypothesis made by (*Rowe 1962*), which should not apply to systems that dissipate energy during loading. Rowe's conclusions through an analysis that does not rely on energy minimization assumptions The resulting stress-dilatancy theory, superior to all other attempts to relate shear strength to dilation, can be best expressed in the form expressly (*Salgado et al. 2000*),

$$N = M.N_c \qquad (3)$$

Where,

N = flow number = $б_1 / б_3$ = stress obliquity

$N_c$ = critical-state flow number = $(б`_1/ б`_3)_c$ = stress obliquity at critical state

M = dilatancy number = $1- dε_v /dε_1$

$dε_v$ = volumetric strain increment

$dε_1$= major principal strain increment = axial strain increment in tri-axial compression tests. N, M, and $N_c$ are given in terms of Φ, $Φ_c$ and ψ by the following expressions:

$$N = (1 + \sin\Phi) / (1 - \sin\Phi) = \tan^2(45 + \Phi/2) \qquad (4)$$

$$N_c = (1 + \sin\Phi_c) / (1 - \sin\Phi_c) = \tan^2(45 + \Phi_c/2) \qquad (5)$$

$$M = (1 + \sin\psi) / (1 - \sin\psi) = \tan^2(45 + \psi/2) \qquad (6)$$

The dilatancy angle, in turn, is defined as

$$\sin\psi = (d\varepsilon_1 / k.d\varepsilon_3 + 1) / (d\varepsilon_1 / k.d\varepsilon_3 - 1) \quad (7)$$

Where,

$d\varepsilon_1$ and $d\varepsilon_3$ = principal strain increments; k = 1 for plane strain; and k = 2 for tri-axial test conditions.

**2.3 Dilatancy Index:-**

The extra angle of shearing of 'dense' soil is correlated to its rate of dilation and thence to its relative density and mean effective stress, combined in a new relative dilatancy index. Research on the shear strength of sands for practical applications has two main branches: the first one focuses on the prediction of the peak friction angle of dilating sands, while the second one focuses on the prediction of un-drained shear strength of loose sands. Pressure and void ratio dependence of shear strength is acknowledged for in both research fields. For drained shear, there are some outstanding contributions [*de Beer (1965), Lee & Seed (1967), Marsal (1967), Bolton (1986) Maeda & Miura (1999a), Maeda & Miura (1999b*)]. For un-drained shear, main contributions are [*Castro (1975), Castro & Poulos (1977), Poulos (1981), Been & Jefferies (1985), Been et al (1991), Ishihara (1993), Verdugo & Ishihara (1996)*]. For drained shear of dilating sands, it is a common practice to compute the peak friction angle $\Phi$ as the sum of the critical state friction angle $\Phi_c$ and a dilatancy term $\psi$ which in turn depends on void ratio e and effective mean pressure p.

*Bolton (1986*) reviewed a large number of tri-axial and plane-strain test results for 17 clean sand and proposed a much simpler relationship between $\Phi$, $\Phi_c$ and $\psi$ which he found to be operationally equivalent as (*Parry, 1995*)

$$\Phi = \Phi_c + 0.8\psi \quad (8)$$

The relationship between the peak friction angle $\Phi_p$ and the critical-state friction angle $\Phi_c$ can be written for both tri-axial and plane-strain test. So that the dilatancy angles for both types of test are expressed in terms of the same quantity $I_R$, referred to as the dilatancy index,

$$\Phi_p = \Phi_c + 5I_R \qquad (9)$$

for plane-strain conditions,

$$\Phi_p = \Phi_c + 3I_R \qquad (10)$$

for tri-axial conditions,

$$I_R = D_r\ (Q - \ln 100p`_p / P_A) - R \qquad (11)$$

Where

$D_r$ = relative density expressed as a number between 0 and 1

$P`_p$ = mean effective stress at peak strength

$P_A$ = reference stress (=100 kPa = 0.1 N/mm$^2$) in the same units as $p`_p$

Q and R = fitting parameters.

Eqs. (9) and (10) are valid for $0 \leq I_R \leq 4$. For higher values of $I_R$ the value of the peak friction angle is taken as the value calculated from (9) or (10) with $I_R = 4$.

# Chapter 3

# Experimental Procedures

## 3.1 Material Used:-

The silty sand and clean sand were procured from the beds of river at Wazirabad Bridge.

## 3.2 Material Properties:-

The shear strength of sand may be expressed in terms of a number of intrinsic parameters ($\Phi_c$, Q and R) (*Bolton 1986*). The intrinsic parameters are a function of the nature of sand and thus changes with fines content for a given soil density. A series of tri-axial tests were performed to assess how the shear strength of sand changes as an increasing percent of low plastic fines is prepared. In order to explain the effect of fines on the behavior of clean sand, an experimental program was developed. The experimental study was carried out for fine content in the range of 2.9 to 4.3%. A series of tri-axial shear tests, relative density tests and model plate load test were performed to assess the effect of fine content on angle of internal friction, minimum and maximum void ratios of clean sand.

The effective size ($D_{10}$), the mean grain size ($D_{50}$), coefficient of uniformity ($C_u$), and coefficient of curvature ($C_c$) are calculated. A summary of the experimental program is given in Table (01), (02) & (03). The Sand after washing on 75 micron sieve, the coarser fraction is used for the testing. The coefficient of uniformity & curvature fo clean sand **$C_u$ is 1.67 & $C_c$ is 0.86**, and the mean grain size **$D_{50}$ is 0.25mm.** The maximum and minimum void ratio's of clean sand are $e_{max}$ and $e_{min}$ are **0.78 and 0.50**. Its specific gravity of silt and sand is **2.63** & **2.67**. The liquid limit and plastic limit are **25% &14%**.

**Table 01(a): Characterization of silty sand**

| Sample | $D_{10}$(mm) | $D_{30}$(mm) | $D_{50}$(mm) | $D_{60}$(mm) | $C_c$ | $C_u$ |
|---|---|---|---|---|---|---|
| A | 0.152 | 0.184 | 0.256 | 0.27 | 0.825 | 1.776 |
| B | 0.139 | 0.178 | 0.224 | 0.265 | 0.860 | 1.906 |
| C | 0.122 | 0.173 | 0.219 | 0.26 | 0.944 | 2.131 |
| D | 0.1 | 0.167 | 0.211 | 0.254 | 1.098 | 2.540 |
| E | 0.093 | 0.153 | 0.209 | 0.25 | 1.007 | 2.688 |
| F | 0.09 | 0.15 | 0.201 | 0.246 | 1.016 | 2.733 |

The sample depositional methods are as:-

- **Slurry Deposition:-**

The slurry deposition (SD) method used in this study was similar to that presented by [*Kuerbis and Vaid (1988) and Kuerbis (1989*)]. To ensure full saturation, the sand sample was boiled the night before testing, similar to the water sedimentation technique. Rather than depositing the soil directly into the split mold, it first was placed into a mixing container, where it was thoroughly mixed before being deposited into the mold. The soil and mixing container is inserted into the mold and then the mixing container is extracted leaving the soil in place.

- **Mixed Dry Deposition:-**

Mixed dry deposition (MDD) is very similar to slurry deposition, except that the soil is prepared and deposited in a dry state.

- **Air Pluviation:-**

Specimens reconstituted by air pluviation (AP) were formed by raining sand through a dispersing screen at the top of a long tube with an equivalent inside diameter to the split mold (101mm). The tube was placed on top of the split mold extension, which rested on the split mold. A variation in drop height often is used to create specimens of different

densities [*Miura and Toki (1982), Vaid and Negussey (1984b), (1988), Rad and Tumay (1987*)]. In order to form a specimen of uniform density, *Vaid and Negussey (1984b*) suggested that the fall height should remain constant with the top of the specimen as it is formed.

### 3.3 Advantages of Slurry deposition method:-

To obtain the homogenous sample, the slurry deposition method of *Kuerbis and Vaid (1988)* was appropriate. This method has the following advantages:-

1. This method produces loose to dense samples in the commonly observed density ranges of in situ soils.

2. The samples are easy to saturate.

3. The samples have a homogenous fabric and fairly uniform void ratio throughout.

4. There is no particle segregation, regardless of gradation of fines content.

5. The method simulates the natural soil deposition mode and is easy to duplicate.

### 3.4 Preparation of Samples:-

The samples were prepared by first estimating the weights of sand needed for desired fines content. There amounts of sand were mixed in cylindrical Plexiglas tube completely filled with de-aired water. The sands are thoroughly mixed by vigorous shaking of Plexiglas tube for approximately 10 minutes to achieve sample uniformity. After that, the cap of Plexiglas tube is removed, a very small amount of de-aired water is added to raise the water level back to the top of the tube and tube is topped with a high density polythene film.

The tube containing the slurry is quickly inverted and positioned inside the tri-axial sample spilt mould, where a stretched, thin membrane completely filled with de aired water is already in place. The contents of the tubes are released in to the membrane by raising the tube. Densification of the sample is accomplished by carefully and symmetrically tapping the sides of the sample mould immediately after the slurry deposition. Because the mass of sand is used in sample can be accurately estimated.

The testing apparatus used to perform the tests is automatic tri-axial testing system (Soil engineering equipment). A load cell to measure the axial load without any piston friction is located inside the pressure chamber. The axial strain was measured locally using high resolution submergible LVDTs, and externally. The details of the test apparatuses were described by [*Fioravante et al. (1994b), Jamiolkowski et al. (1994b), and Lo Presti et al. (1994)*]. Ninety tests on Yamuna sand were performed at the Swati Structure Solutions Pvt. Ltd. New Delhi. The axial strain was measured along with volume changes the majority of the silty sand tests.

**3.5 Procedures:-**

Dry sample:-

a) Put the non-porous cap on the bottom pedestal and the rubber membrane slid over it and tie it with the bottom pedestal of the base O-ring.

b) Put the split mould over the base and the rubber membrane taking through it inside and stretch over it at the top.

c) Weigh the soil in dish to make a sample of required dry density.

d) For loose dry samples, allow the soil to fall freely and rapidly from a tunnel. For dense samples pour the soil in the mould in layers and compact it by the tamping without rupturing the membrane.

e) The sample was allowed to saturate for 10 min and a confining pressure applied during loading.

f) Operate the vacuum pump and carefully remove the mould without jarring the sample.

g) Assemble the cell and fill it with water to exert a confining pressure.

h) Raise the loading plat-form of the compression machine to bring the ram in contact with the loading cap.

i) Set the dial gauge on proving ring to zero to compensate for the load due to cell pressure and piston friction.

j) Take 25 readings of the proving ring at interval of 25 divisions till sample fails or 20% strain is achieved.

k) Repeat the test for higher cell pressure such as 100,150,200,300 and 400 kPa.

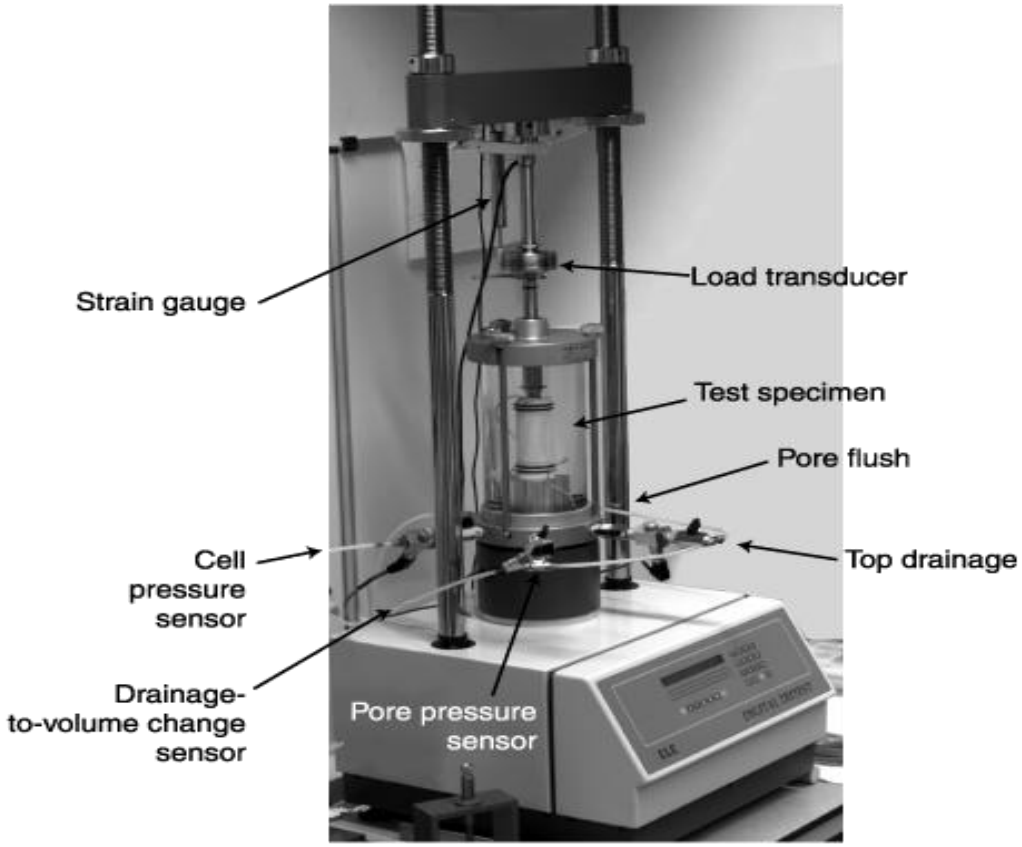


Figure A: Typical tri-axial test apparatus (http://www.geotechdata.info/geotest/triaxial-test)

# Chapter 4

# Project Sample Pictures


Figure B: Tri–axial testing (during loading)

Figure C: Tri–axial testing (picture at the failure of sample)

# Chapter 5

# Analysis of Results

In order to analysis the results the following sections and formulae were used:-

## 5.1 Void Ratio:-

The maximum and minimum void ratios were determined by using the following relations:

$$e_{max} = [(G.\gamma_w / \gamma_{min}) - 1] \quad (13)$$

$$e_{min} = [(G.\gamma_w / \gamma_{max}) - 1] \quad (14)$$

where,

G = specific gravity of sand

$\gamma_w$ = unit weight of water

$\gamma_{min}$ = minimum dry density

$\gamma_{max}$ = maximum dry density

The value of $\gamma_{min}$ and $\gamma_{max}$ were determined as per the IS: 2720-part 14. Form the above value of $\gamma_{min}$ and $\gamma_{max}$ and the relative densities. The value of $\gamma_n$ was calculated as follows:-

$$D_r = [\gamma_{max} (\gamma_n - \gamma_{min})] / [\gamma_n (\gamma_{max} - \gamma_{min})] \text{ x}100 \quad (15)$$

From the values of $\gamma_n$ obtained from above void ratio at $\gamma_d$ also calculated:

$$e = [(G.\gamma_w / \gamma_n) - 1] \quad (16)$$

### 5.2 Peak and Critical State Shear Strength:-

The peak and critical- state friction angles are obtained according to,

$$\sin\Phi = (б`_1 - б`_3) / (б`_1 + б`_3)$$

where,

$(б`_1 / б`_3)$ = effective principal stress ratio or stress obliquity

#### 5.2.1 Critical State:-

Critical state is defined as that where the shear stress and volume change are constant with increasing shear strain (*Attkinson 2007)*

The critical state friction angle is given as,

$$\sin\Phi_c = (б_1 - б_3)_c / (б_1 + б_3)_c \qquad (17)$$

where,

$(б_1 / б_3)_c$ = effective principal stress ratio at critical state,

Similarly peak state friction angle given as:

$$\sin\Phi_p = (б_1 - б_3)_p / (б_1 + б_3)_p \qquad (18)$$

where,

$(б_1 / б_3)_p$ = effective principal stress ratio at peak state

## 5.3 List of Tables:-

**Table 01(b): Consolidated drained test data sheet**

| Sample | Confining Pressure ($б_3$) (kPa) | Diameter (D) (mm) | Length (L) (mm) | Area (A) ($mm^2$) | Volume (V)($mm^3$) |
|---|---|---|---|---|---|
| Yamuna Sand | 100kPa | 38 | 78 | 1134 | 85058.6 |
| Yamuna Sand | 200kPa | 38 | 78 | 1134 | 85058.6 |
| Yamuna Sand | 400kPa | 38 | 78 | 1134 | 85058.6 |

**Table 02: Work program for tri-axial test**

| Nomenclature | Total Tests | Accepted Results | Silt (%) | $\sigma_3$(kPa) | P`$_p$(kPa) |
|---|---|---|---|---|---|
| $D_m^{0.256}D_{r39.3}$ | 3 | 1 | 2.9 | 100 | 147 |
| $D_m^{0.256}D_{r39.3}$ | 3 | 1 | 2.9 | 200 | 293 |
| $D_m^{0.256}D_{r39.3}$ | 3 | 1 | 2.9 | 400 | 563 |
| $D_m^{0.224}D_{r46.67}$ | 2 | 1 | 3.2 | 100 | 155 |
| $D_m^{0.224}D_{r46.67}$ | 2 | 1 | 3.2 | 200 | 294 |
| $D_m^{0.224}D_{r46.67}$ | 1 | 1 | 3.2 | 400 | 538 |
| $D_m^{0.219}D_{r23.33}$ | 2 | 1 | 3.3 | 100 | 186 |
| $D_m^{0.219}D_{r23.33}$ | 2 | 1 | 3.3 | 200 | 303 |
| $D_m^{0.219}D_{r323.33}$ | 2 | 1 | 3.3 | 400 | 622 |
| $D_m^{0.211}D_{r20}$ | 2 | 1 | 3.4 | 100 | 134 |
| $D_m^{0.211}D_{r20}$ | 2 | 1 | 3.4 | 200 | 294 |
| $D_m^{0.211}D_{r20}$ | 2 | 1 | 3.4 | 400 | 573 |
| $D_m^{0.209}D_{r16.67}$ | 3 | 1 | 3.6 | 100 | 145 |
| $D_m^{0.209}D_{r16.67}$ | 3 | 1 | 3.6 | 200 | 286 |
| $D_m^{0.209}D_{r16.67}$ | 2 | 1 | 3.6 | 400 | 507 |

| | | | | | |
|---|---|---|---|---|---|
| $D_m^{0.201}D_{r71.43}$ | 2 | 1 | 4.3 | 100 | 182 |
| $D_m^{0.201}D_{r71.43}$ | 2 | 1 | 4.3 | 200 | 294 |
| $D_m^{0.201}D_{r71.43}$ | 2 | 1 | 4.3 | 400 | 497 |
| $D_m^{0.256}D_{r60.7}$ | 1 | 1 | 2.9 | 100 | 159 |
| $D_m^{0.256}D_{r60.7}$ | 1 | 1 | 2.9 | 200 | 306 |
| $D_m^{0.256}D_{r60.7}$ | 1 | 1 | 2.9 | 400 | 609 |
| $D_m^{0.224}D_{r63.33}$ | 1 | 1 | 3.2 | 100 | 186 |
| $D_m^{0.224}D_{r63.33}$ | 1 | 1 | 3.2 | 200 | 293 |
| $D_m^{0.224}D_{r63.33}$ | 1 | 1 | 3.2 | 400 | 529 |
| $D_m^{0.219}D_{r40}$ | 1 | 1 | 3.3 | 100 | 175 |
| $D_m^{0.219}D_{r40}$ | 1 | 1 | 3.3 | 200 | 317 |
| $D_m^{0.219}D_{r40}$ | 1 | 1 | 3.3 | 400 | 564 |
| $D_m^{0.211}D_{r43.33}$ | 1 | 1 | 3.4 | 100 | 129 |
| $D_m^{0.211}D_{r43.33}$ | 1 | 1 | 3.4 | 200 | 285 |
| $D_m^{0.211}D_{r43.33}$ | 1 | 1 | 3.4 | 400 | 585 |
| $D_m^{0.209}D_{r36.67}$ | 1 | 1 | 3.6 | 100 | 186 |
| $D_m^{0.209}D_{r36.67}$ | 4 | 1 | 3.6 | 200 | 280 |
| $D_m^{0.209}D_{r36.67}$ | 4 | 1 | 3.6 | 400 | 497 |
| $D_m^{0.201}D_{r83.33}$ | 4 | 1 | 4.3 | 100 | 182 |
| $D_m^{0.201}D_{r83.33}$ | 3 | 1 | 4.3 | 200 | 295 |
| $D_m^{0.201}D_{r83.33}$ | 3 | 1 | 4.3 | 400 | 535 |
| $D_m^{0.256}D_{r75}$ | 3 | 1 | 2.9 | 100 | 220 |
| $D_m^{0.256}D_{r75}$ | 3 | 1 | 2.9 | 200 | 302 |
| $D_m^{0.256}D_{r75}$ | 1 | 1 | 2.9 | 400 | 586 |
| $D_m^{0.224}D_{r70.02}$ | 2 | 1 | 3.2 | 100 | 181 |
| $D_m^{0.224}D_{r70.02}$ | 2 | 1 | 3.2 | 200 | 306 |
| $D_m^{0.224}D_{r70.02}$ | 2 | 1 | 3.2 | 400 | 580 |
| $D_m^{0.219}D_{r66.67}$ | 2 | 1 | 3.3 | 100 | 192 |
| $D_m^{0.219}D_{r66.67}$ | 2 | 1 | 3.3 | 200 | 329 |
| $D_m^{0.219}D_{r66.67}$ | 3 | 1 | 3.3 | 400 | 559 |
| $D_m^{0.211}D_{r66.67}$ | 1 | 1 | 3.4 | 100 | 134 |
| $D_m^{0.211}D_{r66.67}$ | 1 | 1 | 3.4 | 200 | 303 |
| $D_m^{0.211}D_{r66.67}$ | 1 | 1 | 3.4 | 400 | 599 |
| $D_m^{0.209}D_{r56.67}$ | 1 | 1 | 3.6 | 100 | 175 |
| $D_m^{0.209}D_{r56.67}$ | 3 | 1 | 3.6 | 200 | 285 |
| $D_m^{0.209}D_{r56.67}$ | 3 | 1 | 3.6 | 400 | 524 |
| $D_m^{0.201}D_{r87.88}$ | 4 | 1 | 4.3 | 100 | 162 |
| $D_m^{0.201}D_{r87.88}$ | 4 | 1 | 4.3 | 200 | 290 |
| $D_m^{0.201}D_{r87.88}$ | 4 | 1 | 4.3 | 400 | 537 |

| | | | | | |
|---|---|---|---|---|---|
| $D_m^{0.256}D_{r85.7}$ | 2 | 1 | 2.9 | 100 | 177 |
| $D_m^{0.256}D_{r85.7}$ | 3 | 1 | 2.9 | 200 | 307 |
| $D_m^{0.256}D_{r85.7}$ | 1 | 1 | 2.9 | 400 | 589 |
| $D_m^{0.224}D_{r76.54}$ | 1 | 1 | 3.2 | 100 | 185 |
| $D_m^{0.224}D_{r76.54}$ | 2 | 1 | 3.2 | 200 | 310 |
| $D_m^{0.224}D_{r76.54}$ | 2 | 1 | 3.2 | 400 | 584 |
| $D_m^{0.219}D_{r75.23}$ | 3 | 1 | 3.3 | 100 | 196 |
| $D_m^{0.219}D_{r75.23}$ | 2 | 1 | 3.3 | 200 | 332 |
| $D_m^{0.219}D_{r75.23}$ | 1 | 1 | 3.3 | 400 | 564 |
| $D_m^{0.211}D_{r75.23}$ | 3 | 1 | 3.4 | 100 | 167 |
| $D_m^{0.211}D_{r75.23}$ | 2 | 1 | 3.4 | 200 | 304 |
| $D_m^{0.211}D_{r75.23}$ | 2 | 1 | 3.4 | 400 | 603 |
| $D_m^{0.209}D_{r88.9}$ | 1 | 1 | 3.6 | 100 | 184 |
| $D_m^{0.209}D_{r88.9}$ | 1 | 1 | 3.6 | 200 | 293 |
| $D_m^{0.209}D_{r88.9}$ | 1 | 1 | 3.6 | 400 | 541 |
| $D_m^{0.201}D_{r92.03}$ | 1 | 1 | 4.3 | 100 | 175 |
| $D_m^{0.201}D_{r92.03}$ | 2 | 1 | 4.3 | 200 | 302 |
| $D_m^{0.201}D_{r92.03}$ | 2 | 1 | 4.3 | 400 | 540 |
| $D_m^{0.256}D_{r89.3}$ | 3 | 1 | 2.9 | 100 | 179 |
| $D_m^{0.256}D_{r89.3}$ | 2 | 1 | 2.9 | 200 | 310 |
| $D_m^{0.256}D_{r89.3}$ | 3 | 1 | 2.9 | 400 | 594 |
| $D_m^{0.224}D_{r82.32}$ | 1 | 1 | 3.2 | 100 | 190 |
| $D_m^{0.224}D_{r82.32}$ | 4 | 1 | 3.2 | 200 | 312 |
| $D_m^{0.224}D_{r82.32}$ | 2 | 1 | 3.2 | 400 | 591 |
| $D_m^{0.219}D_{r82.67}$ | 2 | 1 | 3.3 | 100 | 199 |
| $D_m^{0.219}D_{r82.67}$ | 2 | 1 | 3.3 | 200 | 338 |
| $D_m^{0.219}D_{r82.67}$ | 2 | 1 | 3.3 | 400 | 570 |
| $D_m^{0.211}D_{r83.45}$ | 3 | 1 | 3.4 | 100 | 172 |
| $D_m^{0.211}D_{r83.45}$ | 1 | 1 | 3.4 | 200 | 308 |
| $D_m^{0.211}D_{r83.45}$ | 1 | 1 | 3.4 | 400 | 608 |
| $D_m^{0.209}D_{r91.13}$ | 1 | 1 | 3.6 | 100 | 189 |
| $D_m^{0.209}D_{r91.13}$ | 1 | 1 | 3.6 | 200 | 297 |
| $D_m^{0.209}D_{r91.13}$ | 2 | 1 | 3.6 | 400 | 544 |
| $D_m^{0.201}D_{r93.15}$ | 2 | 1 | 4.3 | 100 | 183 |
| $D_m^{0.201}D_{r93.15}$ | 2 | 1 | 4.3 | 200 | 303 |
| $D_m^{0.201}D_{r93.15}$ | 1 | 1 | 4.3 | 400 | 554 |
| **Total** | **180** | **90** | - | - | - |

## 5.4 List of Figures:-

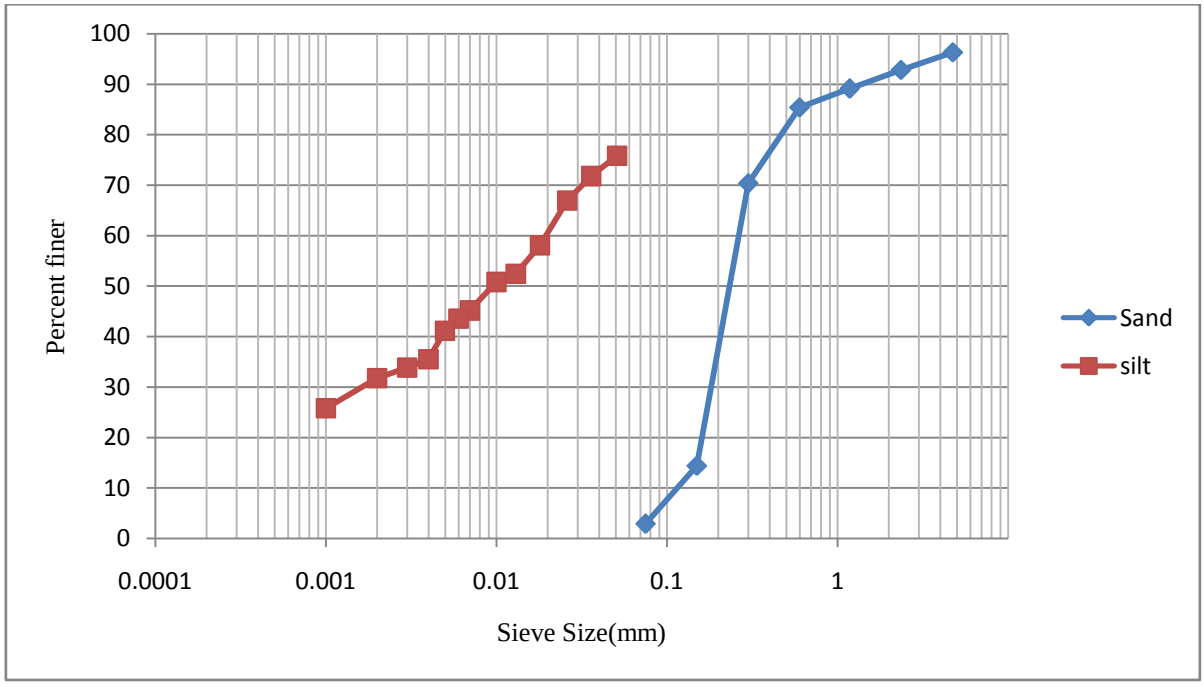


Figure D: Sieve Size v/s Percent finer (Sand &Silt characterization)

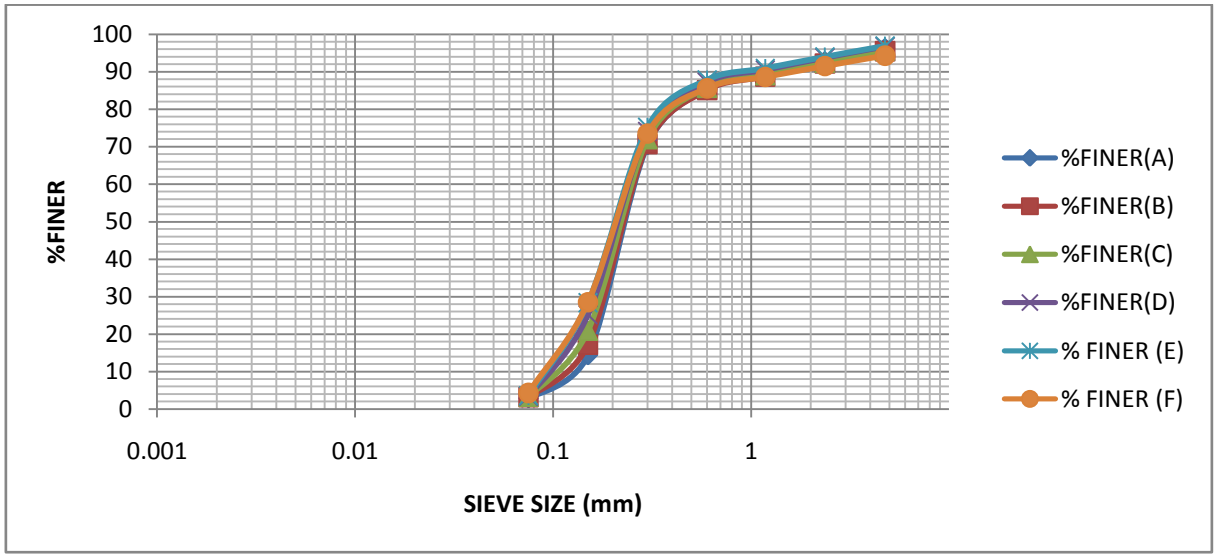


Figure E: Grain Size Analysis

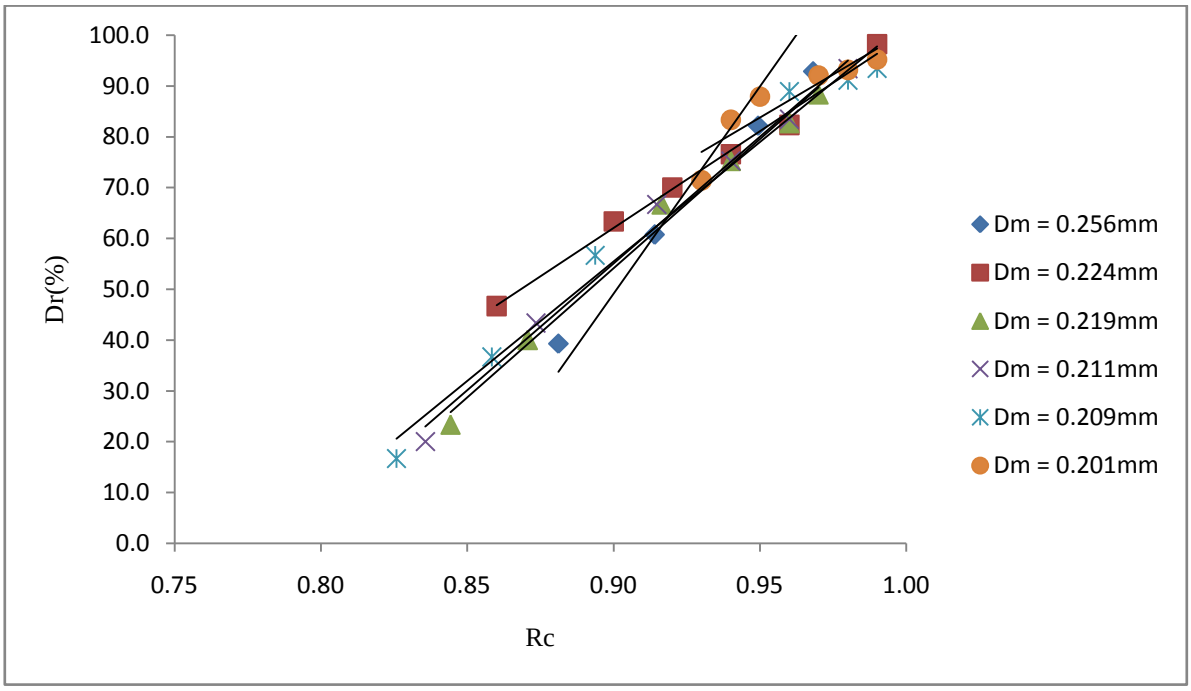


Figure F: $R_c$ v/s $D_r$

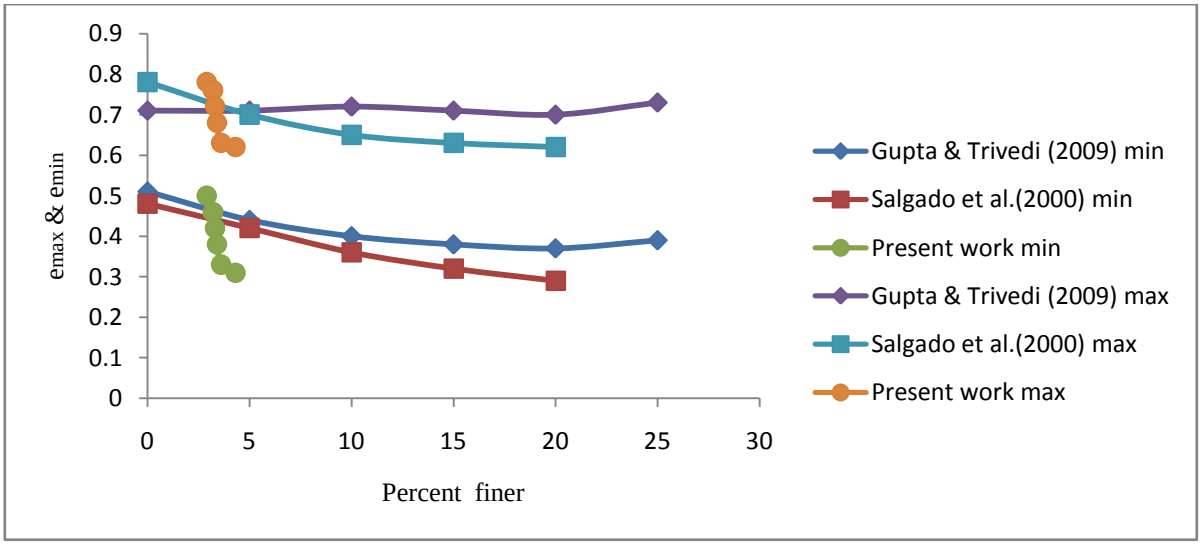


Figure G: Percent finer v/s $e_{max}$ & $e_{min}$

Axial Strain v/s Deviator Stress & Volumetric Strain

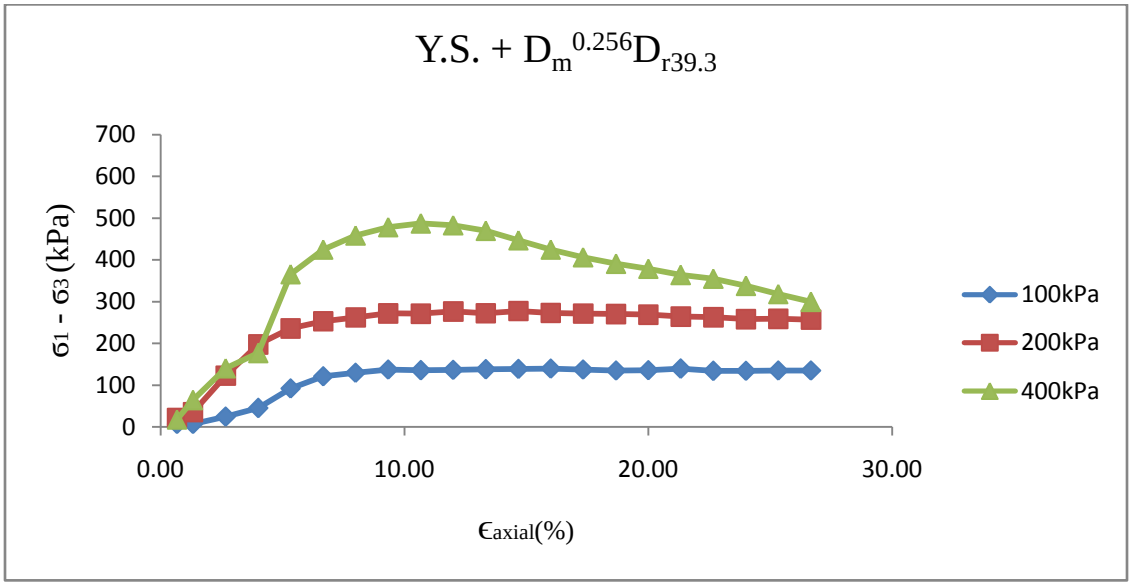


Figure 01(a): Axial Strain v/s Deviator Stress

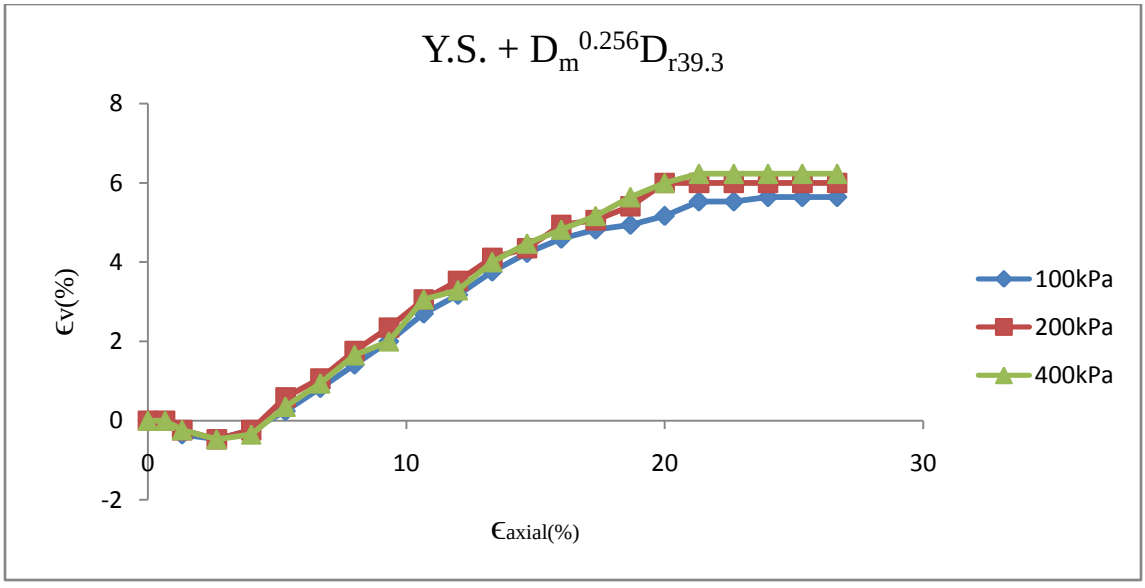


Figure 01(b): Axial Strain v/s Volumetric Strain

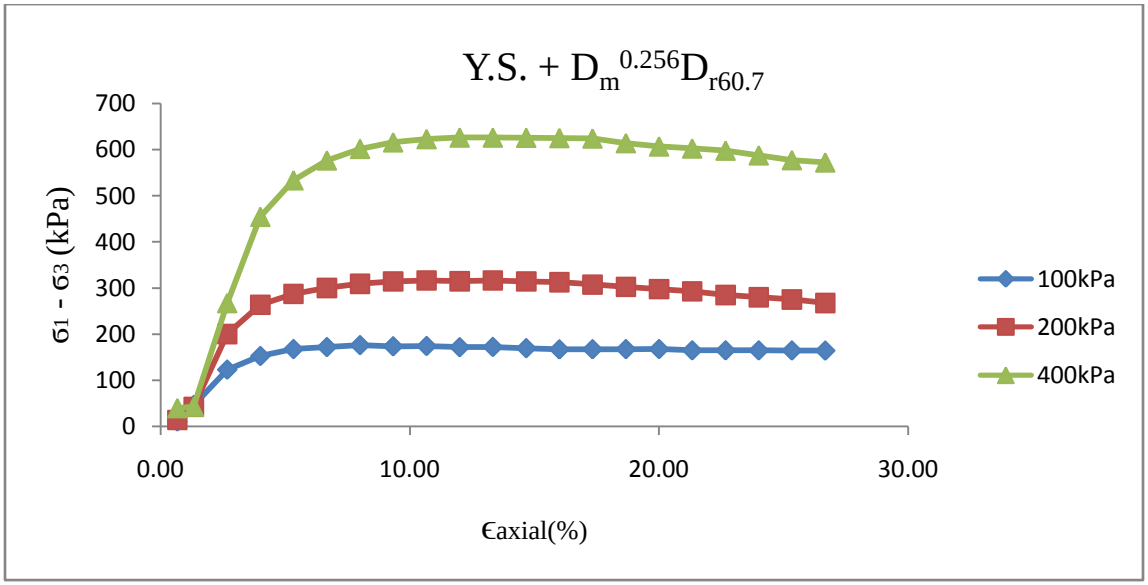


Figure 02(a): Axial Strain v/s Deviator Stress

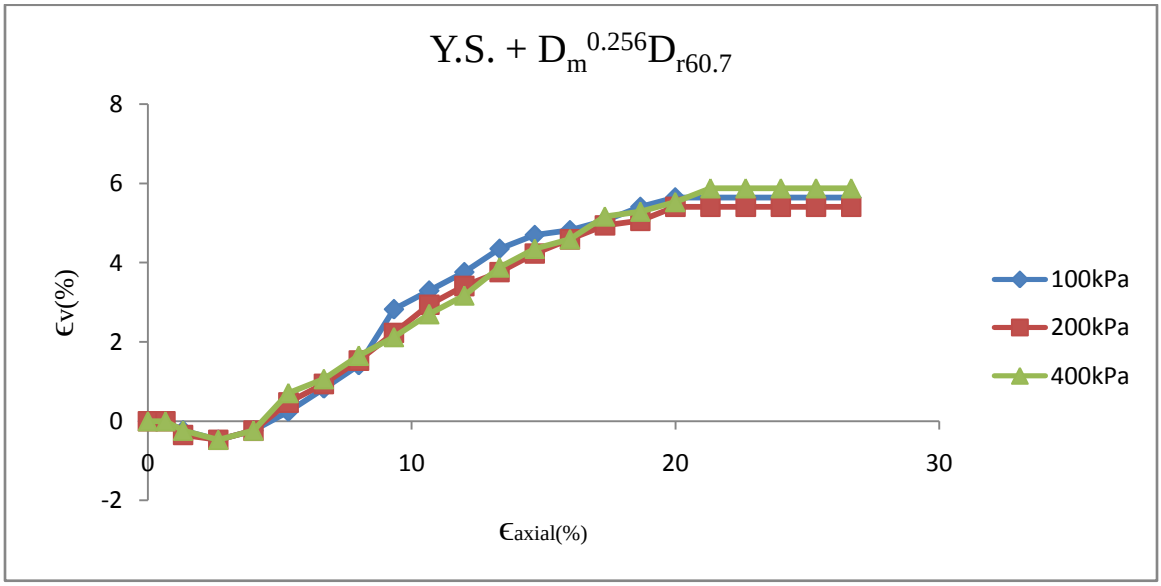


Figure 02(b): Axial Strain v/s Volumetric Strain

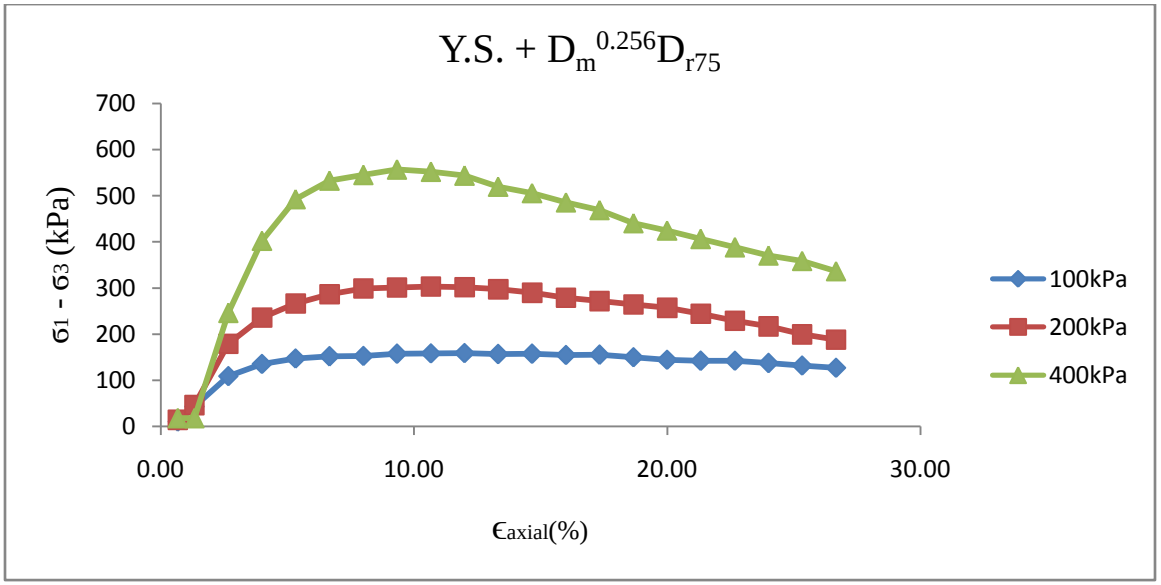


Figure 03(a): Axial Strain v/s Deviator Stress

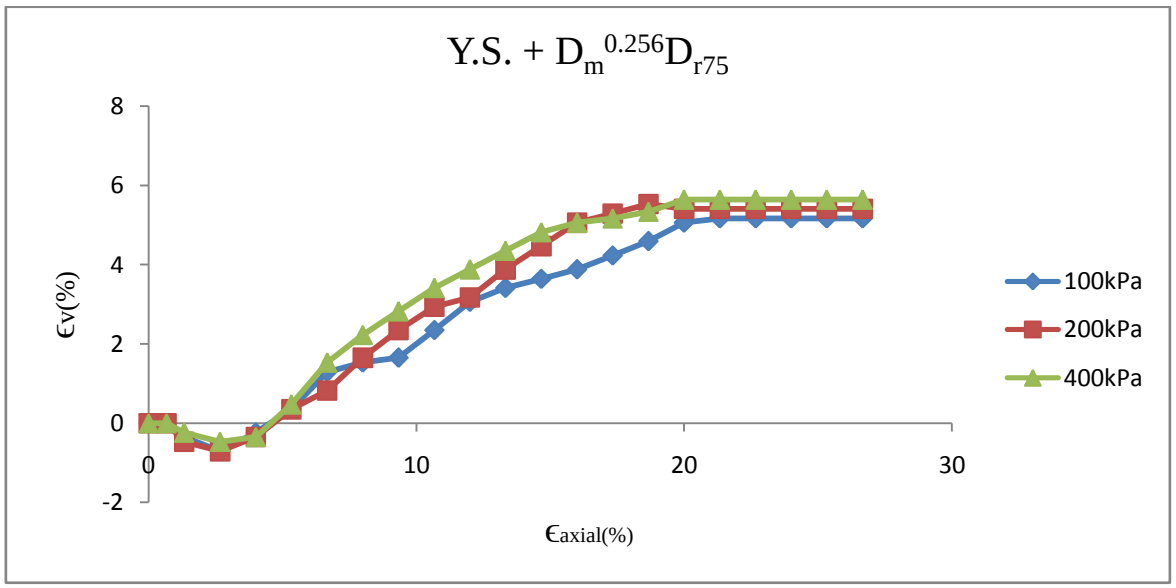


Figure 03(b): Axial Strain v/s Volumetric Strain

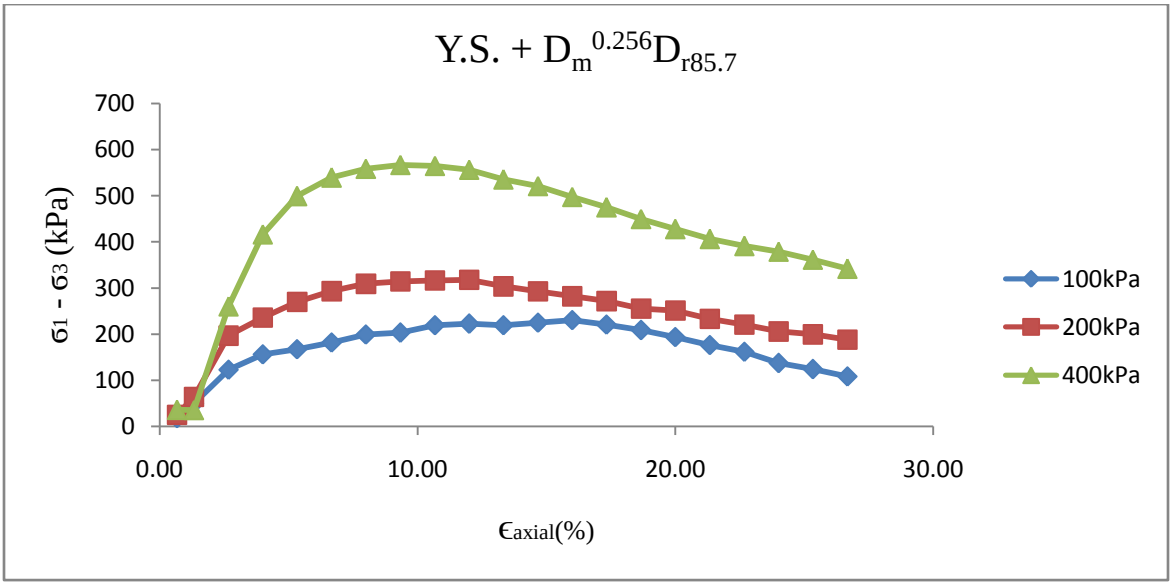


Figure 04(a): Axial Strain v/s Deviator Stress

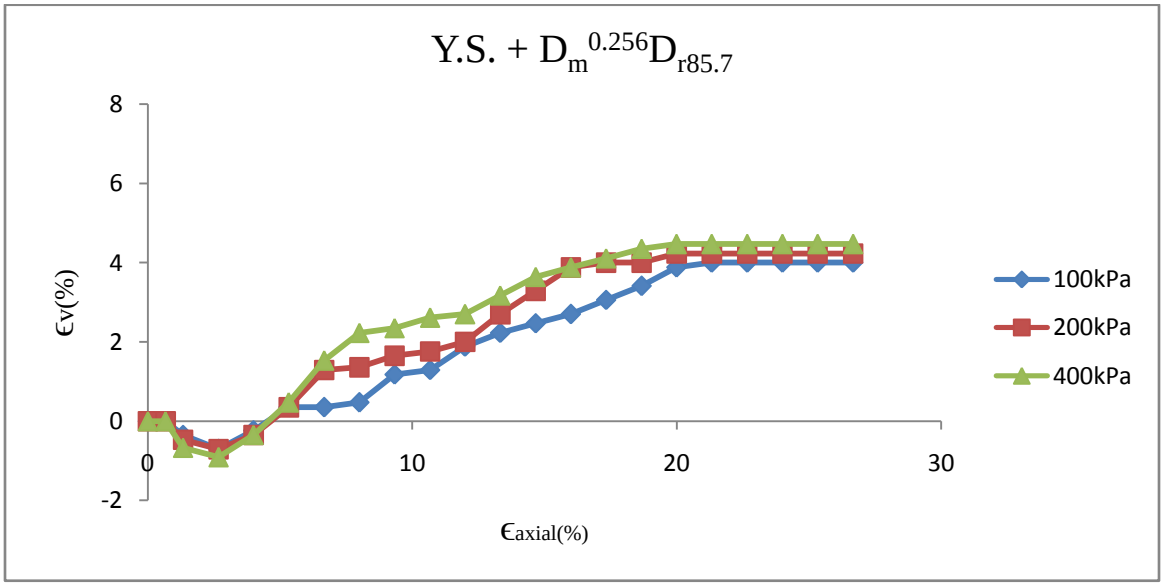


Figure 04(b): Axial Strain v/s Volumetric Strain

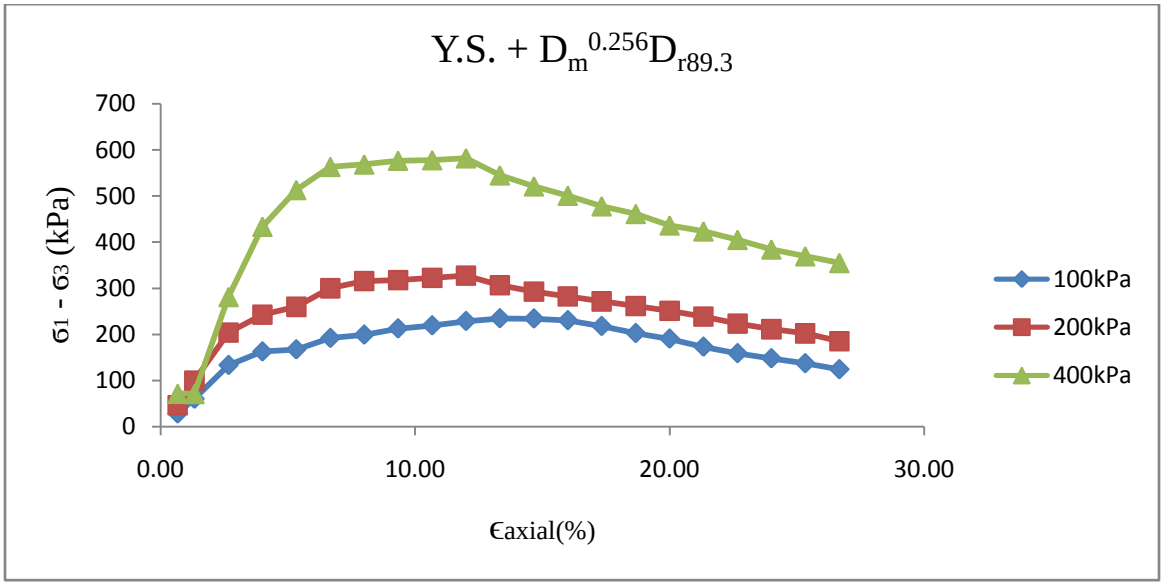


Figure 05(a): Axial Strain v/s Deviator Stress

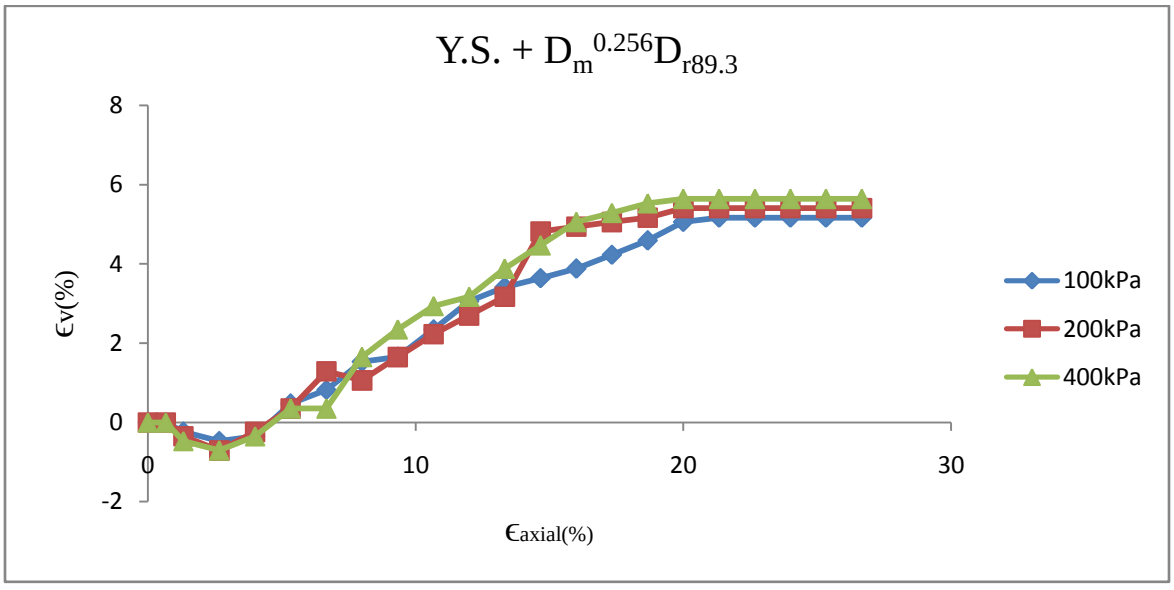


Figure 05(b): Axial Strain v/s Volumetric Strain

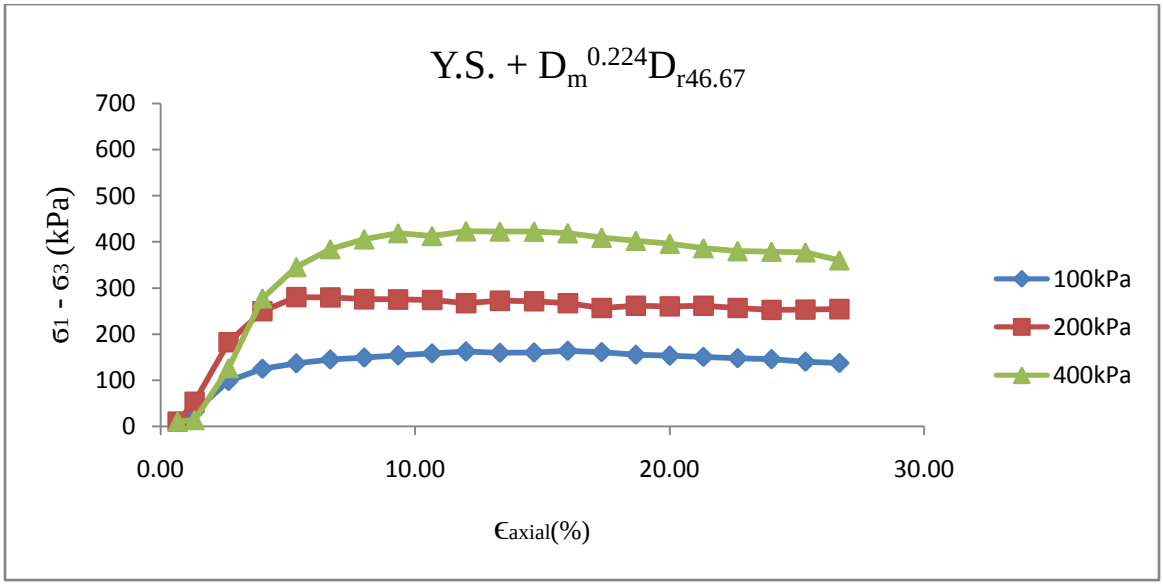


Figure 06(a): Axial Strain v/s Deviator Stress

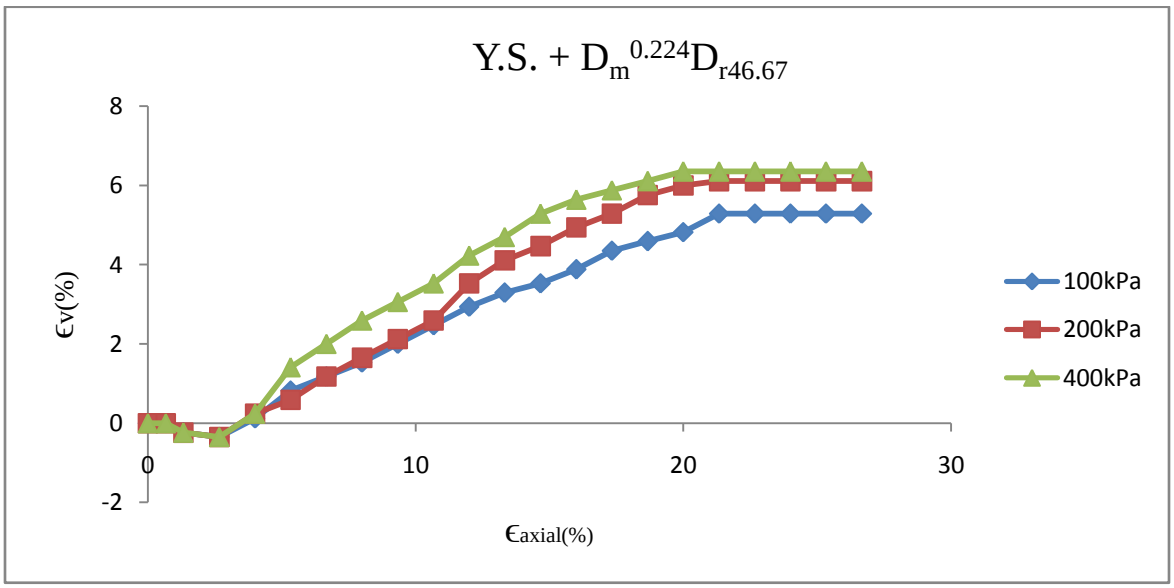


Figure 06(b): Axial Strain v/s Volumetric Strain

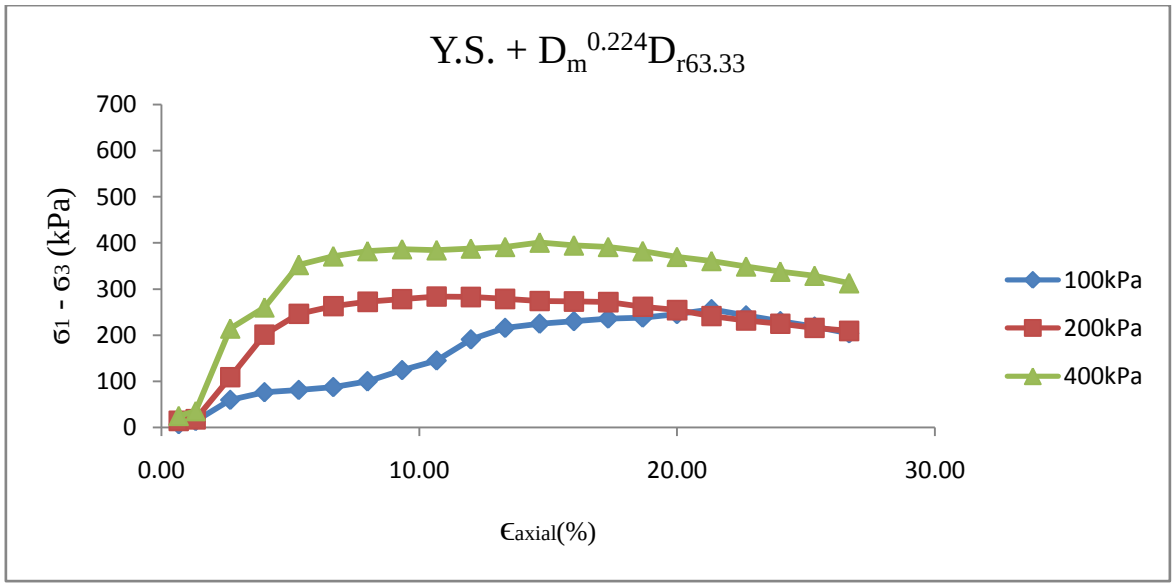


Figure 07(a): Axial Strain v/s Deviator Stress

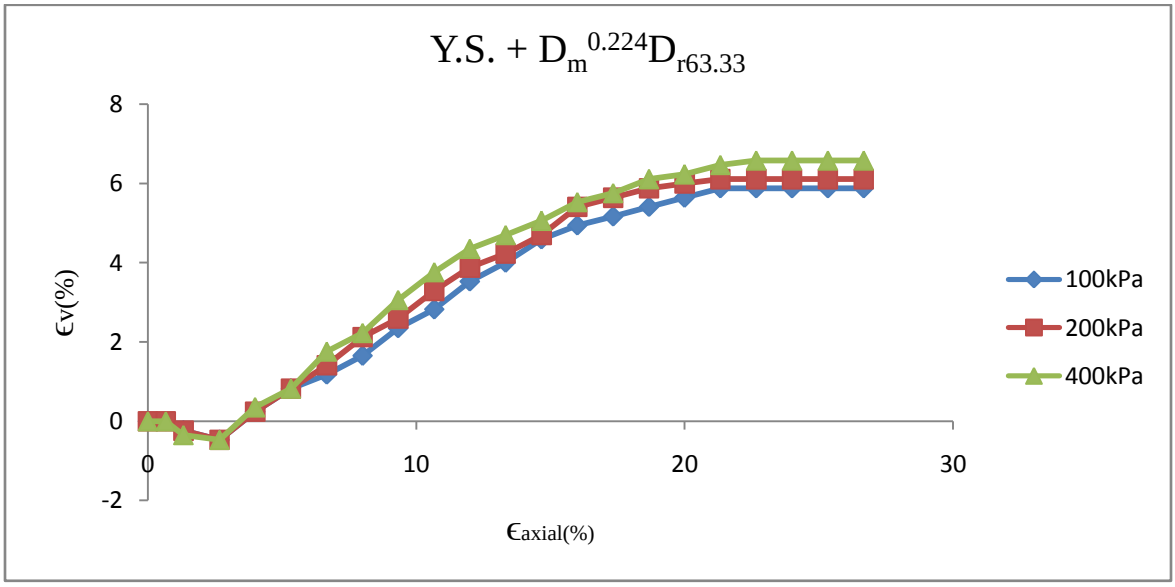


Figure 07(b): Axial Strain v/s Volumetric Strain

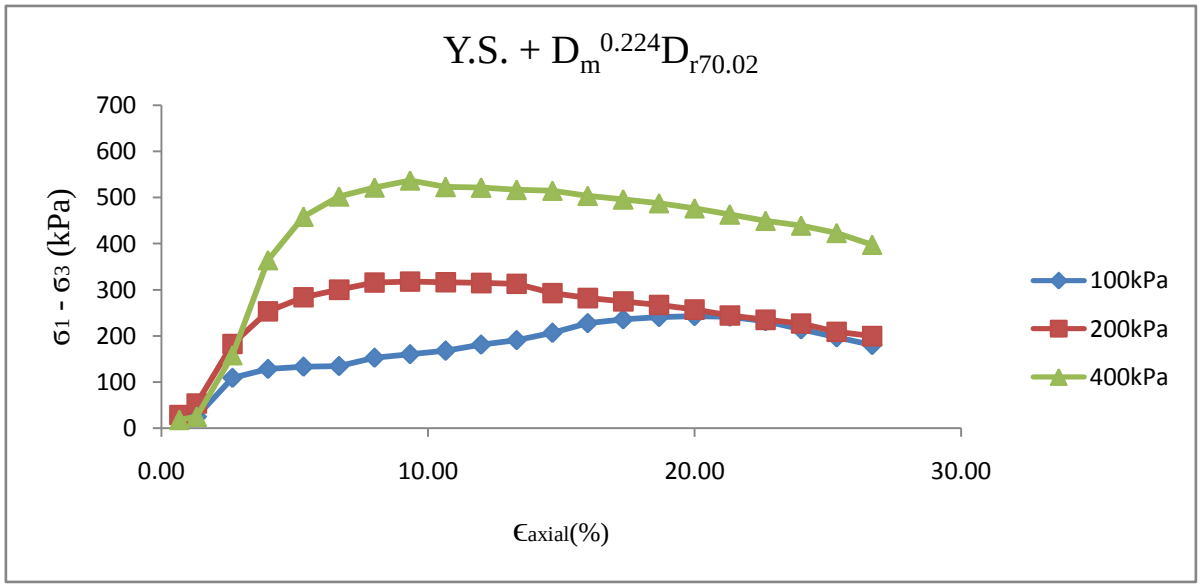


Figure 08(a): Axial Strain v/s Deviator Stress

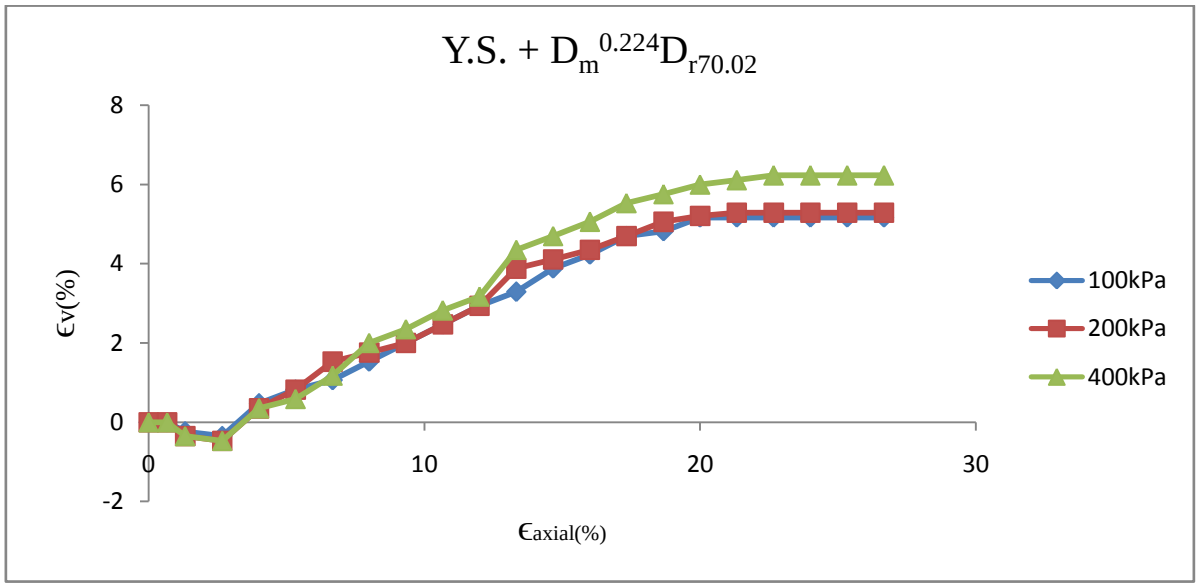


Figure 08(b): Axial Strain v/s Volumetric Strain

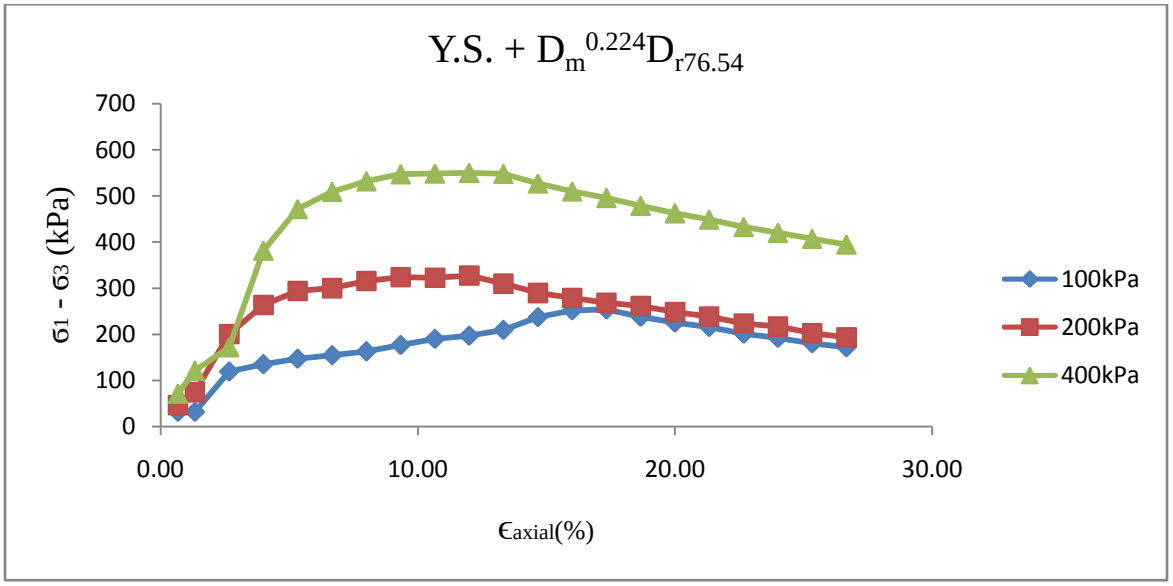


Figure 09(a): Axial Strain v/s Deviator Stress

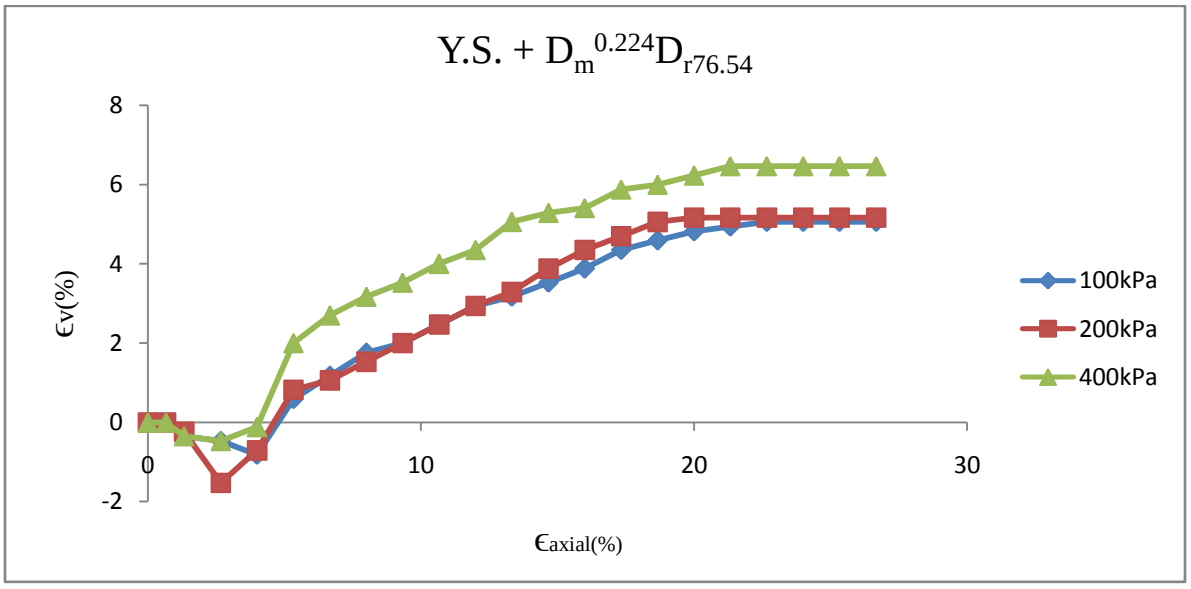


Figure 09(b): Axial Strain v/s Volumetric Strain

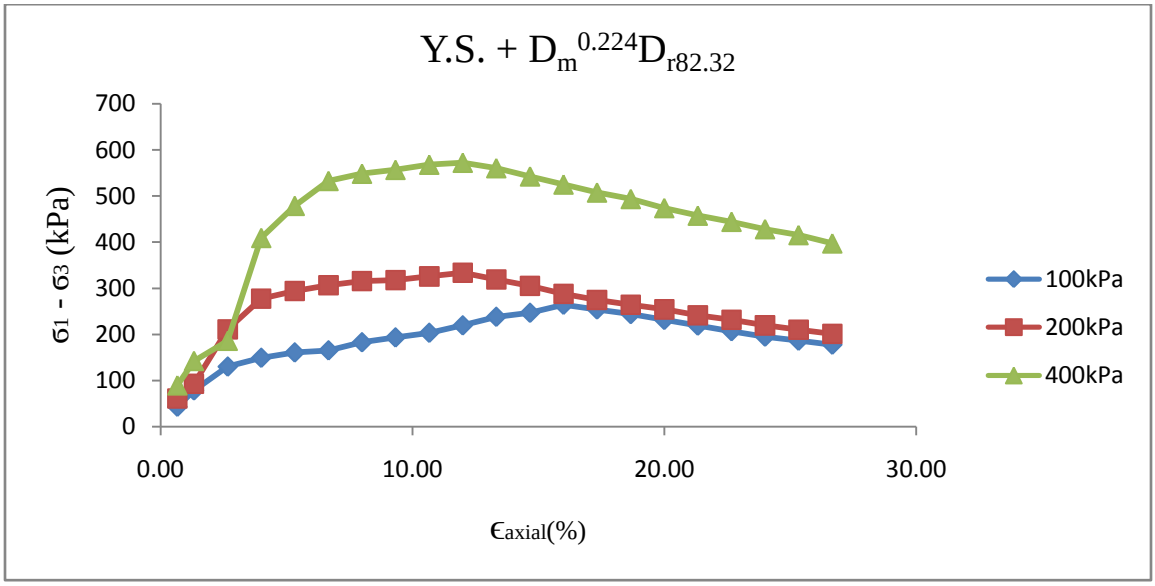


Figure 10(a): Axial Strain v/s Deviator Stress

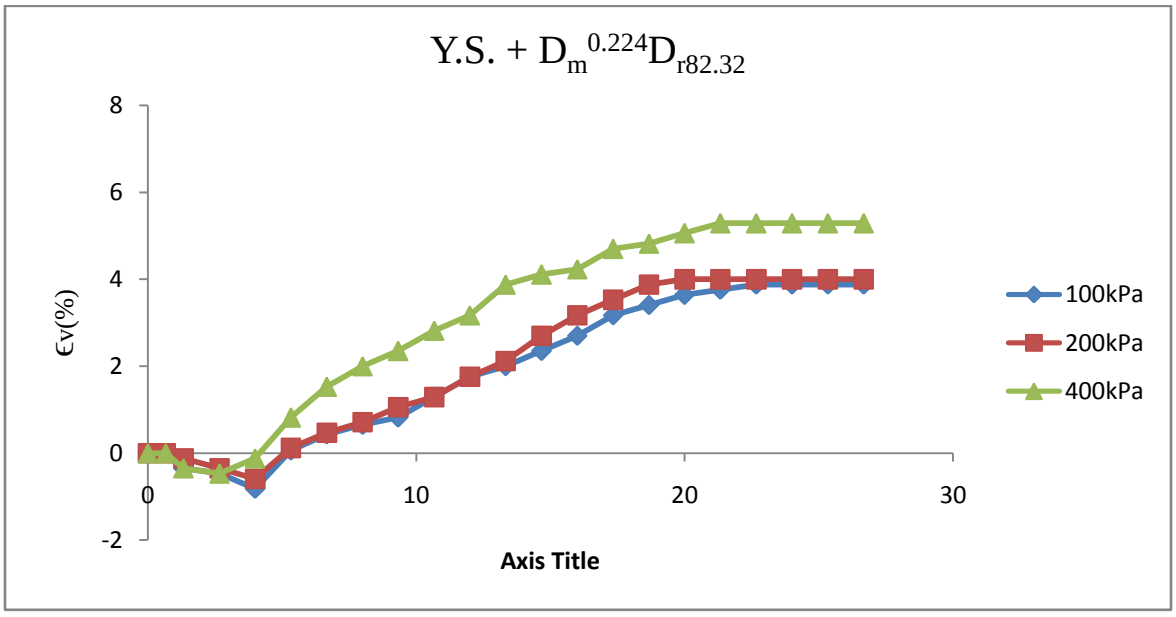


Figure 10(b): Axial Strain v/s Volumetric Strain

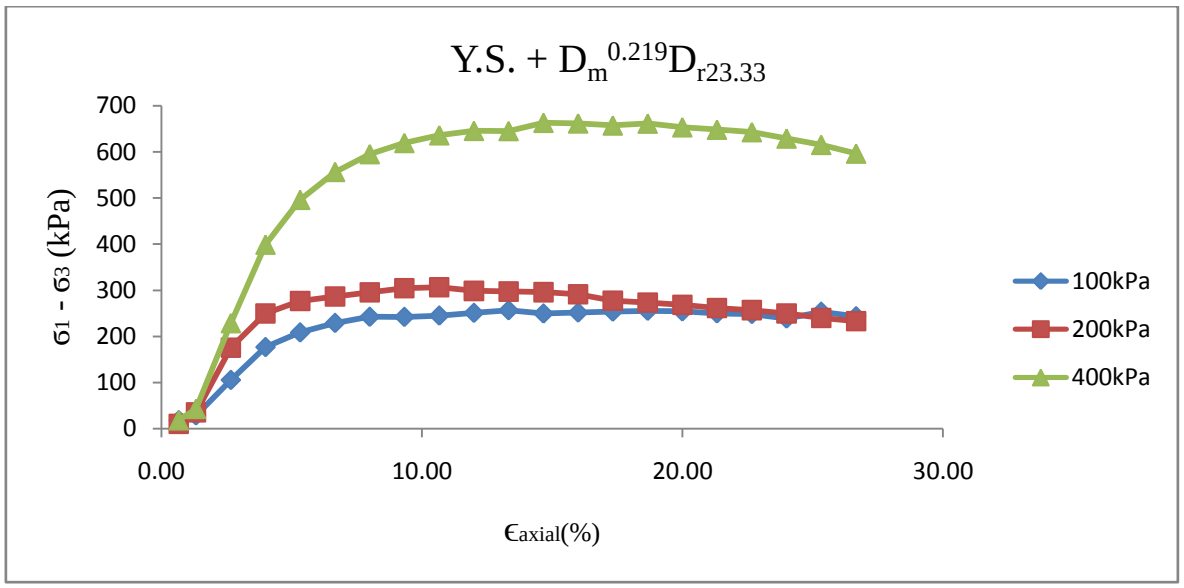


Figure 11(a): Axial Strain v/s Deviator Stress

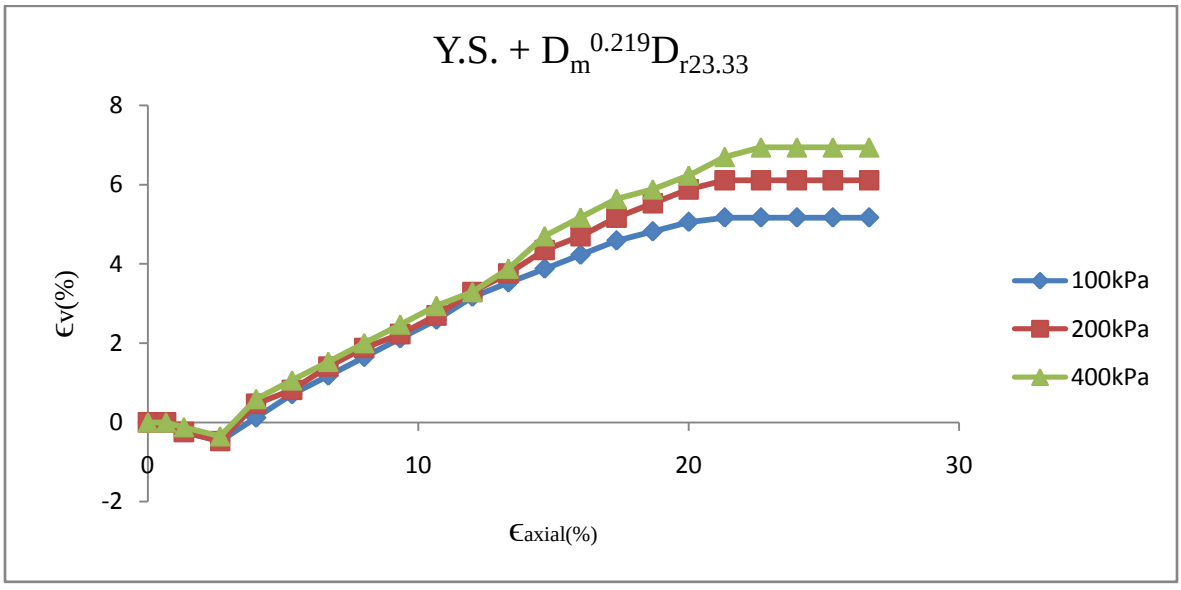


Figure 11(b): Axial Strain v/s Volumetric Strain

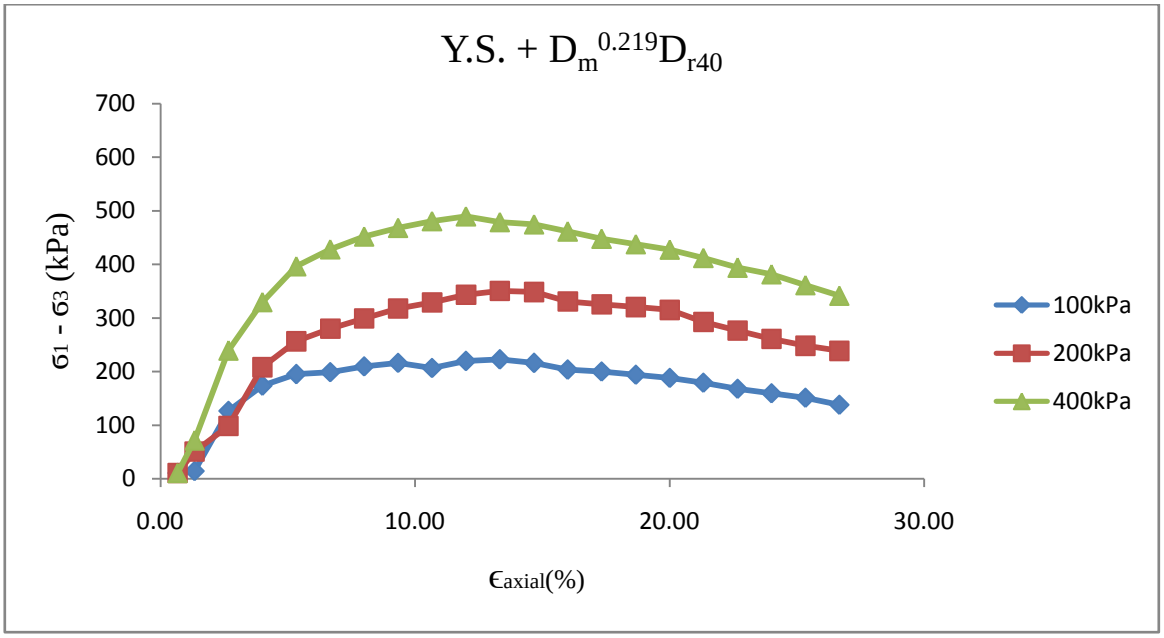


Figure 12(a): Axial Strain v/s Deviator Stress

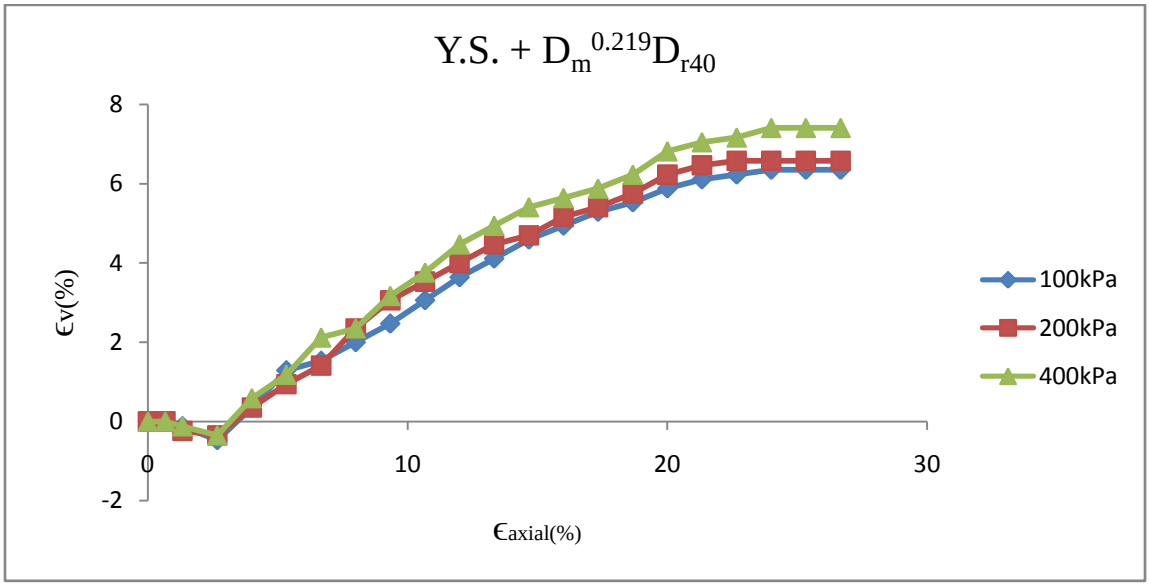


Figure 12(b): Axial Strain v/s Volumetric Strain

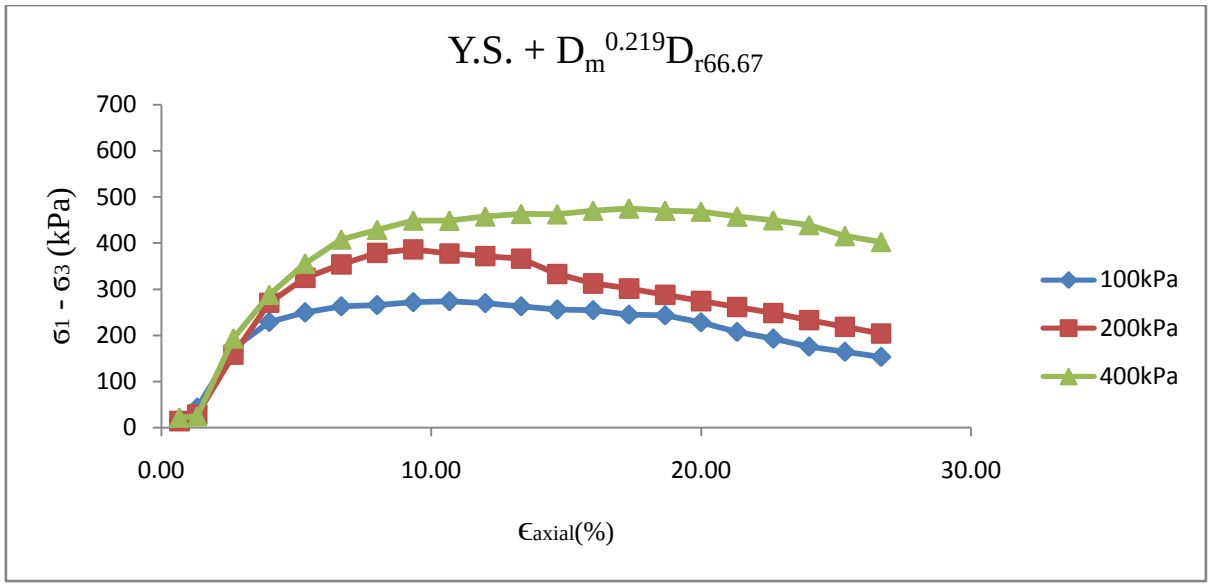


Figure 13(a): Axial Strain v/s Deviator Stress

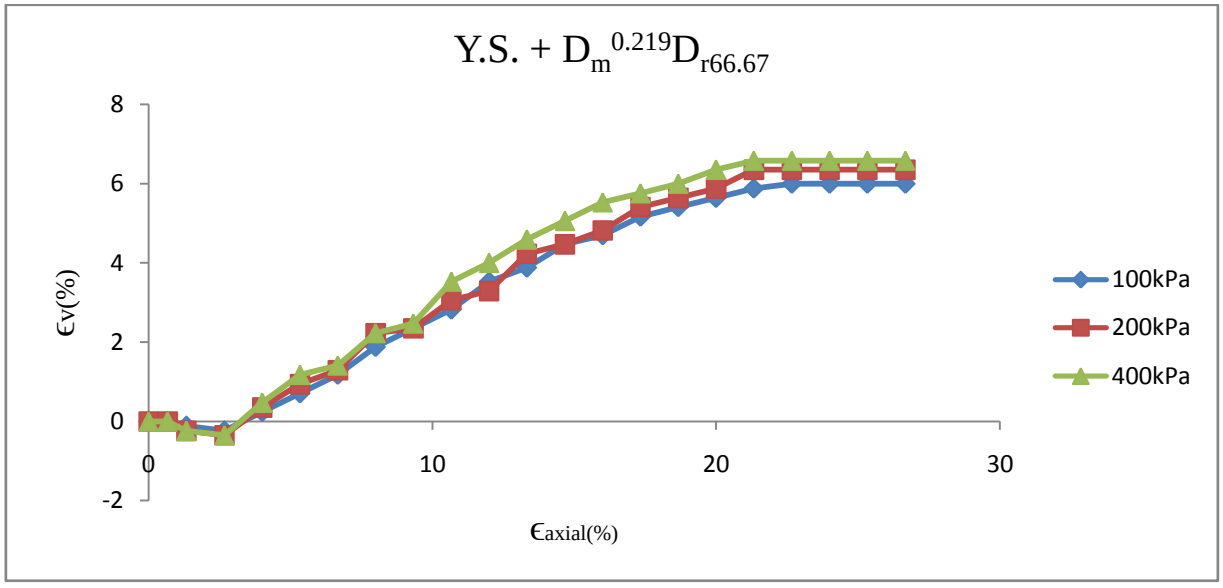


Figure 13(b): Axial Strain v/s Volumetric Strain

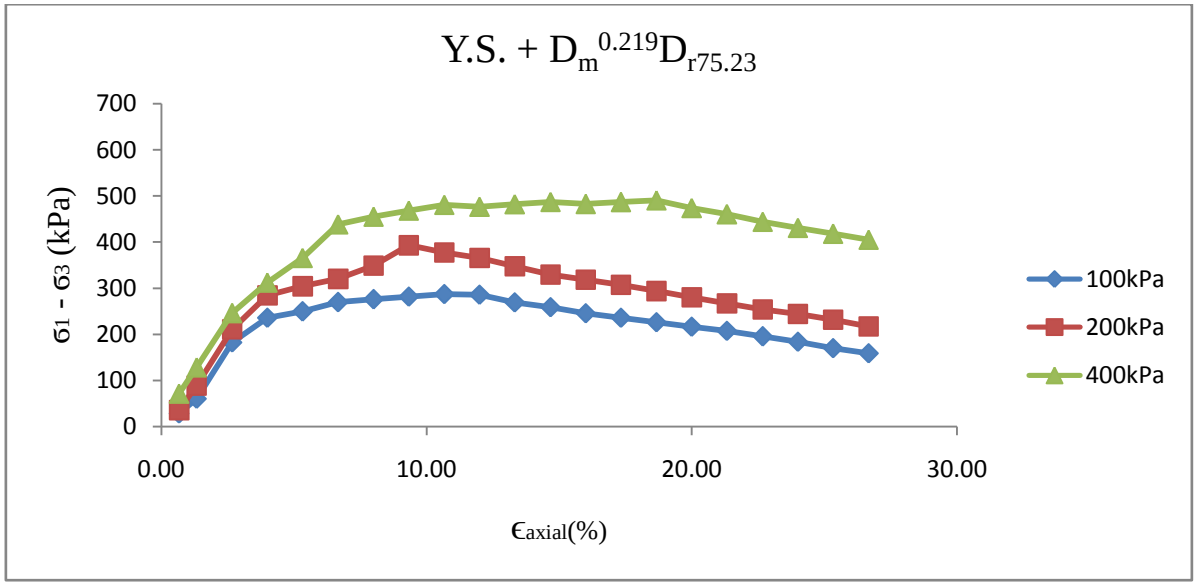


Figure 14(a): Axial Strain v/s Deviator Stress

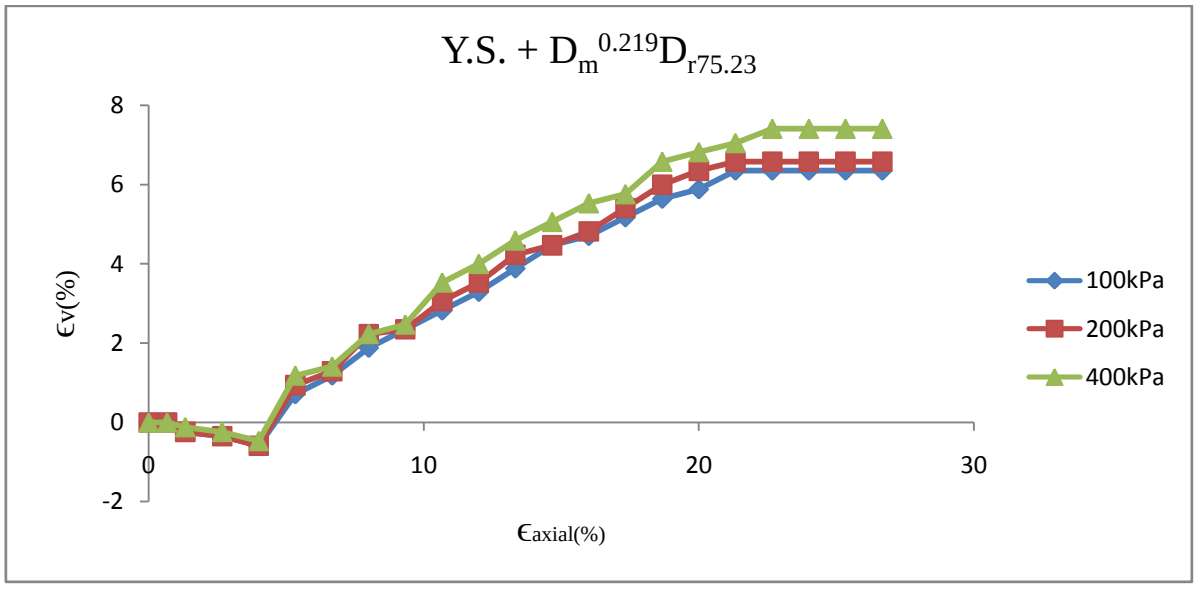


Figure 14(b): Axial Strain v/s Volumetric Strain

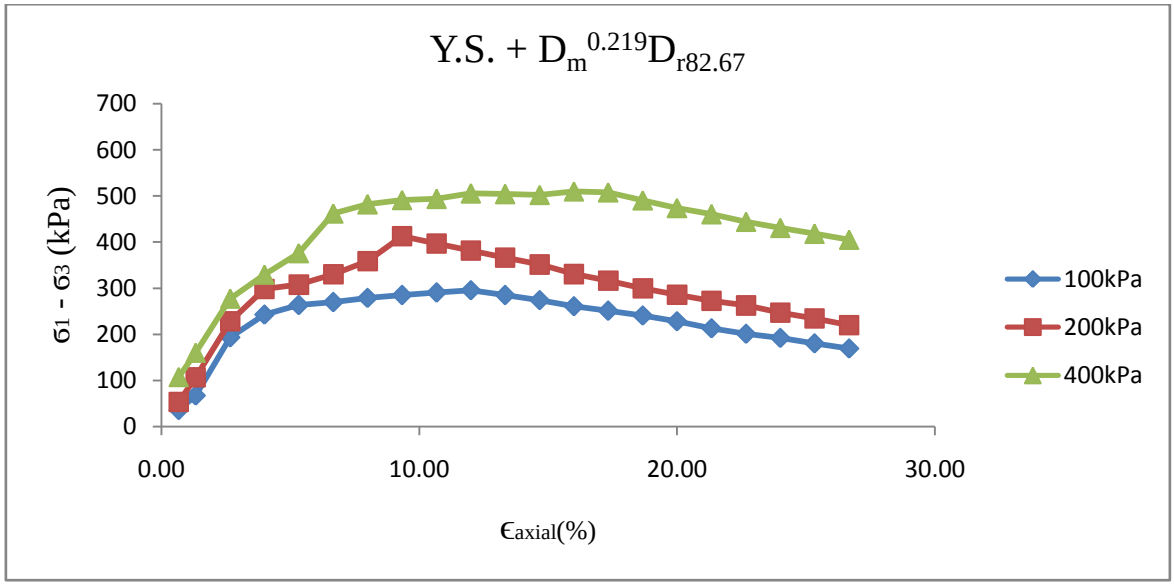


Figure 15(a): Axial Strain v/s Deviator Stress

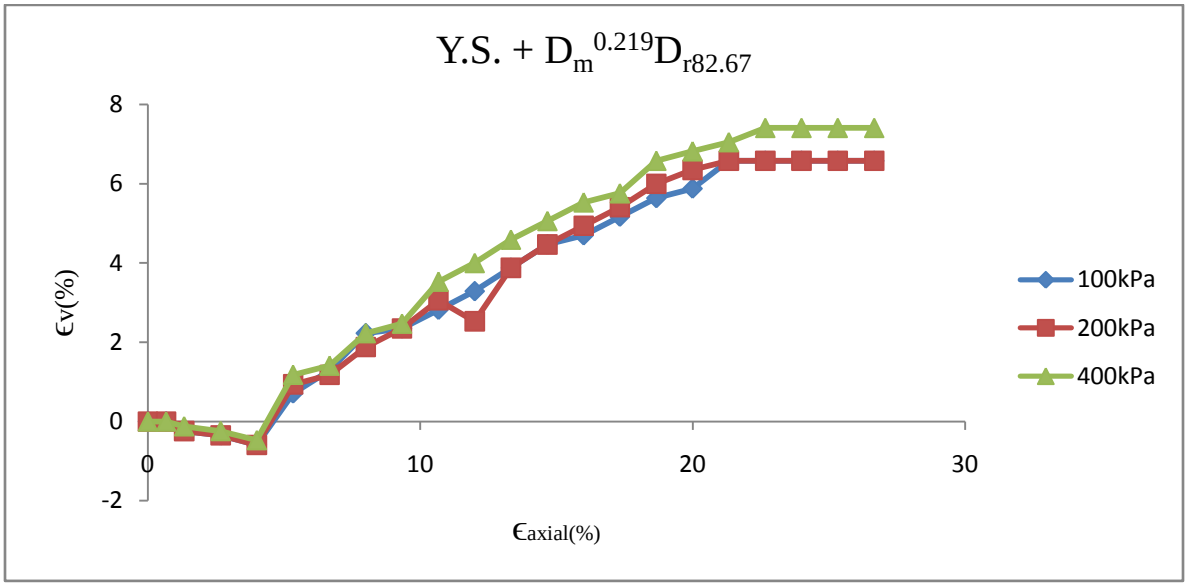


Figure 15(b): Axial Strain v/s Volumetric Strain

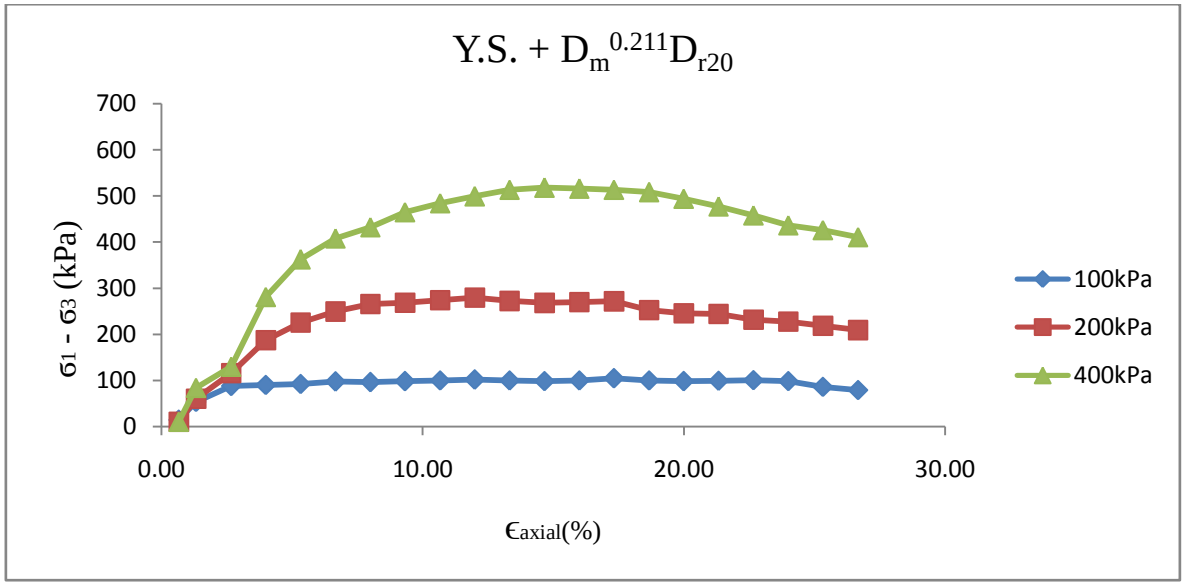


Figure 16(a): Axial Strain v/s Deviator Stress

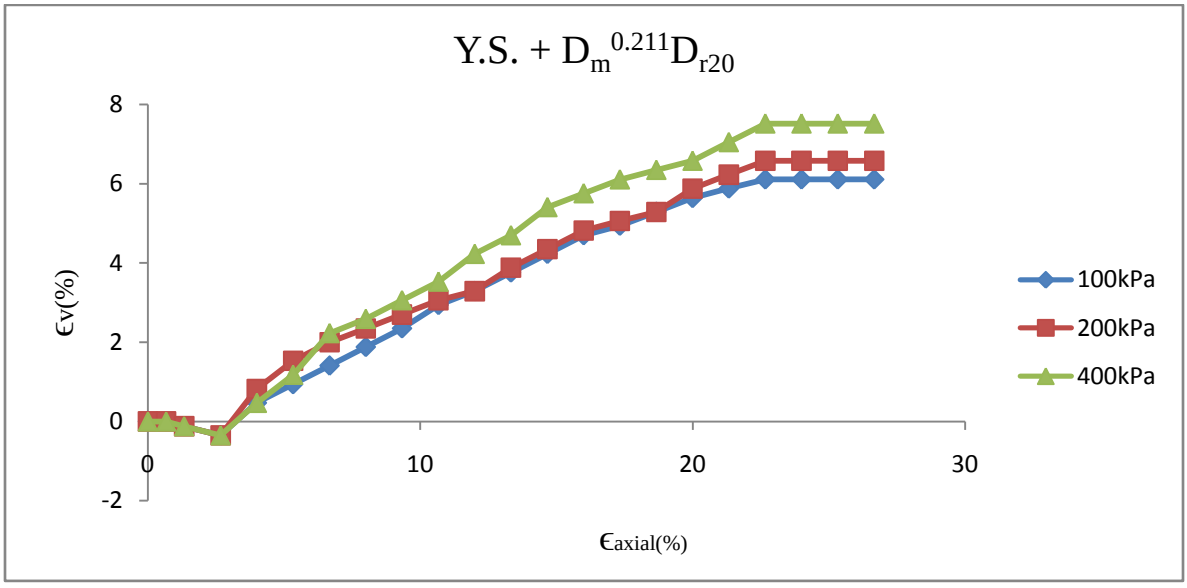


Figure 16(b): Axial Strain v/s Volumetric Strain

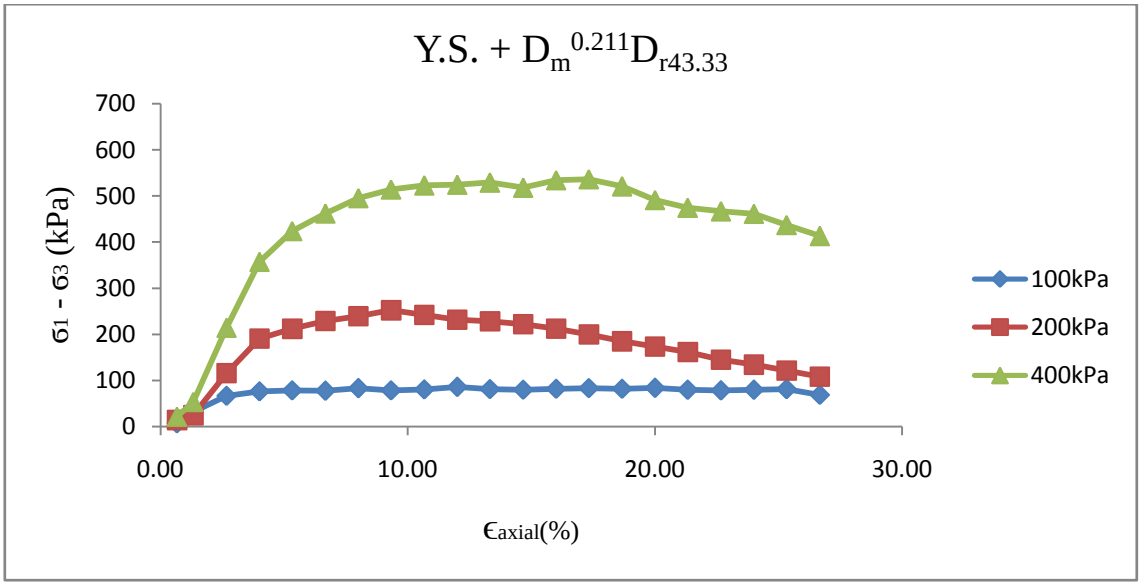


Figure 17(a): Axial Strain v/s Deviator Stress

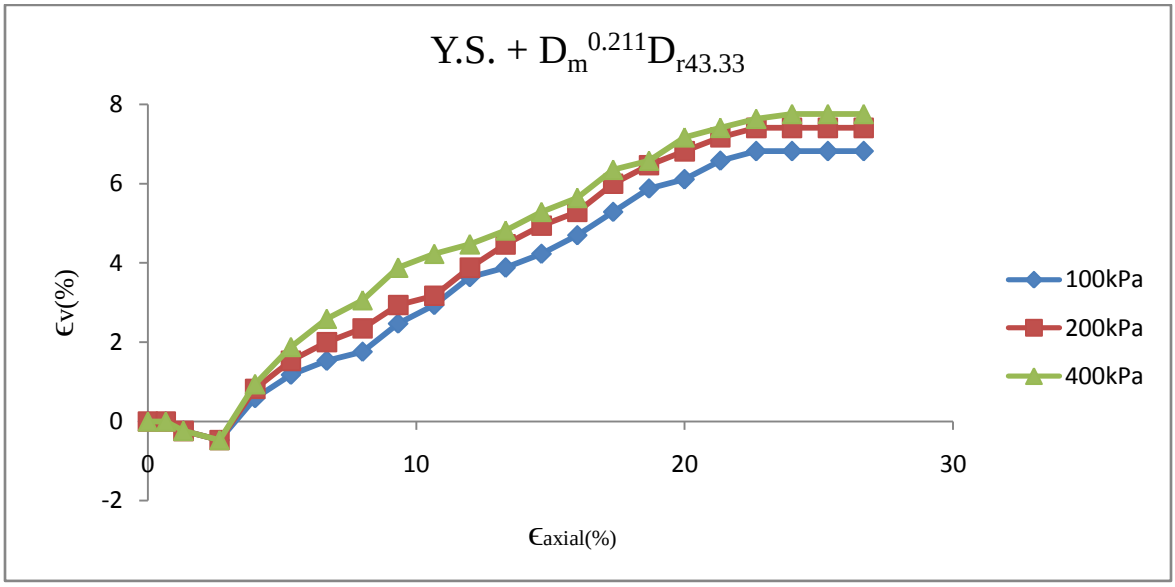


Figure 17(b): Axial Strain v/s Volumetric Strain

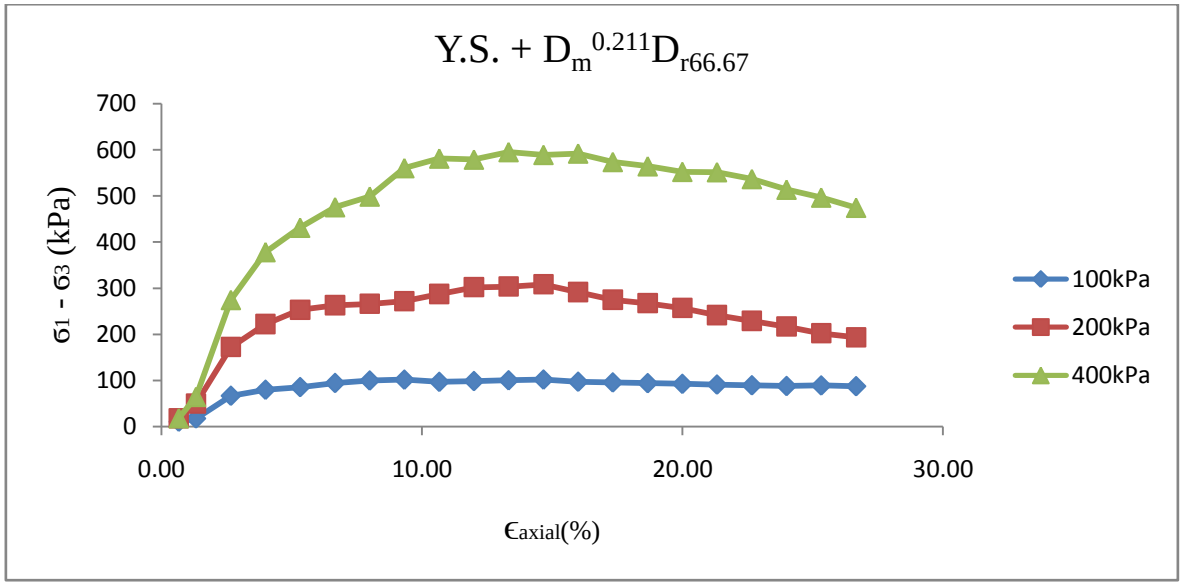


Figure 18(a): Axial Strain v/s Deviator Stress

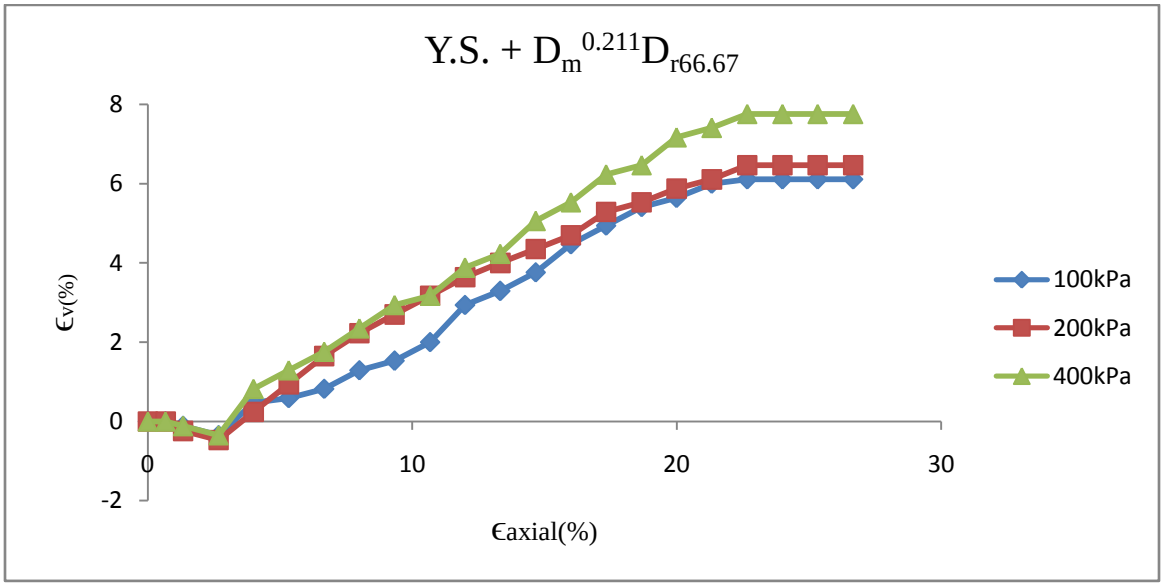


Figure 18(b): Axial Strain v/s Volumetric Strain

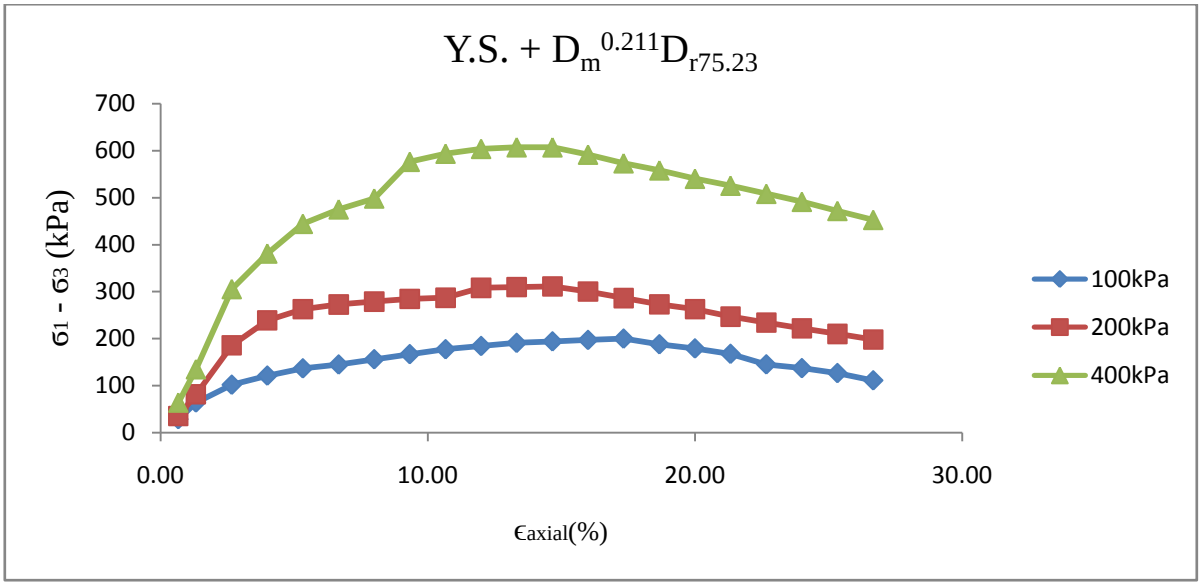


Figure 19(a): Axial Strain v/s Deviator Stress

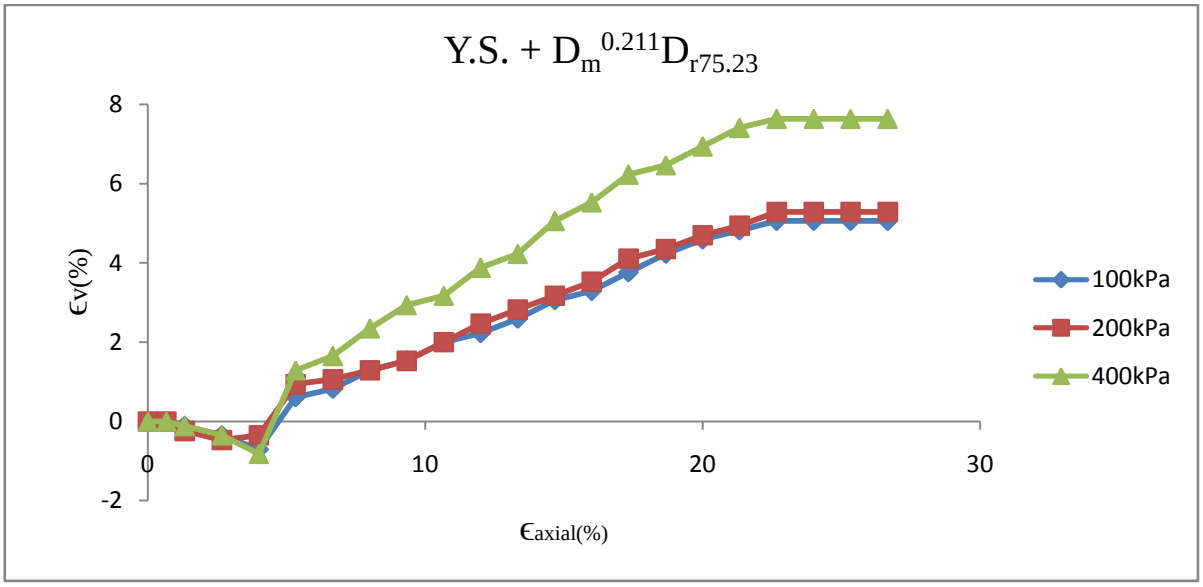


Figure 19(b): Axial Strain v/s Volumetric Strain

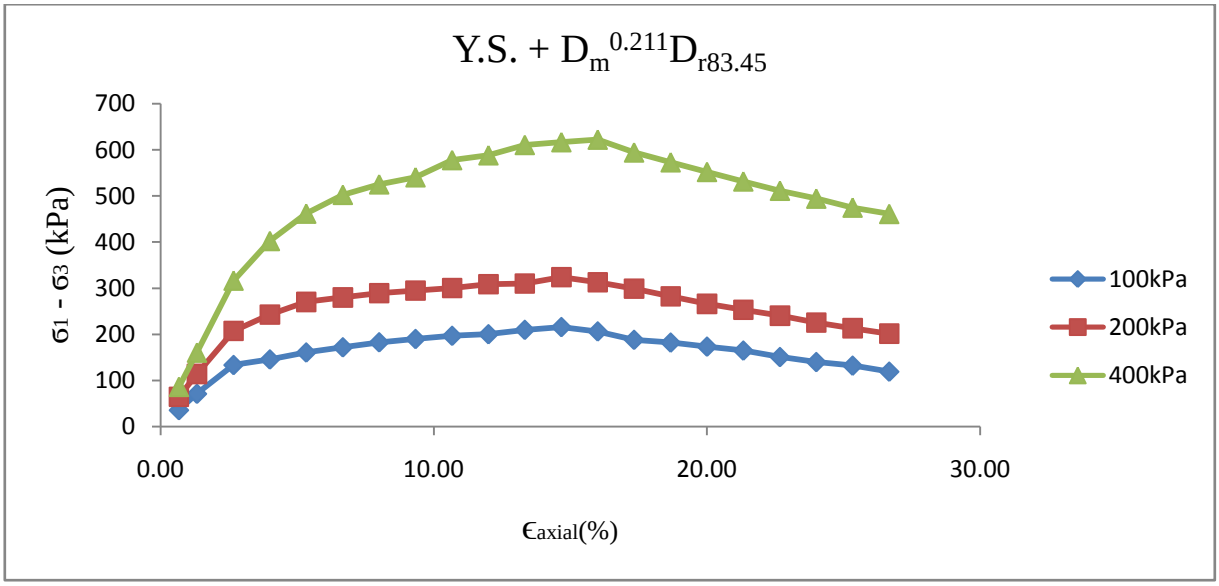


Figure 20(a): Axial Strain v/s Deviator Stress

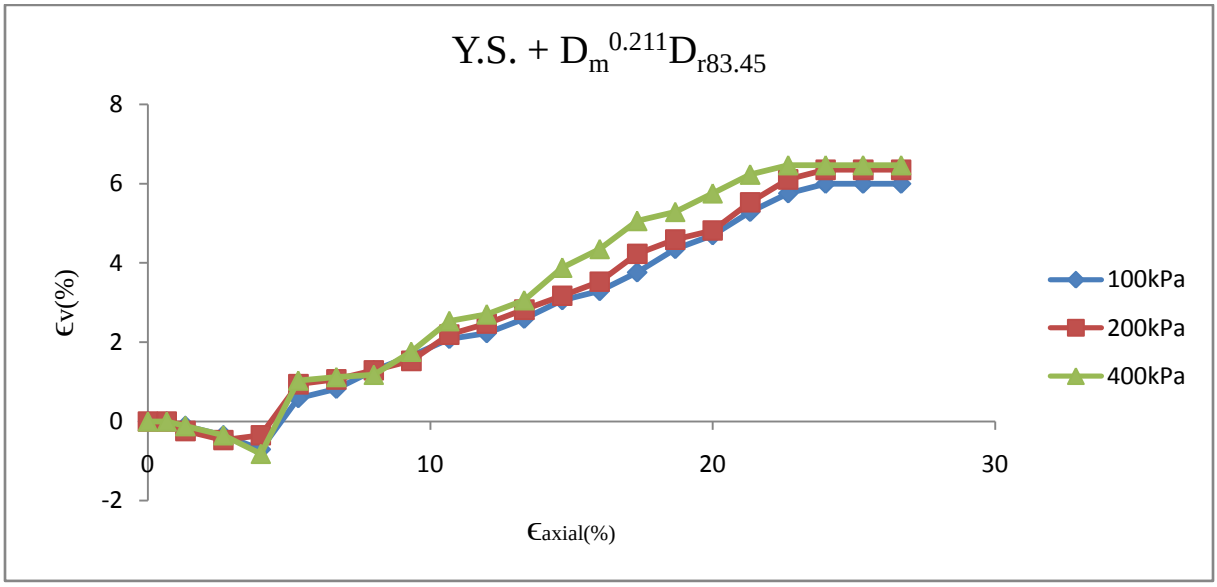


Figure 20(b): Axial Strain v/s Volumetric Strain

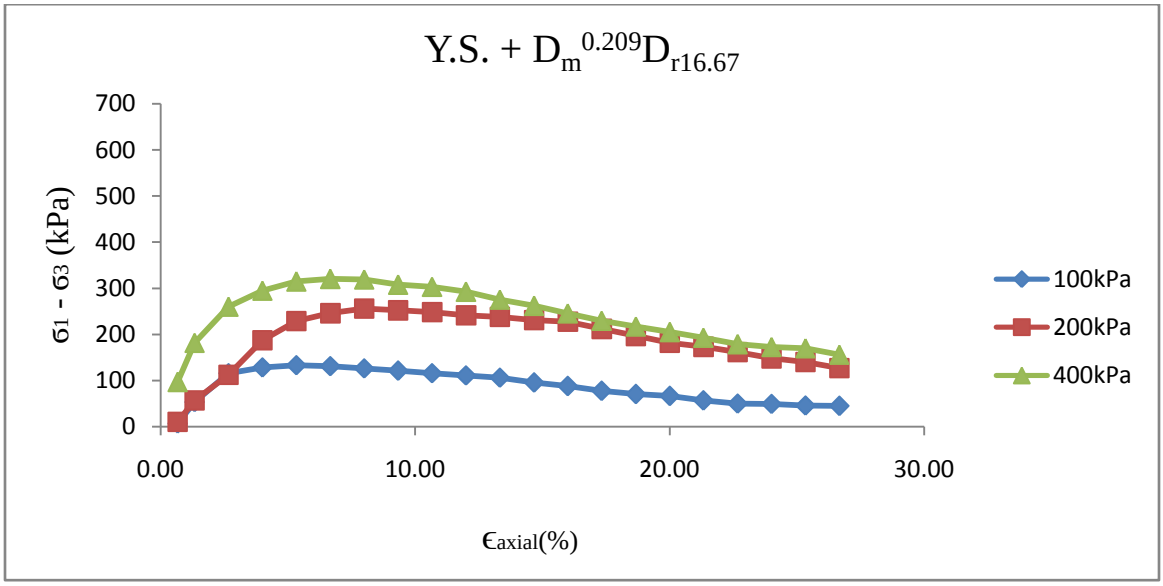


Figure 21(a): Axial Strain v/s Deviator Stress

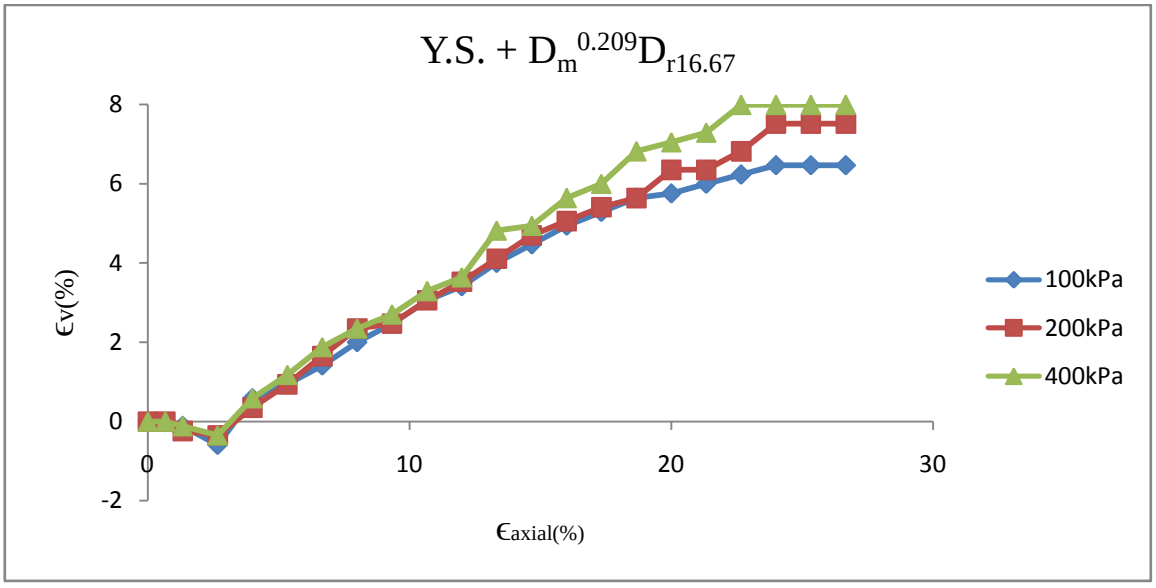


Figure 21(b): Axial Strain v/s Volumetric Strain

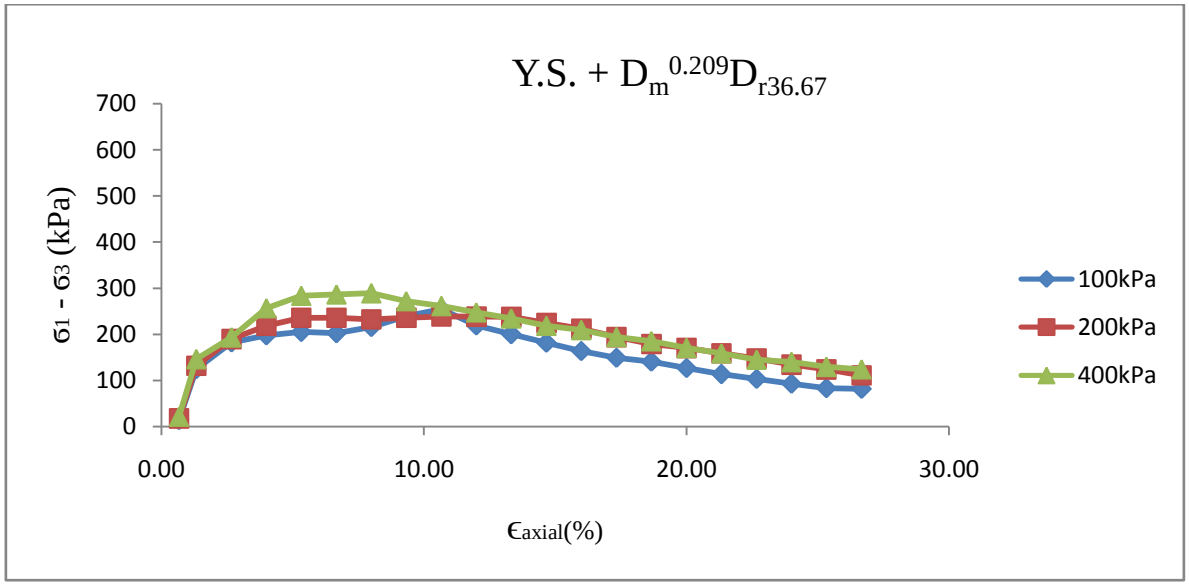


Figure 22(a): Axial Strain v/s Deviator Stress

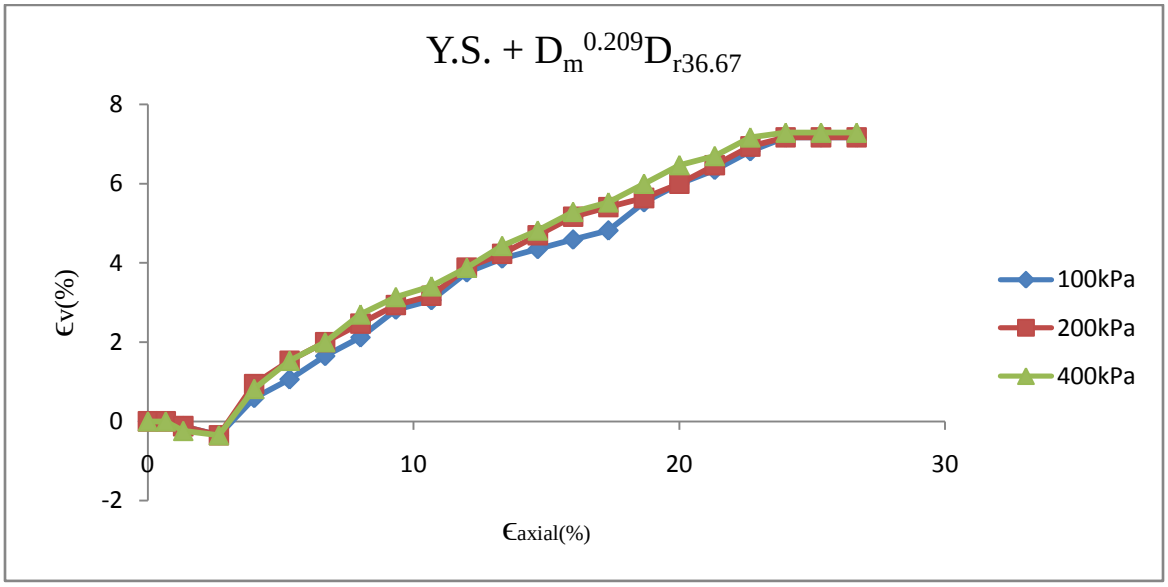


Figure 22(b): Axial Strain v/s Volumetric Strain

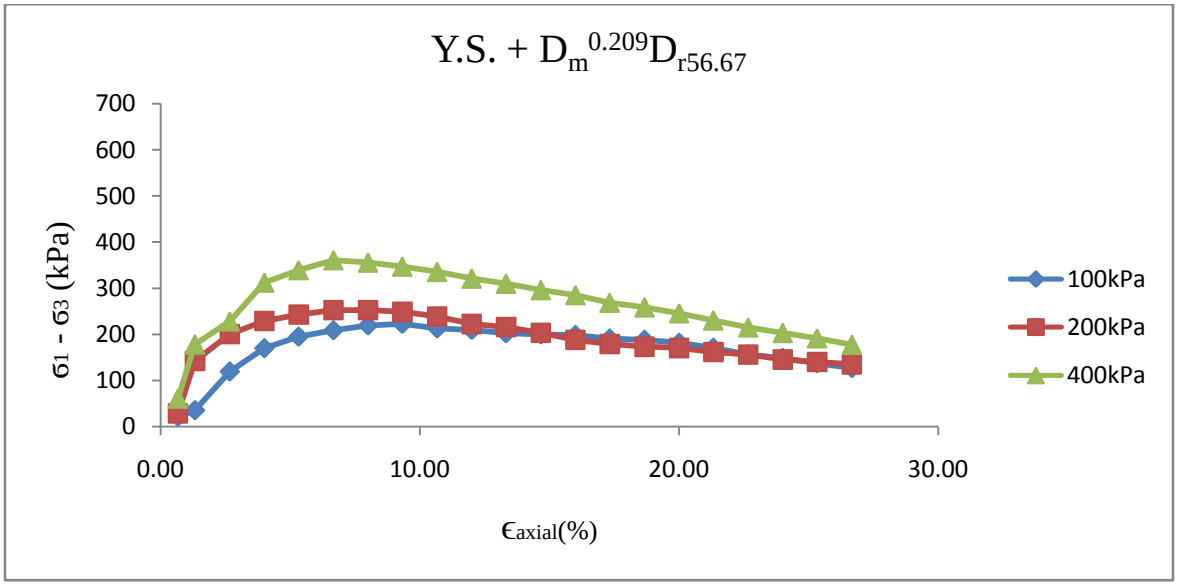


Figure 23(a): Axial Strain v/s Deviator Stress

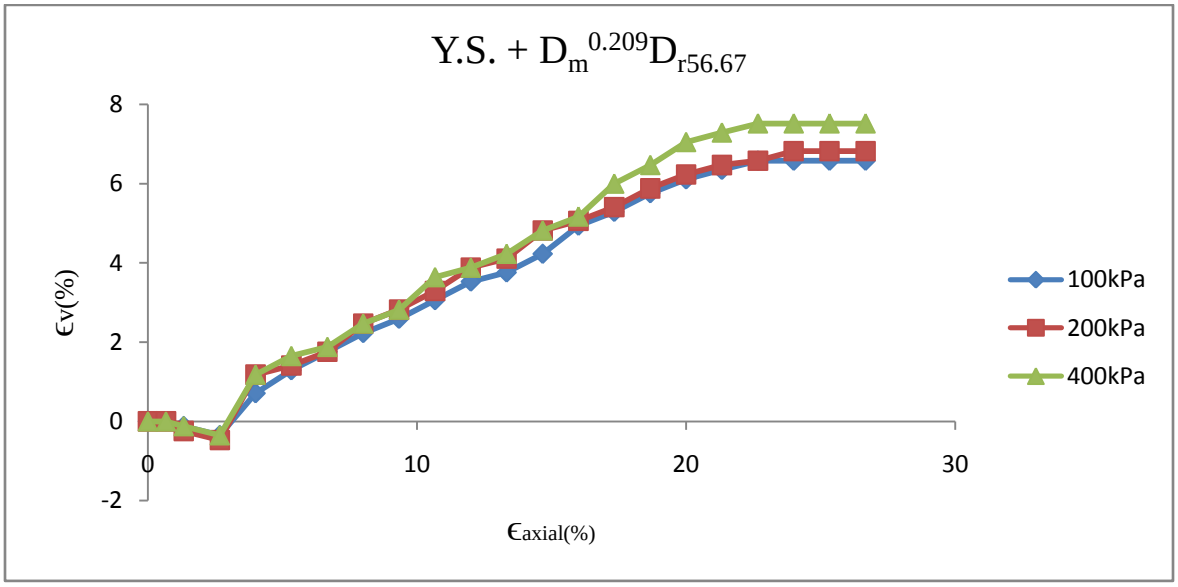


Figure 23(b): Axial Strain v/s Volumetric Strain

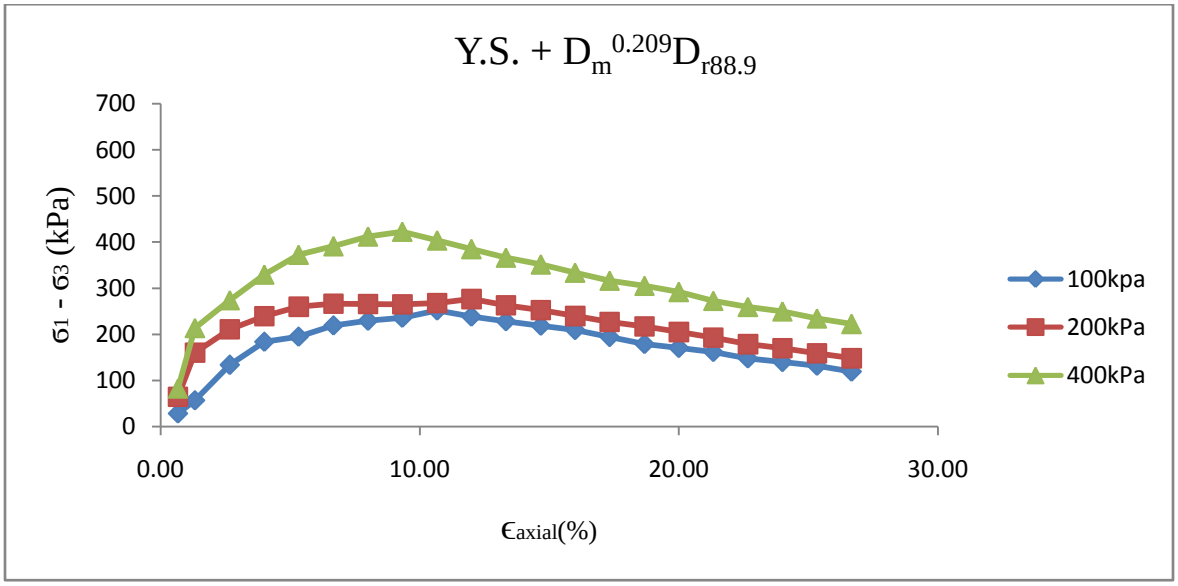


Figure 24(a): Axial Strain v/s Deviator Stress

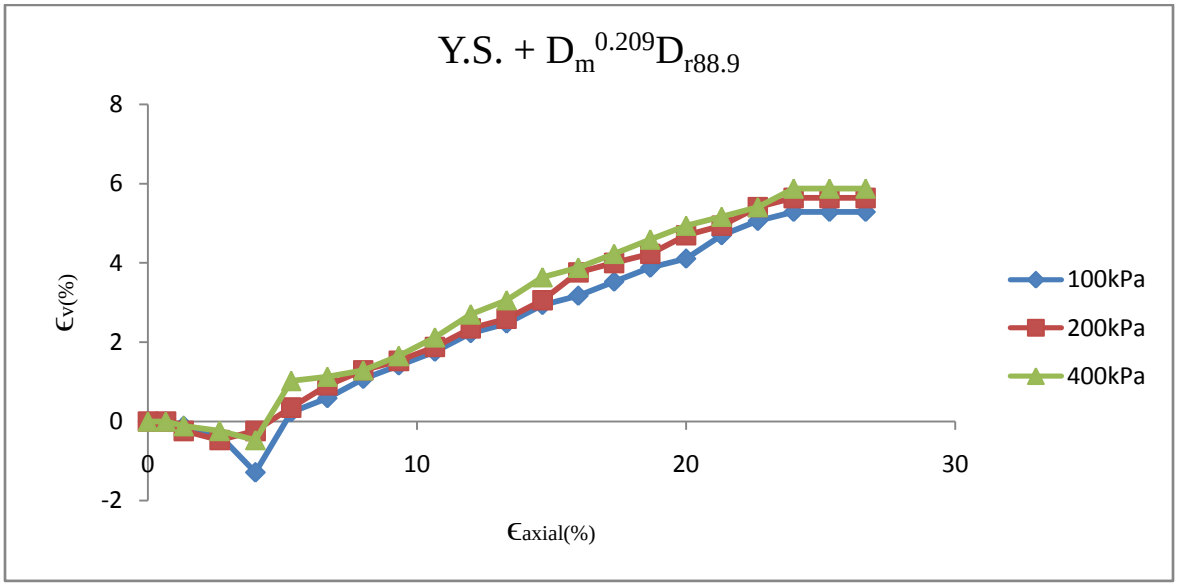


Figure 24(b): Axial Strain v/s Volumetric Strain

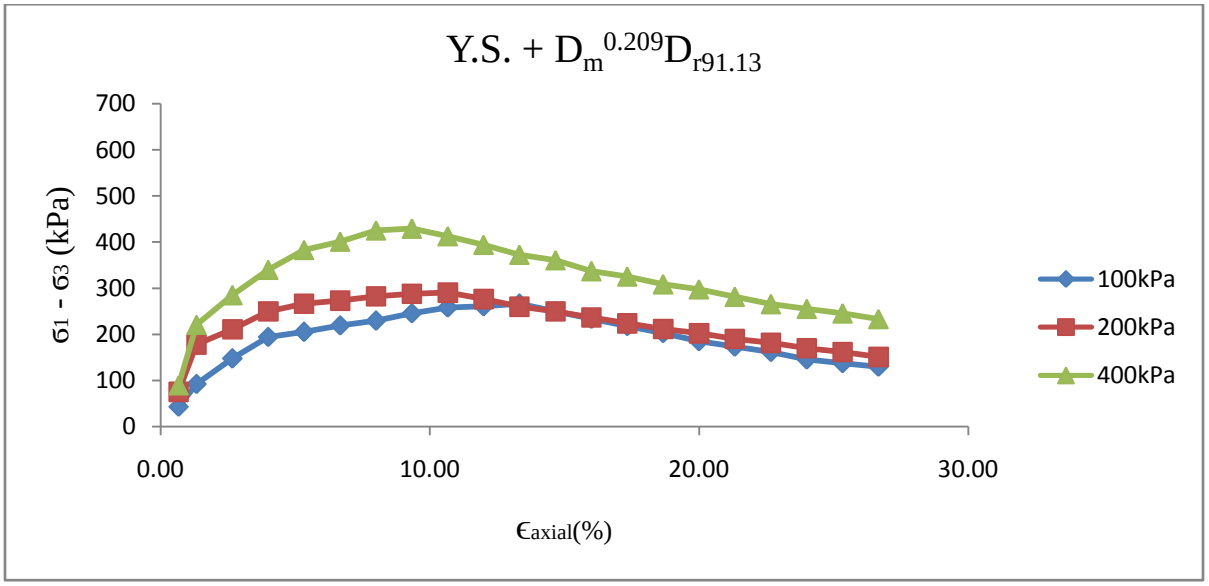


Figure 25(a): Axial Strain v/s Deviator Stress

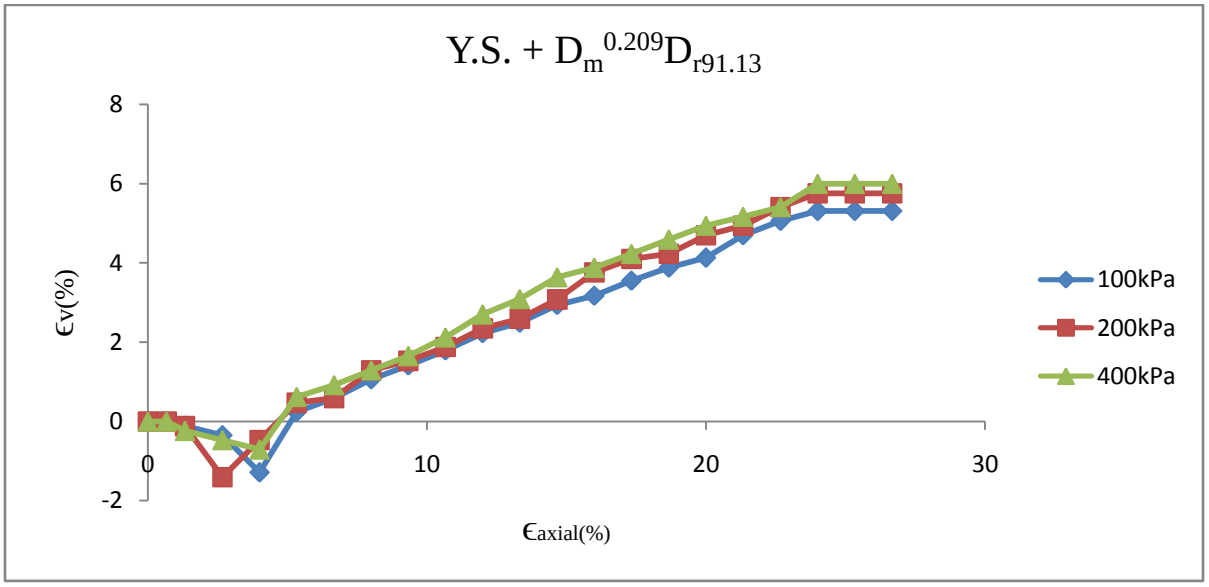


Figure 25(b): Axial Strain v/s Volumetric Strain

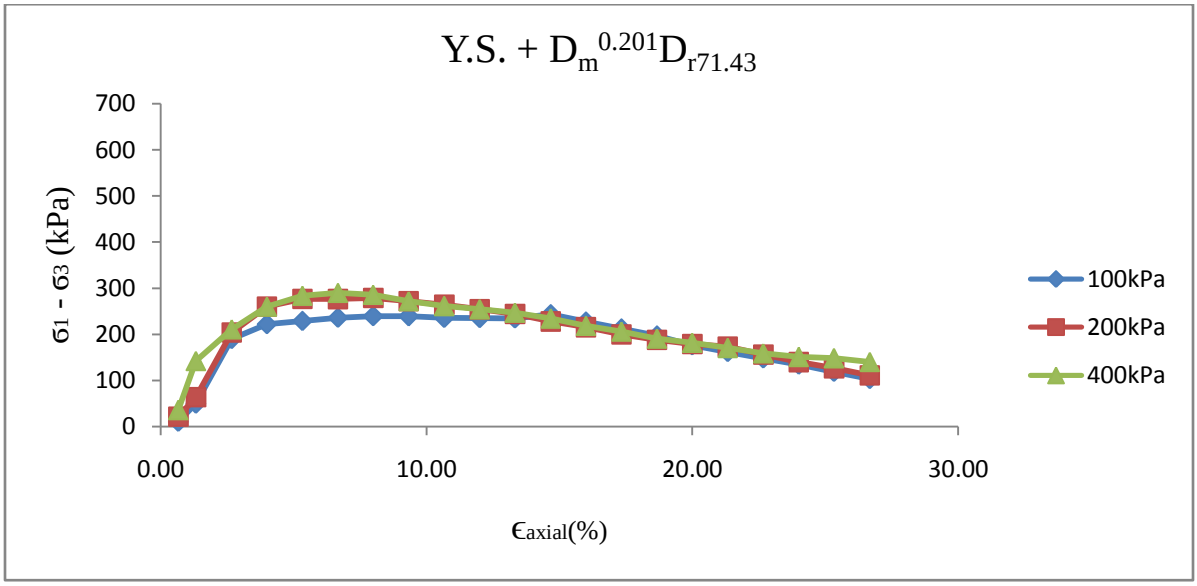


Figure 26(a): Axial Strain v/s Deviator Stress

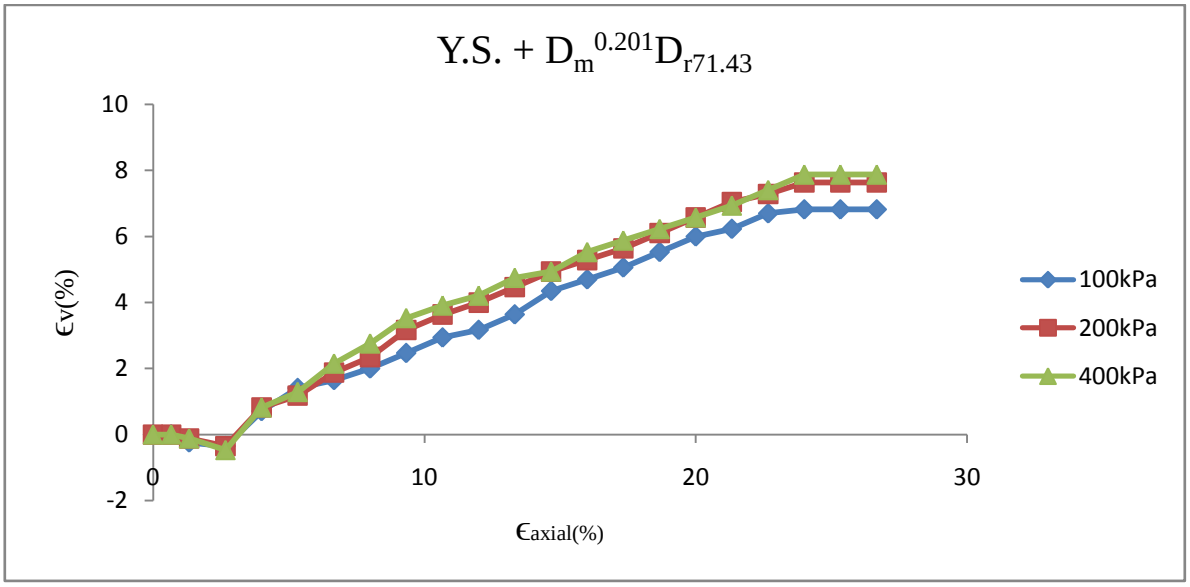


Figure 26(b): Axial Strain v/s Volumetric Strain

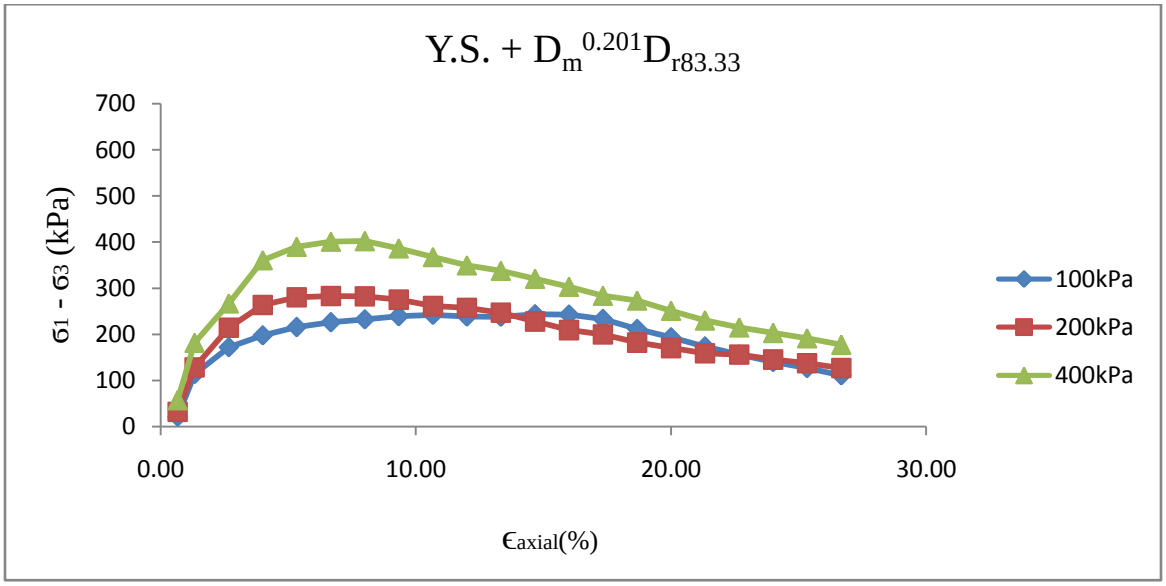


Figure 27(a): Axial Strain v/s Deviator Stress

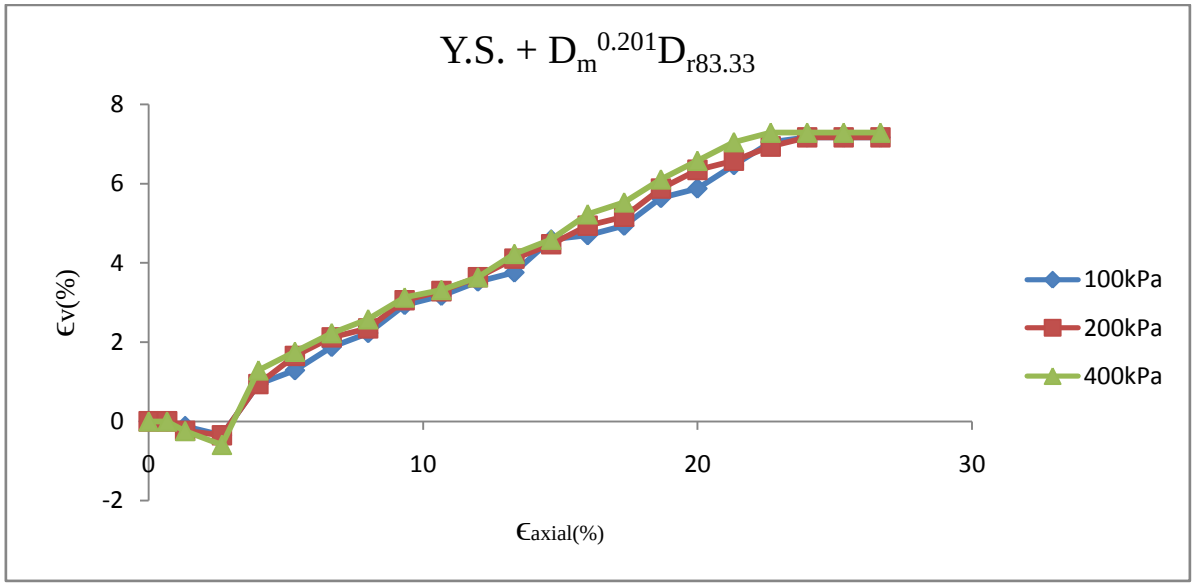


Figure 27(b): Axial Strain v/s Volumetric Strain

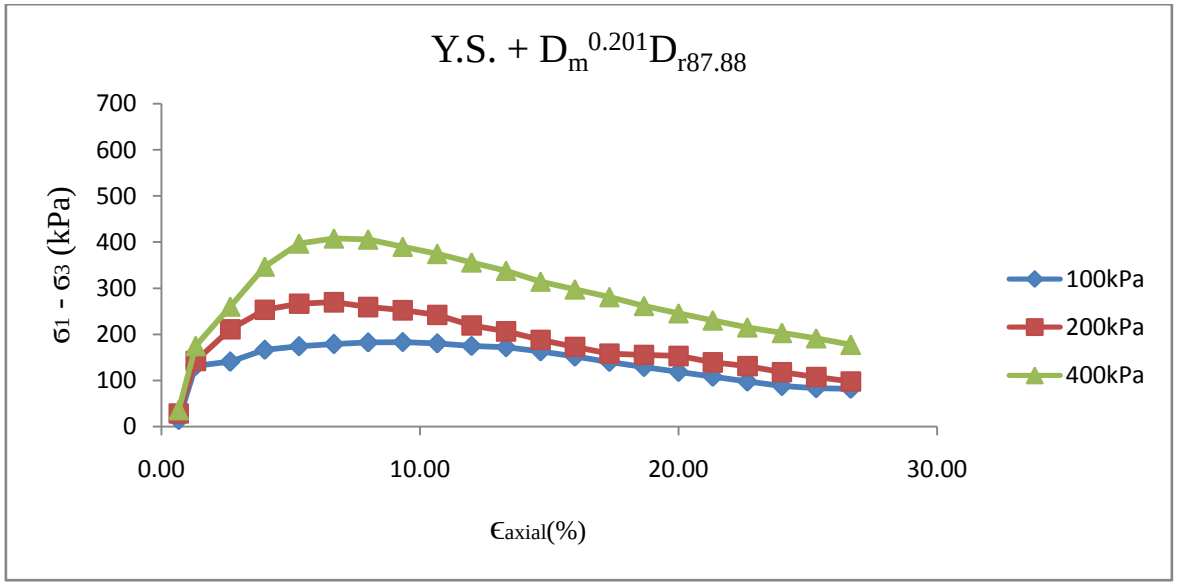


Figure 28(a): Axial Strain v/s Deviator Stress

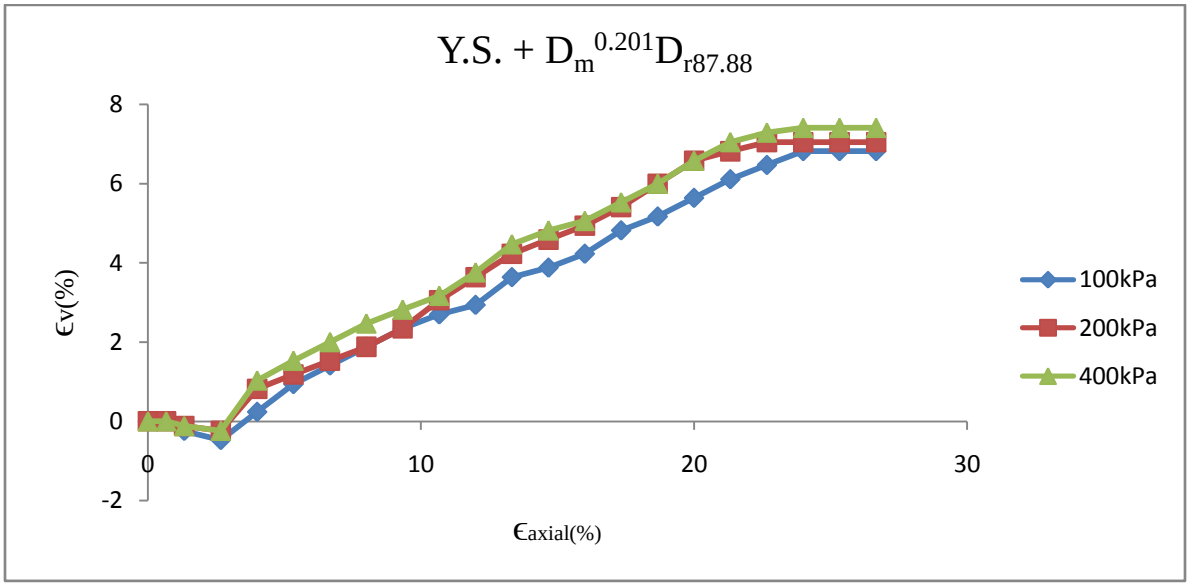


Figure 28(b): Axial Strain v/s Volumetric Strain

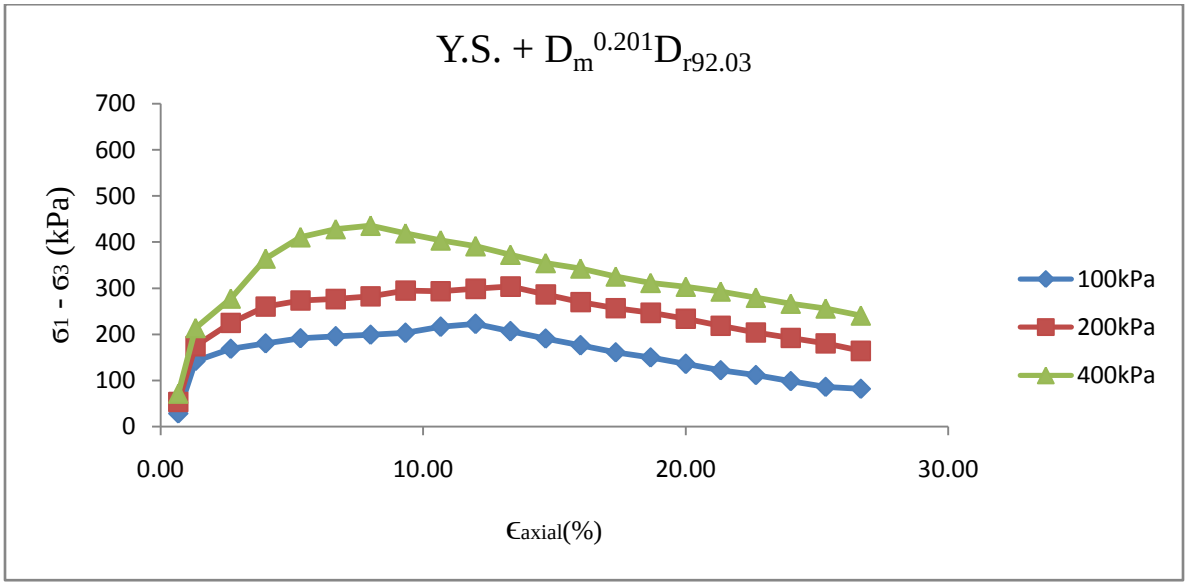


Figure 29(a): Axial Strain v/s Deviator Stress

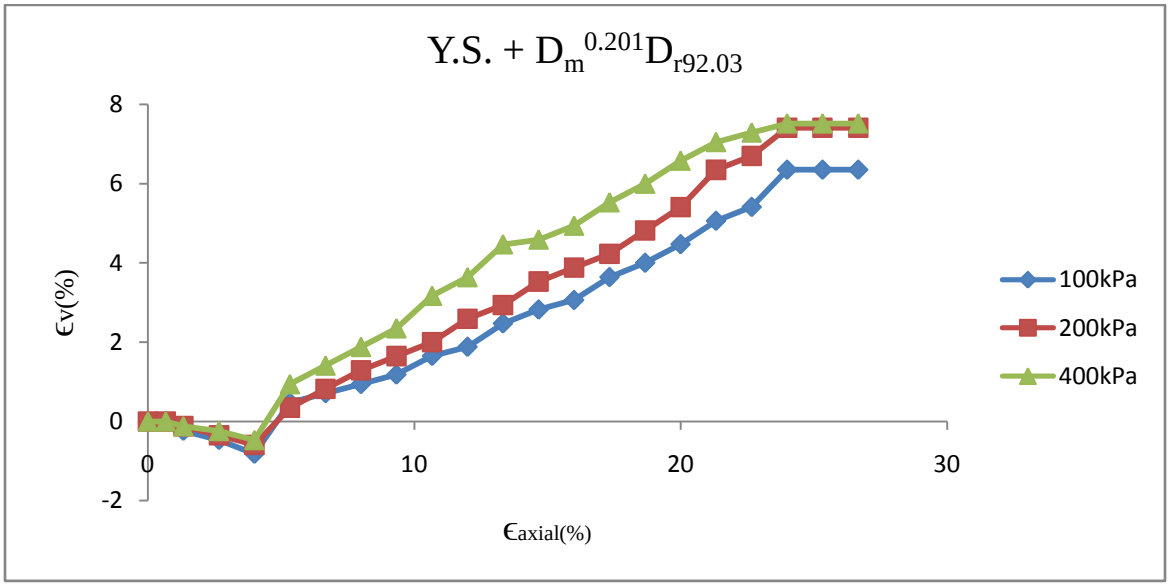


Figure 29(b): Axial Strain v/s Volumetric Strain

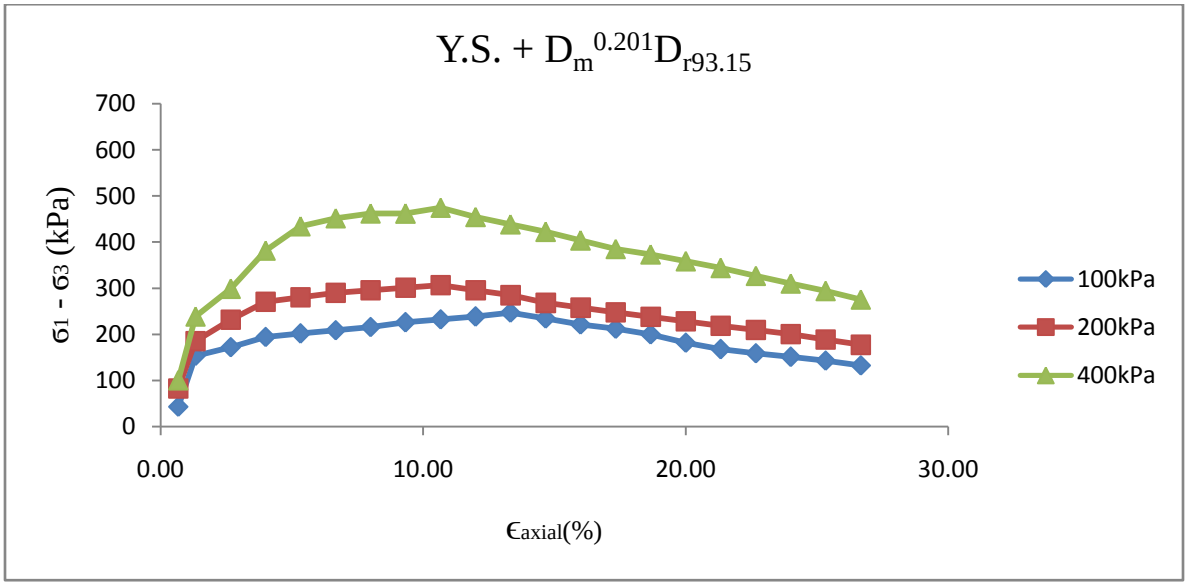


Figure 30(a): Axial Strain v/s Deviator Stress

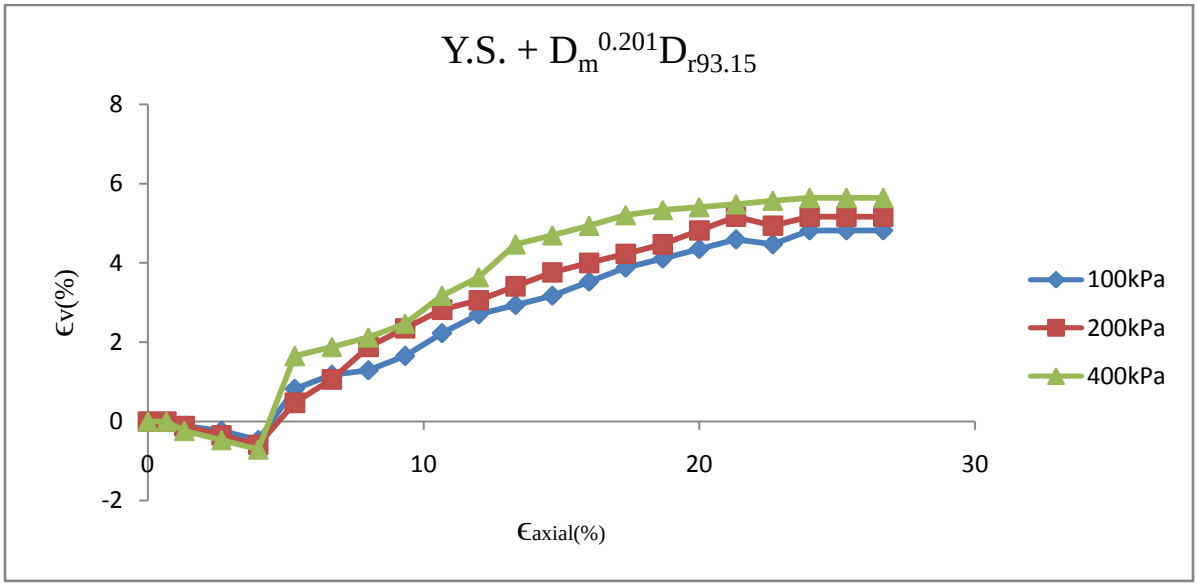


Figure 30(b): Axial Strain v/s Volumetric Strain

# Chapter 6

# Discussions

The analysis of a large number of drained tri-axial compression tests, many of which were carried out with local strain measurement. The tests were performed on consolidated specimens of Yamuna Sand prepared by pluvial deposition in air and allow the following conclusions, all of which refer to the value of confining stress 100, 200 and 400kPa. Table 03 shows the value of intrinsic variables for various sands & silty sand investigated worldwide. Table 05 shows the results of linear regression following equations (11) on the data for Yamuna sand with 2.9, 3.2, 3.3, 3.4, 3.6 and 4.3% silt contents.

**Table 03: Intrinsic variables of some clean sand**

| Sand type | $e_{min}$ | $e_{max}$ | $\Phi_c$ | $G_s$ | $D_{50}$ (mm) | References |
|---|---|---|---|---|---|---|
| Ham river | 0.92 | 0.59 | 33 | - | ~ 0.22 | Bishop & Green (1965) |
| Karlsruhe medium sand | 0.82 | 0.54 | 34 | - | ~ 0.32 | Hettler (1981) |
| Monterey Sand | 0.57 | 0.86 | 37 | - | - | Bolton (1986), Chung et al. (1984) |
| Ticino Sand | 0.57 | 0.93 | 34.8 | 2.69 | 0.55 | Lo Presti (1987), Lo Presti et al. (1992) |
| Toyoura Sand | 0.61 | 0.99 | 35.1 | 2.65 | 0.16 | Lo Presti (1987), Lo Presti et al. (1992) |
| Sacramento River Sand | 0.61 | 1.03 | 33.3 | - | - | Bolton (1986) |
| Hokksund Sand | 0.55 | 0.87 | 36.0 | - | - | Lo Presti (1987), Lo Presti et al. (1992) |
| Ottawa Sand | 0.48 | 0.78 | 29 | - | - | Salgado(2000) |
| Yamuna Sand (Plastic fines 2.9%) | 0.5 | 0.78 | 24.78 | 2.67 | 0.256 | Present work |
| Yamuna Sand (Plastic fines 3.2%) | 0.46 | 0.76 | 25.62 | 2.66 | 0.224 | Present work |
| Yamuna Sand (Plastic | 0.42 | 0.72 | 26.91 | 2.64 | 0.219 | Present work |

| | | | | | | |
|---|---|---|---|---|---|---|
| fines 3.3%) | | | | | | |
| Yamuna Sand (Plastic fines 3.4%) | 0.38 | 0.68 | 27.89 | 2.62 | 0.211 | Present work |
| Yamuna Sand (Plastic fines 3.6%) | 0.33 | 0.63 | 29.01 | 2.64 | 0.209 | Present work |
| Yamuna Sand (Plastic fines 4.3%) | 0.31 | 0.62 | 30.03 | 2.66 | 0.201 | Present work |

**Table 04(a): Dilatancy parameters for clean and silty sands [Salgado et al. (2000)]**

| Silt(%) | $D_{50}$(mm) | Best Fit | | | Trend line with R=0.5 | |
|---|---|---|---|---|---|---|
| | | Q | R | $r^2$ | Q | $r^2$ |
| 0 | 0.25 | 9.0 | 0.49 | 0.93 | 9.0 | 0.93 |
| 5 | 0.25 | 9.0 | -0.5 | 0.98 | 11.0 | 0.92 |
| 10 | 0.25 | 8.3 | -0.69 | 0.97 | 10.6 | 0.87 |
| 15 | 0.25 | 11.4 | 1.29 | 0.97 | 10.3 | 0.96 |
| 20 | 0.25 | 10.1 | 0.85 | 0.95 | 9.5 | 0.95 |

**Table 04(b): Dilatancy parameters for clean and silty sands [Salgado et al. (2010)]**

| $\sigma`_{3p}$ (kPa) | $\sigma`_{mp}$ (kPa) | Best Fit | | | Trend line with R=1 | |
|---|---|---|---|---|---|---|
| | | Q | R | $r^2$ | Q | $r^2$ |
| 4 | 9.3 | 6.9 | 0.47 | 0.928 | 7.7 | 0.914 |
| 6.2 | 14.3 | 6.2 | -0.23 | 0.943 | 8.1 | 0.839 |
| 11.2 | 25.8 | 7.4 | 0.13 | 0.99 | 8.7 | 0.954 |
| 20.8 | 47.2 | 7.5 | 0.03 | 0.987 | 9.0 | 0.945 |
| 50.3 | 108.4 | 8.9 | 0.79 | 0.999 | 9.3 | 0.997 |
| 99.3 | 207.5 | 9.3 | 0.80 | 0.997 | 9.7 | 0.996 |
| 197.2 | 412.4 | 9.6 | 0.73 | 0.999 | 10.0 | 0.997 |

**Table 05: Dilatancy parameters for plastic silty sands [Present work]**

| Silt(%) | $D_{50}$(mm) | Best Fit | | | Trend line with R=1 | |
|---|---|---|---|---|---|---|
| | | Q | R | $r^2$ | Q | $r^2$ |
| 2.9 | 0.256 | 7.23 | 0.5 | 0.818 | 6.56 | 0.783 |
| 3.2 | 0.224 | 8.46 | -0.57 | 0.826 | 6.70 | 0.747 |
| 3.3 | 0.219 | 9.13 | -0.48 | 0.889 | 6.90 | 0.687 |
| 3.4 | 0.211 | 8.88 | -0.72 | 0.736 | 7.20 | 0.621 |
| 3.6 | 0.209 | 8.40 | 0.83 | 0.645 | 8.17 | 0.60 |
| 4.3 | 0.201 | 7.97 | 0.92 | 0.621 | 8.87 | 0.591 |

The following curves were obtained between $D_r$ v/s $I_N$ are shown below as:-

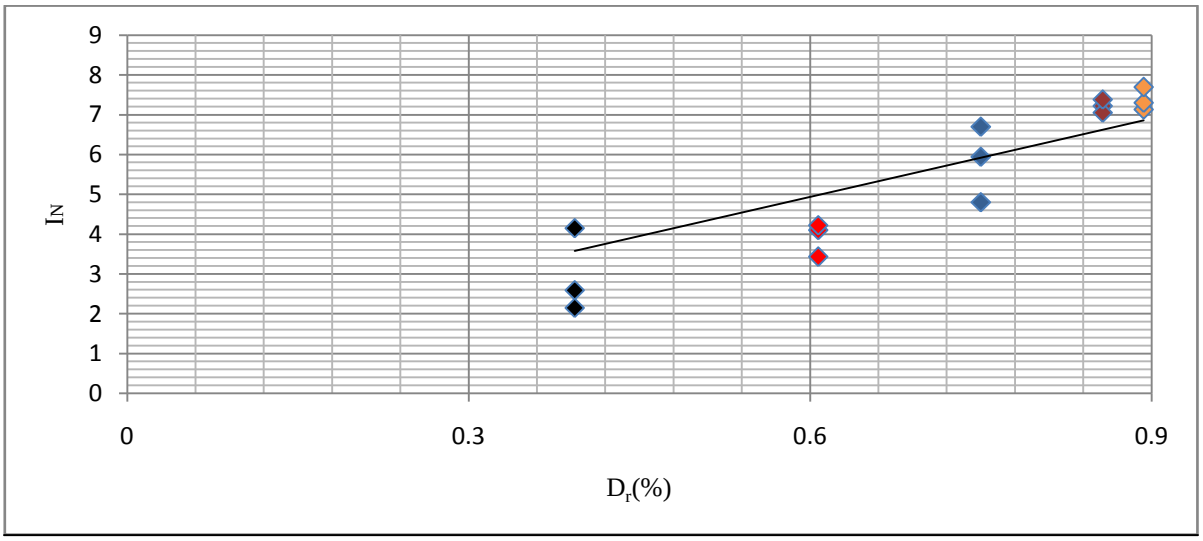


Figure 31(a): $D_r$ v/s $I_N$ (Curve for $D_m^{0.256}$)

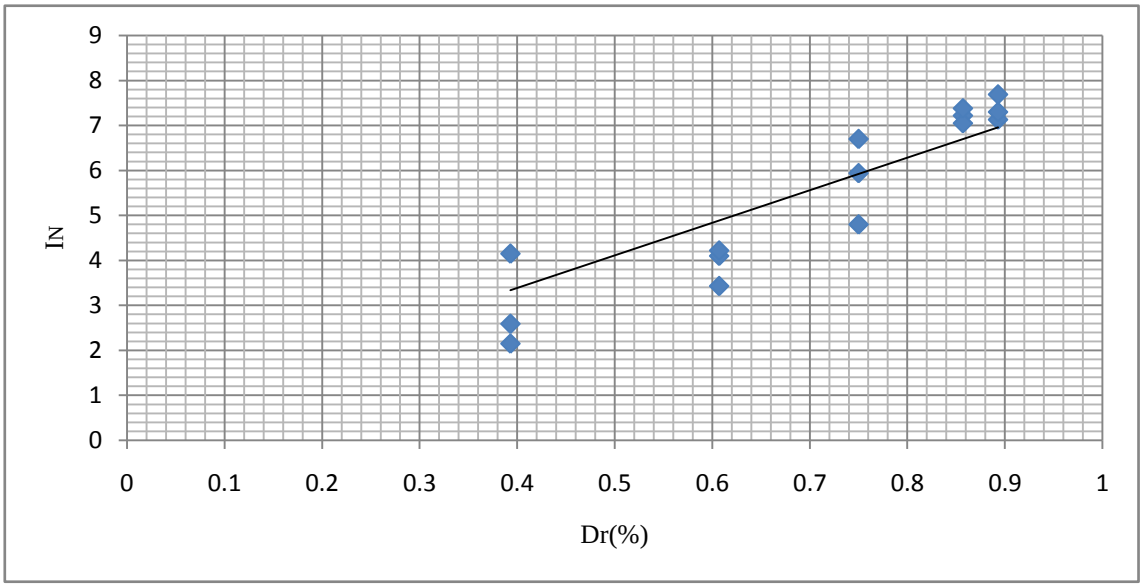


Figure 31(b): $D_r$ v/s $I_N$ (Best Fit Curves for $D_m^{0.256}$)

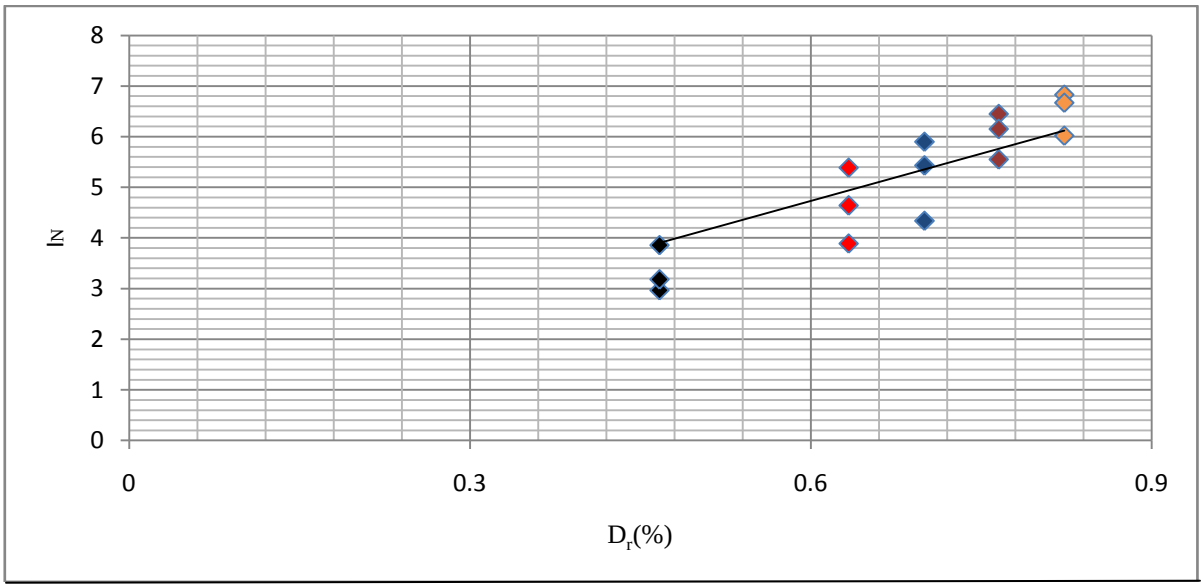


Figure 32(a): $D_r$ v/s $I_N$ (Curve for $D_m^{0.224}$)

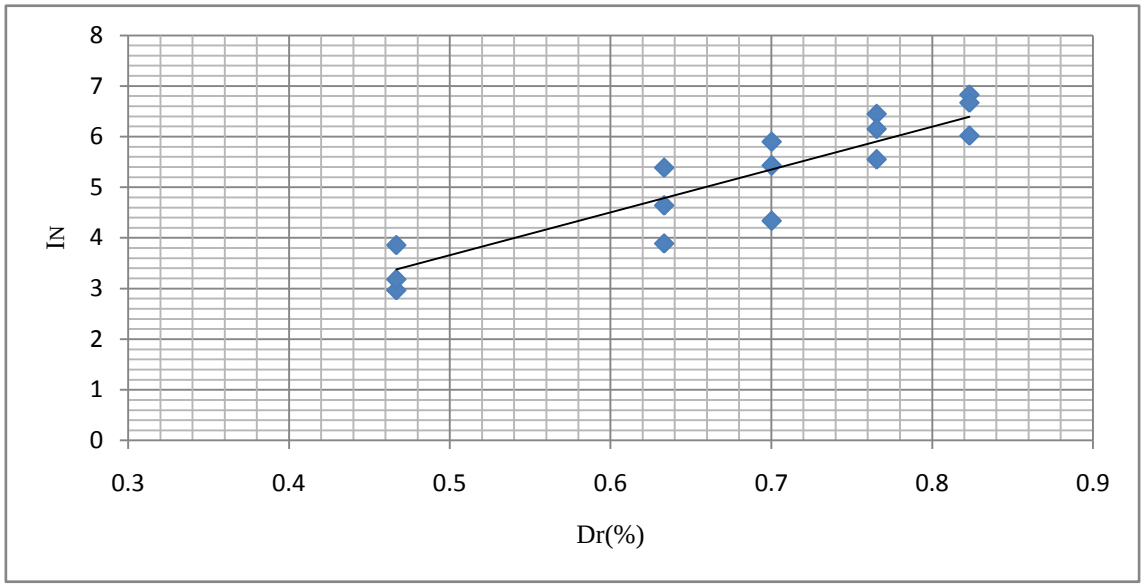


Figure 32(b): $D_r$ v/s $I_N$ (Best Fit Curves for $D_m^{0.224}$)

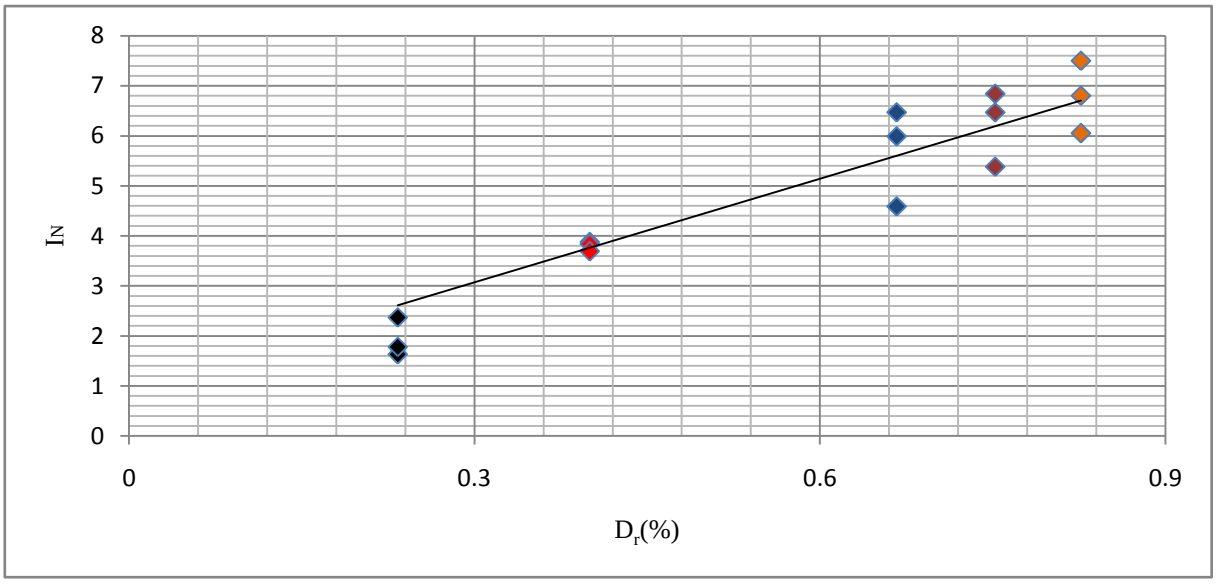


Figure 33(a): $D_r$ v/s $I_N$ (Curve for $D_m^{0.219}$)

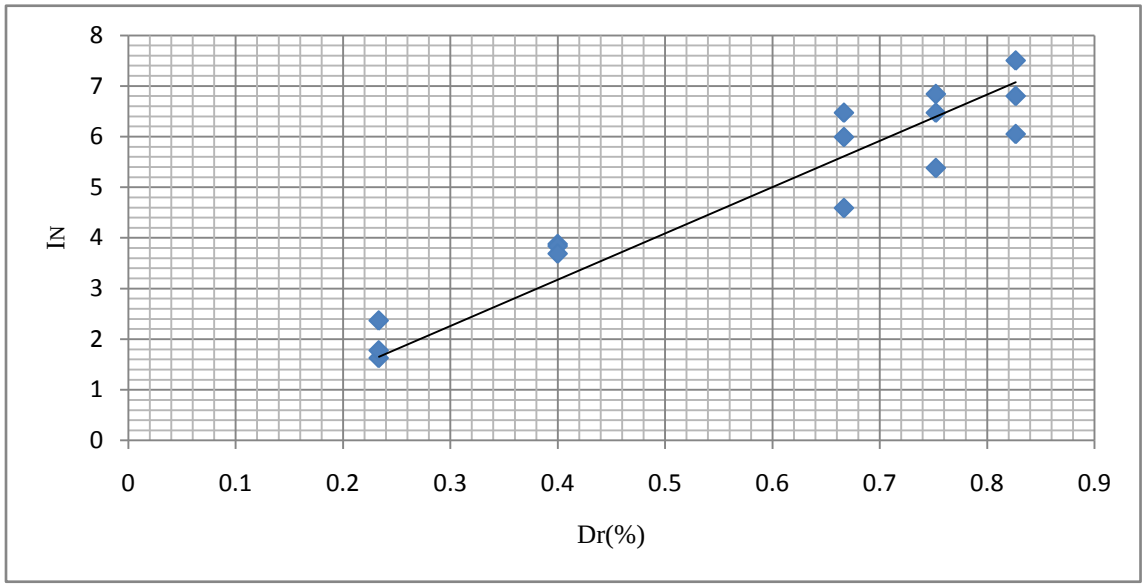


Figure 33(b): $D_r$ v/s $I_N$ (Best Fit Curves for $D_m^{0.219}$)

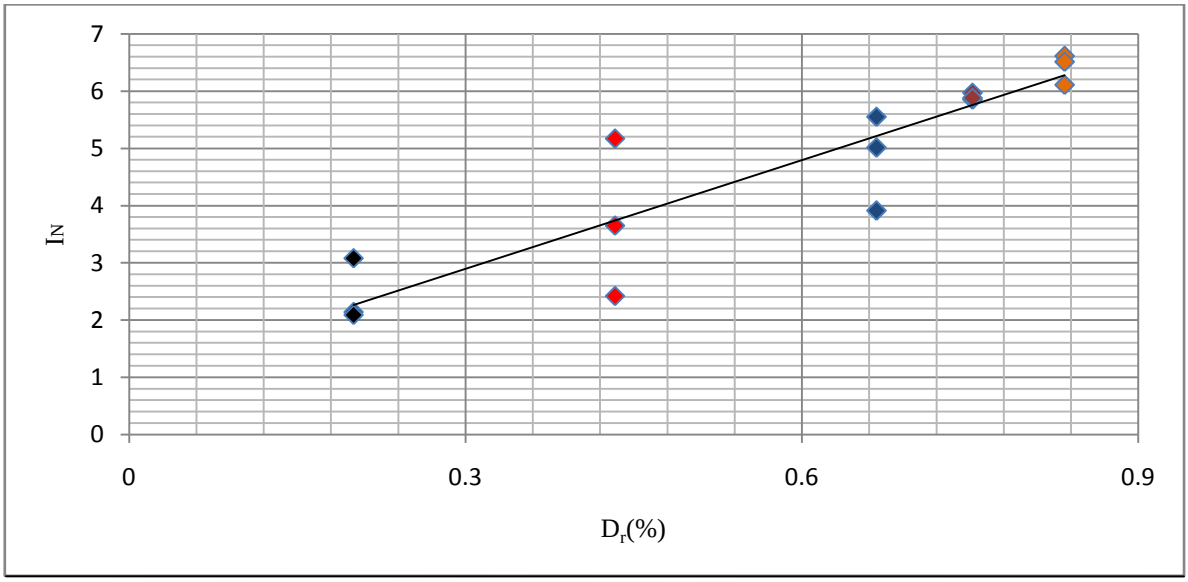


Figure 34(a): $D_r$ v/s $I_N$ (Curve for $D_m^{0.211}$)

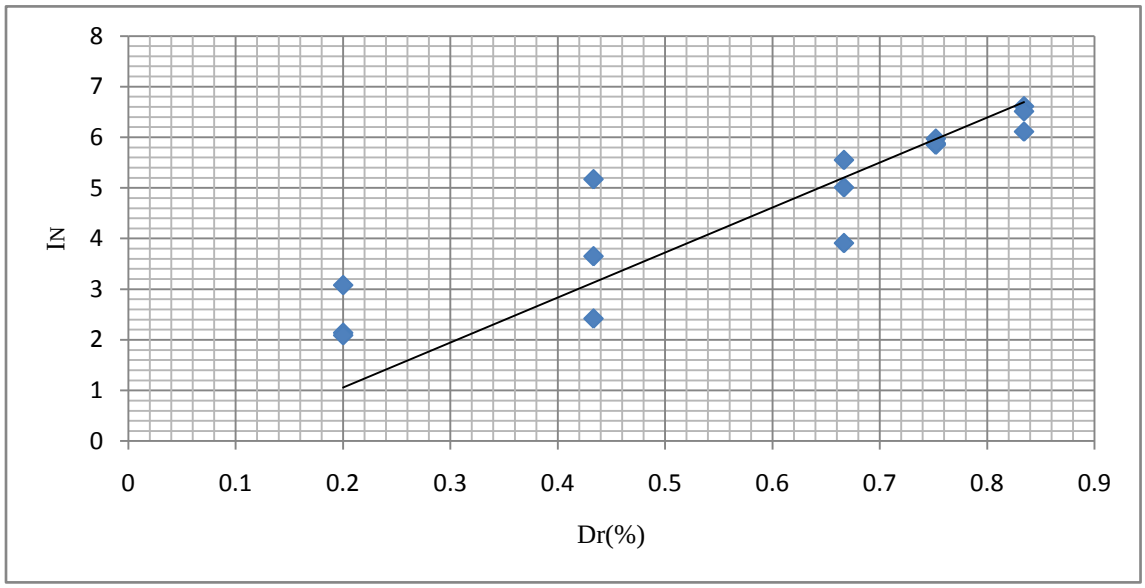


Figure 34(b): $D_r$ v/s $I_N$ (Best Fit Curves for $D_m^{0.211}$)

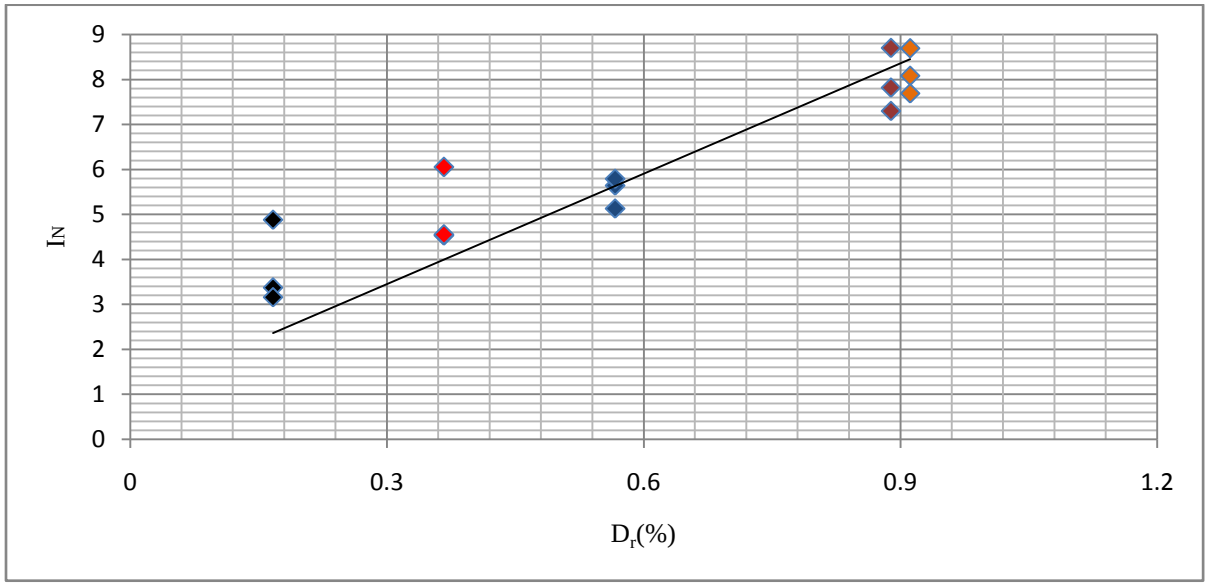


Figure 35(a): $D_r$ v/s $I_N$ (Curve for $D_m^{0.209}$)

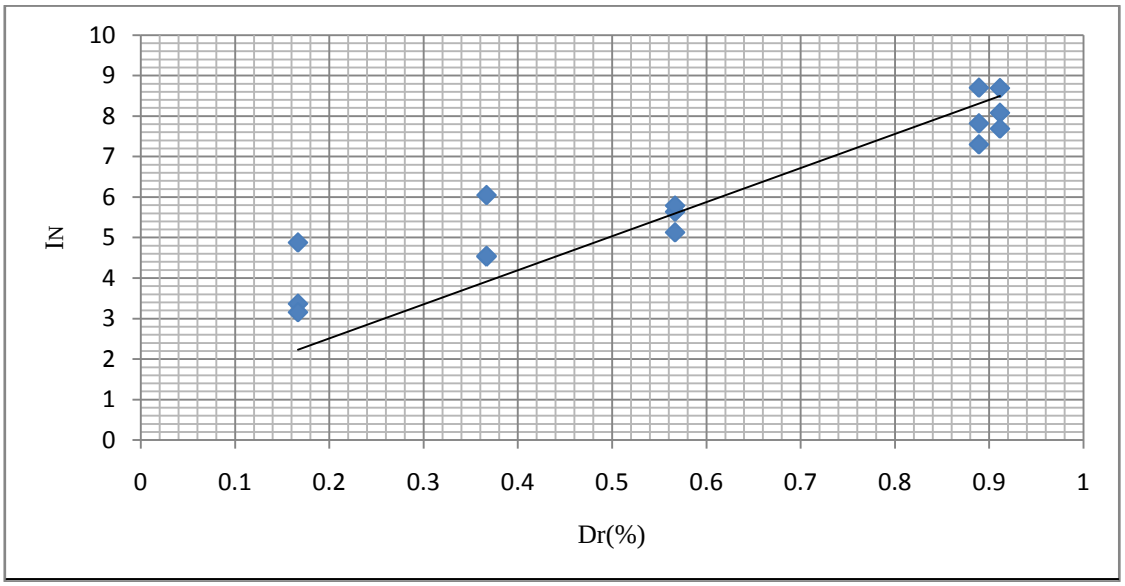


Figure 35(b): $D_r$ v/s $I_N$ (Best Fit Curves for $D_m^{0.209}$)

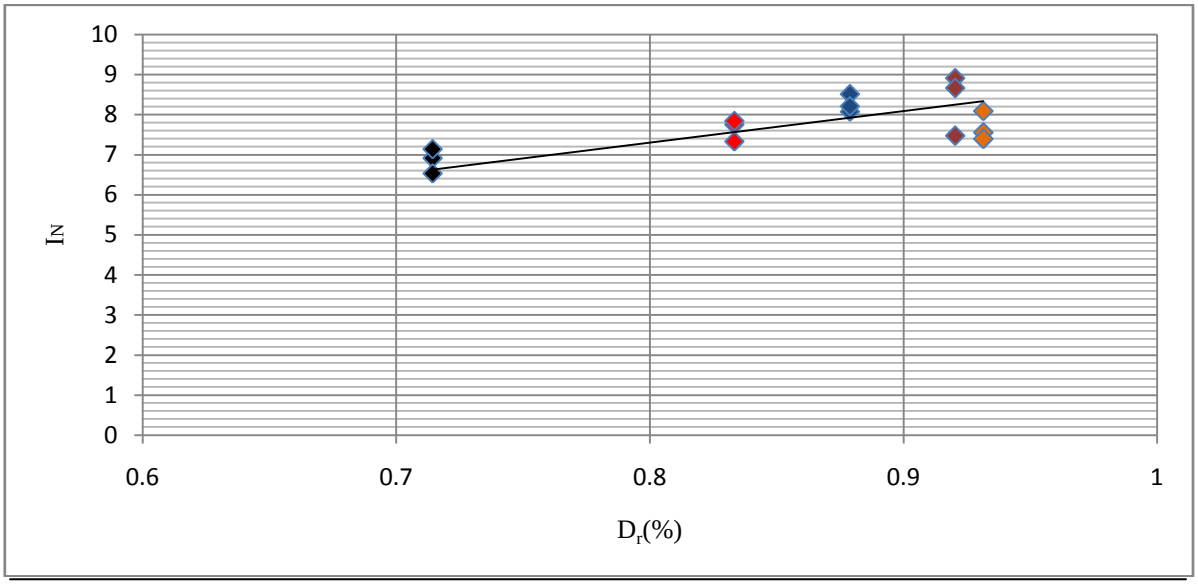


Figure 36(a): $D_r$ v/s $I_N$ (Curve for $D_m^{0.201}$)

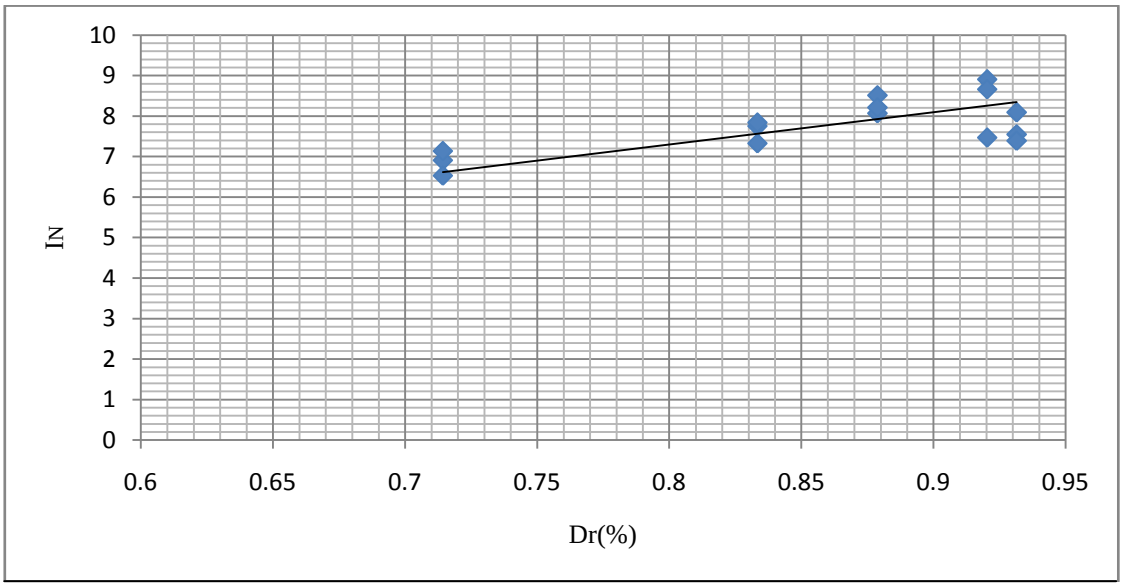


Figure 36(b): $D_r$ v/s $I_N$ (Best Fit Curves for $D_m^{0.201}$)

Bolton (1986) discussed the case in which the calculated peak friction angle results less than the critical-state friction angle. This would be seen when the strains necessary to reach critical-state shear strength are so large that $\Phi_p$ is selected at an earlier, lower value of shear strength. A positive value of R would suggest this type of scenario for very low relative densities. A negative value of R, on the other hand, would imply that the $\Phi_p$ of very loose sand would still be higher than $\Phi_{cs}$. Comparing the findings of Bolton(1986) with that of present work, As per Equation (11), dilatancy increases with increasing Q and increasing with constant value of R. In this work we have evaluate the calculated peak friction angle results less than the critical-state friction angle. This would be seen when the strains necessary to reach critical-state shear strength are so large that $\Phi_p$ is selected at an earlier, lower value of shear strength.

At small shear strains, the shear stress versus shear strain relationship of sand is linear, but for larger shear strains it becomes strongly nonlinear. If the sand is dilative, peak shear strength is reached at axial strains of the order of different percentages. At large strains, the sand reaches its critical state. The peak friction angle ($\Phi_p$) in sand is a result of the combined effects of relative density, mean effective stress, loading path and basic frictional shear strength (as reflected in the value of the critical - state frictional angle). The correlation for peak friction angle proposed by Bolton (1986) and re examined in this work can capture, in a similar manner, the effects of all these factors.

Table 05 summarizes the Q & R values for compression tests on Yamuna Sand obtained by Equation (11) to Yamuna sand datasets corresponding to different confinement levels. The relative densities of the sample for each confining stress level variations from 100, 200 & 400kPa and different fines levels 2.9 to 4.3%. The Q values rise in the (7.23 - 9.13) range, with regression coefficient of (0.818-0.621). Using this data the frictional properties of Yamuna sand with plastic fines can be obtained. We required only the value of percentages of the plastic fines and $D_{50}$. However this needs to be extended for a wide variety of silts obtained in this area and for a wide variety of mean sizes of the Yamuna sand.

# Chapter 7

# Conclusions

As a result of present work we obtained the dilatancy of silty sand. It is observed that slight addition of plastic silty (L.L. = 25% & P.L. = 14%) sand there is a significant change in the Q & R values of silty sand. In fact the value of Q & R attained by (*Bolton1986*) and that attained by (*Salgado et al. 2000*) are not directly applicable, if the fines are plastic. The outcome of present work indicated that Q & R are sensitive to slight addition of fines. If the fines appears to be plastic the value of Q ranges among (7.23 - 9.13).

# Chapter 8

# References


1. Reynolds O. (1885). "On the dilatancy of media composed of rigid particles in contact with experimental illustrations", Phil. Mag. vol. 20, 469-482.

2. Mohr O. (1900). "Welche Umstande Bedingen die Elastizitatsgrenze und den Bruch eines Materials?, *Zeitschrift Des Vereines Deutscher Ingenieure*, vol. 44, 1524-1530, 1572-1577.

3. Bishop A.W. (1954). "Correspondence on shear characteristics of saturated silt measured in tri-axial compression", A. D. M. Penman. *Geotechnique* vol. 4(1), 433-445.

4. Rowe W. and Barden L. (1964). "Importance of free ends in tri-axial testing", *J. Soil Me& Fdns Div. Am. Sot. Cio. Engrs* 90, (SMl) l-27.

5. Wroth C.P. and Bassett R. H. (1965). "A stress-strain relationship for the shearing behavior of a sand", *Geotechnique,* vol. 15(1), 32-56.

6. B.O. Hardin and W.L. Black (1966). "Sand stiffness under various tri-axial stresses", *J. Soil Mechanics and Foundation Engineering Division,* ASCE, 92(SM2), 27–42.

7. Schofield A.N. and Wroth C.P. (1968). "Critical state soil mechanics." *McGraw-hill,* London.

8. Selig E.T. and Ladd R. S. (1973). ‘‘Evaluation of relative density measurement and applications.’’ Evaluation of relative density and its role in geotechnical projects involving cohesionless soils, ASTM STP 523, ASTM, West Conshohocken, Pa., 487–504.

9. Reades D.W. and Green G.E. (1976). “Independent stress control and tri-axial extension tests on sand”, *Geotechnique,* vol. 26(4), 551-576.

10. Shirley D. J. and Hampton L. D. (1977). ‘‘Shear-wave measurements in laboratory sediments.’’ *J. Acoust. Soc*. Am., vol. 63(2), 607–613.

11. Poulos S. (1981). “The steady state of deformation”, *Journal Geotechincal Engineering Division*, ASCE, vol. 107(5), 553-562.

12. Fukushima S. and Tatsuoka F. (1984). “Strength and deformation characteristics of saturated sand at extremely low pressures”, *Soils and Foundations*, vol. 24(4), 30-48.

13. Yu P. and Richart F. E. Jr. (1984). ‘‘Stress ratio effect on Shear modulus of dry sands.’’ *J. Geotech. Engg*., ASCE, vol. 110(3), 331–345.

14. Wood D. M. (1984). “On stress parameters”, *Geotechnique,* vol. 34(2), 282-287.

15. Been K. and Jefferies M. (1985). “A state parameter for sands”, *Geotechnique,* vol. 35(2), 99-112.

16. Wroth C.P. and Houlsby G.T. (1985). “Soil mechanics—property characterization and analysis procedures”, *In: Proc. 11th Int. Conf. SMFE, San Francisco*, vol. (1), 1–55.

17. Bolton M.D. (1986). “The strength and dilatancy of sands”, *Geotechnique*, vol. 36(1) 65–78.

18. Diego C.F. Lo Presti (1987). ‘‘Mechanical behavior of Ticino sand from resonant column tests,’’ PhD thesis, *Politecnico di Torino*, Turin, Italy.

19. Kuerbis R., Negussey D. and Vaid Y. P. (1988). ‘‘Effect of gradation and fines content on the un-drained response of sand.’’ Hydraulic fill structures, *Geotechnical Spec*. Publ. No. 21, ASCE, New York, 330–345.

20. Kuerbis R. and Vaid Y.P. (1988). ‘‘Sand sample preparation— The slurry deposition method.’’ *Soil and Found*, Tokyo, vol. 28(4), 107–118.

21. Sladen J.A. and Oswell J.M. (1989). “The behavior of very loose sand in the tri-axial compression test”, Can Geotech. J., vol. 26(1), 103-113.

22. Wood D.M. (1990). “Soil behavior and Critical state soil mechanics”, *Cambridge University*, New York.

23. Vaid Y., Chung E. K.F. and Keurbis R. H. (1990). “Stress path and steady state”, *Can. Geotech. J*. vol. 27(1), l-7.

24. Been K., Jefferies M. and Hachey J. (1991). "The Critical state of sands" *Geotechnique,* vol. 41(3), 365-381.

25. Jamiolkowski M., Leroueil S. and Diego C. F. Lo Presti (1991). ''Theme lecture: Design parameters from theory to practice.'' *Proc., Geo-Coast*'91, 1–41.

26. Diego C.F. Lo Presti, Pedroni S. and Crippa V. (1992). ''Maximum dry density of cohesionless soil by pluviation and by ASTM D 4253-83: a comparative study.'' *Geotech. Testing J*., vol. 15(2), 180–189.

27. Jefferies M. (1993). "Nor-Sand: A simple critical state model for sand", *Geotechnique,* vol. 43(1), 91-103.

28. Tatsuoka F., Siddiquee M.S.A., Park C., Sakamoto M. and Abe F. (1993). "Modeling stress-strain relations in sand", *Soils and Foundations*, vol. 33(2), 60–81.

29. Wood D.M., Belkheir K. and Liu D. (1993). "Strain softening and state parameter for sand modeling", *Geotechnique,* vol. 44(2), 335-339.

30. Vaid Y.P. (1994). ''Liquefaction of silty soils.'' Ground failures under seismic conditions, *Geotechnical Spec. Publ*. No. 44, Shamsher Prakash and Panos Dakoulas, eds., ASCE, New York, 1–16.

31. Parry R.H.G., (1995). "Mohr Circle stress path and Geotechnics." E & FN Spoon, London.

32. Viggiani G., and Atkinson J.H. (1995a). ‘‘Interpretation of bender element tests.’’ *Geotechnique,* London, vol. 45(1), 149–154.

33. Viggiani G. and Atkinson J.H. (1995b). ‘‘Stiffness of fine-grained soil at very small strains.’’ *Geotechnique*, London, vol. 42(2), 249–265.

34. Schanz T. and Vermeer P.A. (1996). ‘‘Angles of friction and dilatancy of sand.’’ *Geotechnique*, London, vol. 46(1), 145–151.

35. Salgado R., Boulanger R.W., and Mitchell J.K. (1997a). ‘‘Lateral stress effects on CPT liquefaction resistance correlations.’’ *J. Geotech. And Geoenvir. Engg*., ASCE, 123(8), 726–735.

36. Salgado R., Mitchell J.K., and Jamiolkowski M. (1997b). ‘‘Cavity expansion and penetration resistance in sand.’’ *J. Geotech. and Geoenvir. Engg*., ASCE, vol. 123(4), 344–354.

37. Arulnathan R., Boulanger, R.W., and Riemer, M.F. (1998). ‘‘Analysis of bender element tests.’’ *Geotechnical Testing J*., vol. 21(2), 120–131.

38. Bandini P. (1999). ‘‘Static response and liquefaction of silty sands”, Master thesis, *Purdue University*, West Lafayette, Ind.

39. Maeda K. and Miura K. (1999a). “Confining stress dependency of mechanical properties of sands”, *Soils and Foundations,* vol. 39(1), 53-67.

40. Maeda K., and Miura K. (1999b). "Relative density dependency of mechanical properties of sands", *Soils and Foundations,* vol. 39(1), 69-79.

41. Li., X.S. (2002), "A sand model with state dependent dilatancy", *Geotechnique,* vol. 52(3), 173-186.

42. Salgado R., Bandini P. and Karim A. (2000). "Shear Strength and Stiffness of Silty Sand", *Journal of Geotechnical and Geo-environmental Engineering,* vol. 126(5), 451–462.

43. Yamashita S., Jamiolkowski M. and Diego C.F. Lo Presti (2000). "Stiffness Non Linearity of three sands", *Journal of Geotechnical and Geo-Environmental Engineering*, vol. 126(10), 929–938.

44. Wang Q., and Lade, P.V. (2001). "Shear banding in true tri-axial tests and its effect on failure in sand", *J.Engg. Mech.*, vol. 127(8), 754-761.

45. Santamarina J.C. and Cho G.C. (2001). "Determination of Critical State Parameters in Sandy Soils—Simple Procedure," *Geotechnical Testing Journal,* GTJODJ, vol. 24(2), 185–192.

46. Trivedi A. and Sud V.K. (2002). "Grain characteristics and engineering properties of coal ash", *Granular Matter 4, Springer-Verlag,* 93-101.

47. Trivedi A. and Sud V.K. (2004). "Collapse Behavior of Coal Ash", *Journal of Geotechnical and Geo-Environmental Engineering*, vol. 130(4), 403-415.

48. Alshibli K.A. and Williams H.S. (2005). "A true tri-axial apparatus for soil testing with mixed boundary conditions", *Geotech. Test. J.*, 28(6), 534-543.

49. Brandon T.L., Rose A.T. and Duncan J.M. (2006). "Drained and Un-drained Strength Interpretation for Low-Plasticity Silts", *Journal of Geotechnical and Geoenvironmental Engineering*, vol. 132(2).

50. Atkinson J. (2007). "The Mechanics of Soils and Foundations" (Through critical state soil mechanics), Professor of Soil Mechanics, City University, McGraw-Hill, London.

51. Gupta R. and Trivedi A. (2009). "Effects of non-plastic fines on the behavior of loose sand an experimental study", *EJGE*, vol. 14, Bund. B.1-14.

52. Chakraborty T. and Salgado R. (2010). "Dilatancy and Shear strength of sand at low Confining Pressure", *Journal of Geotechnical and Geo-Environmental Engineering*, ASCE, vol. 136(3), 527-534.

53. Trivedi A. (2010). "Strength and dilatancy of jointed rocks with granular fill", *Acta, Geotechnica*, vol. 5(1), 15-31.

54. Trivedi A. (2012). "Estimating insitu Deformation of Rock Masses Using a Hardening Parameter and RQD", *International Journal of Geomechanics*, doi:10.1061/(ASCE)GM.1943-5622.0000215.

55. http://www.geotechdata.info/geotest/triaxial-test